

Università degli Studi di Napoli

“Federico II”



**DEPARTMENT OF CHEMICAL, MATERIALS AND INDUSTRIAL  
PRODUCTION ENGINEERING**

XXIX Course

PhD school in

INDUSTRIAL PRODUCT AND PROCESS ENGINEERING

“The drilling of CFRP and Ti6Al4V stacks:  
an innovative approach”

Supervisor:

Prof.

**Antonino Squillace**

Head of the Doctorate School:

Prof.

**Giuseppe Mensitieri**

Ph.D. candidate:

**Filomena Impero**

A.Y. 2016/17

## INDEX

<b>Introduction</b>	<b>1</b>
<b>1 New generation materials for high speed transport</b>	<b>4</b>
1.1 Titanium in the Aircraft Industry	6
1.1.1 Facts about Titanium	6
1.1.2 Titanium Designations	8
1.1.3 Corrosion Characteristics	9
1.1.4 Titanium Advantages	10
1.1.5 Titanium in Aircraft Construction	10
1.2 Composite materials	11
1.2.1 Advantages/Disadvantages of Composites	12
1.2.2 Composite safety	13
1.2.3 Fibre Reinforced Materials	14
1.2.4 Laminated Structures	14
1.3 Aluminium alloys	17
1.3.1 Cast alloys	19
1.3.2 Wrought aluminium alloys	21
1.3.3 Effect of Alloying Element	23
<b>2 The drilling in assembly of aero-structures</b>	<b>26</b>
2.1 The tools	26
2.1.1 Geometry	27
2.1.2 Materials	31
2.1.3 Coatings	33
2.2 Issues in drilling of materials	35
2.2.1 Issues in drilling of CFRP	35
2.2.2 Issues in drilling of titanium alloys	38
2.2.3 Issues in drilling of CFRP-Ti stacks	40
2.3 Strategies and cutting fluids	41

<b>3</b>	<b>The Drilling of stacks: a comparison between Wet and Cryogenic conditions</b>	<b>47</b>
3.1	Materials & methods	47
3.1.1	The used tool	48
3.1.2	The workpieces	49
3.1.3	Drilling machine	50
3.1.4	Process conditions	52
3.1.5	Measuring instruments	53
3.2	Results & discussions	55
3.2.1	Thrust forces	56
3.2.2	Torque	60
3.2.3	Hole diameters	65
3.2.4	Burr height	75
3.3	Conclusions	77
<b>4</b>	<b>The Drilling of stacks: the Long Run Campaign</b>	<b>80</b>
4.1	Materials & methods	80
4.1.1	The used tools	80
4.1.2	The workpieces	81
4.1.3	The drilling conditions and evaluated outputs	81
4.2	Results & discussions	82
4.2.1	Thrust forces	82
4.2.2	Torque	85
4.2.3	Hole diameters	89
4.2.4	Burr height	91
4.2.5	Tools visual inspection	93
4.3	Conclusions	97
<b>5</b>	<b>Conclusion</b>	<b>99</b>

Airframe industries are increasing the implementation of composite/metal stacks due to their high strength to weight ratio in order to increase fuel efficiency and cycle life. Among these materials, carbon fiber reinforced plastics (CFRP) and titanium (Ti) are increasing in popularity. For example, the structural weight of the Boeing 787 and the F-22 contains 14% and 39% titanium content, respectively. In terms of composites, the Boeing 787 has a 51% structural weight content while the F-22 has a 36% structural weight content. Structural components made from composites are generally attached to titanium rather than aluminum due to galvanic corrosion that occurs between composite/aluminum stacks. Titanium alloys are also popular with various applications, which include and are not limited to biomedical implant materials and sporting goods (golf club heads, bicycle frames, etc.).

When it comes to machining for CFRP and titanium, both are difficult-to-cut materials. CFRP is highly abrasive (two- and three-body abrasion), requiring tools with high hardness to resist its abrasive nature. Its anisotropic properties submit the tool to various cutting loads (varying ply orientation combined by a matrix material). Temperature during machining must be kept minimal to prevent matrix degradation. The tool edge must be kept sharp for higher quality. Titanium has a low thermal conductivity (6.7W/m-K), which leads to high temperature gradients localized on the cutting edge. With high temperatures, titanium is chemically reactive, leading to adhesion and diffusion, and ultimately tool failure. Titanium undergoes work hardening and has a high hot hardness. Cyclic forces also occur due as drilling titanium produces segmented chips, which can lead to mechanical fatigue failure. In every material, but especially in CFRP and titanium, hole quality is important for fatigue life performance of the structures assembled via fasteners.

While drilling each material individually is well known to be difficult, drilling CFRP/Ti stacks is even more challenging. When drilling CFRP, diamond like carbon (DLC) has the good performance. For high-speed titanium machining, tungsten carbide (WC) is the

optimal tool material. However, when machining CFRP, WC tools undergo two- and three-body abrasion, resulting with spalling, as the cobalt binder is easily abraded by composite fibers and titanium. When drilling titanium, the removal of tool material grains with the titanium adhesion, otherwise known as attrition, can occur. On top of these, drilling both materials together can lead to increased surface defects. High cutting temperatures can produce damages around the CFRP at the CFRP/Ti interface as the temperature passes the limit the matrix can withstand. A damage ring may also occur due to severe rounding of the tool cutting edge. Stiff titanium chips at high feeds can produce surface damage to CFRP borehole. When drilling CFRP, the titanium adhesion from the previous hole acts as a cutting edge, producing more fiber pullout to occur when drilling CFRP in the next hole due to the lower sharpness of the acting titanium adhesion. Cutting speeds and feeds also affect hole surface roughness in both CFRP and titanium.

This thesis focuses on hole quality for the drilling of carbon fiber reinforced plastics and titanium stacks and lightly covers preliminary results in identifying tool wear mechanisms. There are five chapters in this thesis, and an Introduction.

The Introduction, provides a glance at the motivation and problem this research is attempting to solve.

The first chapter, New generation materials for high speed transports, brings forth ample knowledge from past to present research vital to this report as well as to the continuation of this research; a special eye has been put on the aeronautic sector and the most common materials used in making aero structures.

The second chapter, the drilling in assembly of aero-structures, describes in details the drilling in all its aspects, dealing deeply the drilling of both CFRP and titanium alloys and finally the issues of drilling of stacks of these materials.

The drilling of stacks a comparison between Wet and Cryogenic conditions, chapter 3, describes the experiments conducted in the first experimental campaign of this study and introduces the equipment used for the experiment analysis. In particular, the influence of cooling conditions and process parameters have been deeply investigated.

The fourth chapter, The Drilling of stacks in the long Run Campaign, presents the results collected throughout the experiments carried out on the long run campaign with the aim to define the highest possible number of holes that can be produced in tolerance with a single tool. It provides a discussion of the results.

The final chapter, chapter 5, is the conclusion ascertained by the results.

## 1. New generation materials for high-speed transports

---

### Introduction

This chapter deals with the most important materials that are used in the modern aircraft industry for making aerostructure. Along all its history, this industry has always used materials characterized by good mechanical properties and a low weight.

The first material to be used was the wood, since at that time, the beginning of the last century, it represented the best choice. Year by year, as more and more materials were available, the wood was progressively replaced by steel and, above all, aluminium alloys.

In the last decades, the composite materials (mainly Carbon Fibre Reinforce Plastics, CFRP, but also Glass Fibre Reinforced Plastics) have been used firstly for secondary structures, then for horizontal stabilizers and wings, and finally, thanks to the Boeing 787, for the entire fuselage.

In the following picture the percentages of main materials used in this aircraft are reported.

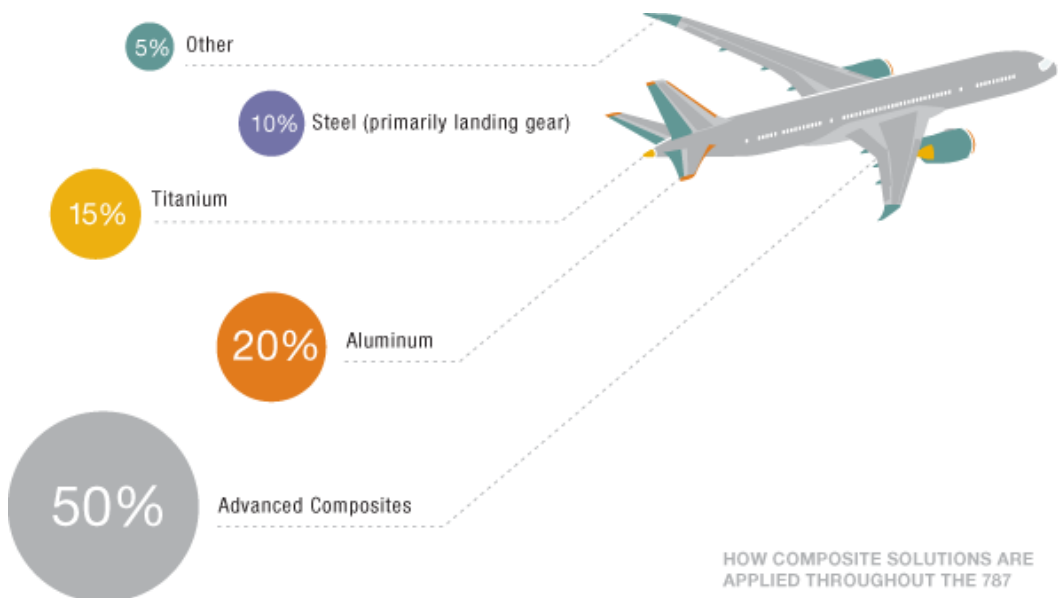
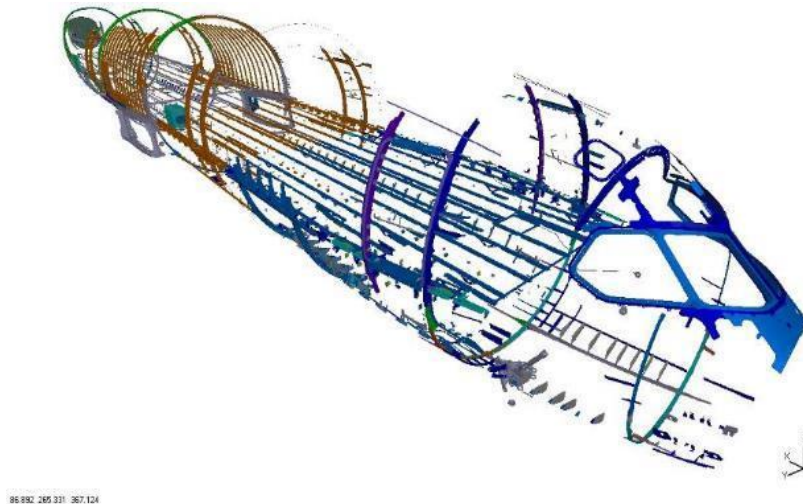


Fig. 1.1 – The main materials used in the Boeing 787.

The wider use of CFRP has determined also an increased use of titanium alloys. In fact, those part of the CFRP aero-structure that are heavily stressed by concentrated loads, have to be made using this metal.

The following figure reports, as an example, the numerous titanium parts belonging to the fuselage of the Boeing 787:



*Fig. 1.2 – Titanium parts in the fuselage of the Boeing 787.*

The reasons leading to the choice of this metal are fundamentally two. The former is due to the good electrochemical compatibility between carbon fibres and titanium: this prevents any problem of corrosion due to the galvanic coupling of different materials. The latter is due to the similar values of coefficients of thermal expansion of the two materials that prevents problems regarding the occurrence of inner stresses in large structures exposed to very wide ranges of temperatures, normally wider than 100°C.

In the following, the two mains materials, CFRP and titanium (and its alloys) will be briefly described, in order to understand better, in the rest of this work, all the issues arising in the drilling of both parent materials and their stacks. To conclude the chapter, a brief description of aluminium alloys will be given, since these alloys represented, and still represent, the most important family of materials in aeronautic.

## **1.1 Titanium in the Aircraft Industry**

Aircraft construction requires the use of materials that can withstand the severe pressures of flight at high altitudes, as well as constant exposure to the elements. Traditionally, aircraft were constructed of steel, but lighter, more durable materials are now used to extend the life of aircraft and make them more energy efficient.

### **1.1.1 Facts About Titanium**

Titanium is classified as a metal with chemical element symbol of Ti and an atomic number of 22. Titanium has the highest weight-to-strength ratio of any metal, which makes it useful for a variety of industries in which parts must have superior strength but not add to the overall weight of the product. Titanium is as strong as steel but 45% lighter. It is also corrosion resistant, which makes it a preferred metal for a number of outdoor uses. Titanium can be made into an alloy with a number of metals, such as iron, aluminium, molybdenum and vanadium. Reverend William Gregor discovered titanium in 1791. Martin Heinrich Klaproth named it in honour of the Titans of Greek mythology. Titanium can be found in abundance in the earth. It is always found bonded to other elements in its natural form. It must be extracted and purified through a number of processes.

A crude separation of titanium ore was accomplished in 1825. In 1906, a sufficient amount of pure titanium was isolated in metallic form to permit a study. Following this study, in 1932, an extraction process was developed which became the first commercial method for producing titanium. The United States Bureau of Mines began making titanium sponge in 1946, and 4 years later the melting process began.

The use of titanium is widespread. It is used in many commercial enterprises and is in constant demand for such items as pumps, screens, and other tools and fixtures where corrosion attack is prevalent. In aircraft construction and repair,

titanium is used for fuselage skins, engine shrouds, firewalls, longerons, frames, fittings, air ducts, and fasteners.

Titanium is used for making compressor disks, spacer rings, compressor blades and vanes, through bolts, turbine housings and liners, and miscellaneous hardware for turbine engines.

Titanium, in appearance, is similar to stainless steel. One quick method used to identify titanium is the spark test. Titanium gives off a brilliant white trace ending in a brilliant white burst. Also, moistening the titanium and using it to draw a line on a piece of glass can accomplish identification. This will leave a dark line similar in appearance to a pencil mark.

Titanium falls between aluminium and stainless steel in terms of elasticity, density, and elevated temperature strength. It has a melting point of 1668°C, low thermal conductivity, and a low coefficient of expansion. It is light, strong, and resistant to stress corrosion cracking. Titanium is approximately 60% heavier than aluminium and about 50% lighter than stainless steel.

Because of its high melting point, high temperature properties are disappointing. The ultimate yield strength of titanium drops rapidly above 450°C. The absorption of oxygen and nitrogen from the air at temperatures above 800°C makes the metal so brittle on long exposure that it soon becomes worthless. However, titanium has some merit for short time exposure up to 1650 °C where strength is not important. Aircraft firewalls demand this requirement.

Titanium is nonmagnetic and has an electrical resistance comparable to that of stainless steel. Some of the base alloys of titanium are quite hard. Heat treating and alloying do not develop the hardness of titanium to the high levels of some of the heat-treated alloys of steel. It was only recently that a heat-treatable titanium alloy was developed. Prior to the development of this alloy, heating and rolling was the only method of forming that could be accomplished. However, it is possible to form the new alloy in the soft condition and heat-treat it for hardness.

Iron, molybdenum, and chromium are used to stabilize titanium and produce alloys that will quench harden and age harden. The addition of these metals also enhances ductility. The fatigue resistance of titanium is greater than that of aluminium or steel.

Titanium becomes softer as the degree of purity is increased. It is not practical to distinguish between the various grades of commercially pure or unalloyed titanium by chemical analysis; therefore, the grades are determined by mechanical properties.

### **1.1.2 Titanium Designations**

The A-B-C classification of titanium alloys was established to provide a convenient and simple means of describing all titanium alloys. Titanium and titanium alloys possess two basic types of crystals: the former named alpha, with a hexagonal close-packed lattice, the latter named beta, with a cubic centred lattice. The former phase is stable at room temperature and up to the so-called beta transus, which is about 880°C for pure titanium.

The latter phase is stable from beta transus up the melting point.

Adding alloying elements to titanium provides a wide range of physical and mechanical properties. Certain alloying additions, notably aluminium, tend to stabilize the alpha phase; that is, they raise the temperature at which the alloy will be transformed completely to the beta phase.

Alloying additions such as chromium, columbium, copper, iron, manganese, molybdenum, tantalum, and vanadium stabilize the beta phase by lowering the temperature of transformation from alpha to beta. Some elements, notably tin and zirconium behave as neutral solutes in titanium and have little effect on the transformation temperature, acting instead as strengtheners of the alpha phase.

Depending on the presence, and the relative percentage, of the two phases, titanium alloys can be classified in A (with a percentage of beta phase lower than 5%), B (with a percentage of beta phase higher than 20%), and C (with a percentage of beta phase ranging from 5 up to 20%).

Their characteristics are:

- A (alpha) - all around performance; good weldability; tough and strong both cold and hot, and resistant to oxidation.
- B (beta) - bendability; excellent bend ductility; strong both cold and hot, but vulnerable to contamination.
- C (combined alpha and beta for compromise performances) - strong when cold and warm, but weak when hot; good bendability; moderate contamination resistance; excellent forgeability.

Titanium is manufactured for commercial use in two basic compositions: commercially pure titanium and alloyed titanium. A-55 is an example of commercially pure titanium. It has yield strength of 400 to 550 MPa and is a general-purpose grade for moderate to severe forming. It is sometimes used for non-structural aircraft parts and for all types of corrosion resistant applications, such as tubing. Type A-70 titanium is closely related to type A-55 but has yield strength of 480 to 650 MPa. It is used where higher strength is required, and it is specified for many moderately stressed aircraft parts. For many corrosion applications, it is used interchangeably with type A-55. Both type A-55 and type A-70 are weldable.

One of the widely-used titanium base alloys is designated as C-110M. It is used for primary structural members and aircraft skin, has 760 MPa minimum yield strength, and contains 8% manganese.

Type A-110AT is a titanium alloy that contains 5% aluminium and 2.5% tin. It also has high minimum yield strength at elevated temperatures with the excellent welding characteristics inherent in alpha-type titanium alloys.

### **1.1.3 Corrosion Characteristics**

The corrosion resistance of titanium deserves special mention. The resistance of the metal to corrosion is caused by the formation of a protective surface film of stable oxide or chemical absorbed oxygen. Film is often produced by the presence of oxygen and oxidizing agents.

Corrosion of titanium is uniform. There is little evidence of pitting or other serious forms of localized attack. Normally, it is not subject to stress corrosion, corrosion fatigue, intergranular corrosion, or galvanic corrosion. Its corrosion resistance is equal or superior to 18-8 stainless steel.

Laboratory tests with acid and saline solutions show titanium polarizes readily. The net effect, in general, is to decrease current flow in galvanic and corrosion cells. Corrosion currents on the surface of titanium and metallic couples are naturally restricted. This partly accounts for good resistance to many chemicals; also, the material may be used with some dissimilar metals with no harmful galvanic effect on either.

#### **1.1.4 Titanium Advantages**

Titanium can withstand long periods of exposure to salt water in marine atmospheres, as well, which makes it of particular value in coastal regions. It is also a very ductile material that can be worked into many shapes. Titanium's melting point is very high, at 1650°C, which makes it able to bear high-heat environments. It is also nonmagnetic and does not conduct heat or electricity well. All of these qualities make it an especially good choice for aircraft parts. Welding of titanium requires special treatment to avoid intrusion of impurities into the weld, which can cause cracking and failure. Machining of titanium must also be done using specific processes to avoid softening and galling of the metal.

#### **1.1.5 Titanium in Aircraft Construction**

Titanium is used in a variety of parts in aircraft construction, both on the exterior framework and in the engine. Titanium can be found on parts for landing gear, internal components of wings, propellers and other components. It can also be found within the aircraft engine, such as the housing, fan blades, pumps, screens and components that may be exposed to high temperatures. Steel and steel alloys are still used extensively in many aircraft because of cost considerations. Titanium is not only an expensive material; the costs involved in properly

machining the metal often make it less feasible for widespread use throughout the aircraft. Titanium alloys are common in aircraft construction with complex compounds used to provide specific qualities for particular parts, such as with aluminium for hydraulic tubing and with tin and chromium for frames and engines.

Titanium is a desirable option for many aircraft parts because of its intrinsic qualities. As this metal becomes more widely used, the cost per unit is expected to drop, making it the metal of choice for the industry.

The increased use of CFRP has noticeably increased the use of titanium alloys even in those parts of the aerostructure that are heavily stressed by concentrated loads and the parts themselves are in contact with CFRP. The reasons of his choice have been detailed reported at the beginning of this chapter.

## **1.2 Composite materials**

In the 1940s, the aircraft industry began to develop synthetic fibres to enhance aircraft design. Starting from that time, composites have been used more and more. When composites are mentioned, most people think of only fiberglass, or maybe graphite or aramids (Kevlar), which are widely used in sport goods. Composites began in aviation, but now are being embraced by many other industries, including auto racing, sporting goods, and boating, as well as defence industry uses.

A “composite” material is defined as a mixture of two or more different materials or things. This definition is so general that it could refer to metal alloys made from several different metals to enhance the strength, ductility, conductivity or whatever characteristics are desired. Similarly, the composition of composite materials is a combination of reinforcement, such as a fibre, whisker, or particle, surrounded and held in place by a matrix (in our case a polymer), forming a structure. Separately, the reinforcement and the resin are very different from their combined state. Even in their combined state, they can

still be individually identified and mechanically separated. One composite, concrete, is composed of cement (resin) and gravel or reinforcement rods for the reinforcement to create the concrete.

### **1.2.1 Advantages/Disadvantages of Composites**

Some of the many advantages for using composite materials are:

- High strength to weight ratio
- Fibre-to- fibre transfer of stress allowed by chemical bonding
- Modulus (stiffness to density ratio) 3.5 to 5 times that of steel or aluminium
- Longer life than metals
- Higher corrosion resistance
- Tensile strength 4 to 6 times that of steel or aluminium
- Greater design flexibility
- Bonded construction eliminates joints and fasteners
- Easily repairable

The disadvantages of composites include:

- Inspection methods difficult to conduct, especially delamination detection
- Lack of long term design database, relatively new technology methods
- Cost
- Very expensive processing equipment
- Lack of standardized system of methodology
- Great variety of materials, processes, and techniques
- General lack of repair knowledge and expertise
- Products often toxic and hazardous
- Lack of standardized methodology for construction and repairs

The increased strength and the ability to design for the performance needs by the product makes composites much superior to the traditional materials used in today's aircraft.

Since composites are more and more used, the costs, design, inspection ease, and information about strength to weight advantages will help composites

become the material of choice for aircraft construction. As it has been reported at the beginning of this chapter, the Boeing Company has been the first in the world to design and make a new aircraft with the entire fuselage completely made of CFRP.

Probably, in the very next future, we will see other examples like this.

### **1.2.2 Composite safety**

Composite products can be very harmful to the skin, eyes, and lungs. In the long or short term, people can become sensitized to the materials with serious irritation and health issues. Personal protection is often uncomfortable, hot, and difficult to wear; however, a little discomfort while working with the composite materials can prevent serious health issues or even death.

Respirator particle protection is very important to protecting the lungs from permanent damage from tiny glass bubbles and fibre pieces. At a minimum, a dust mask approved for fiberglass is a necessity. The best protection is a respirator with dust filters. The proper fit of a respirator or dust mask is very important because if the air around the seal is breathed, the mask cannot protect the wearer's lungs. When working with resins, it is important to use vapour protection. Charcoal filters in a respirator will remove the vapours for a period of time. If you can smell the resin vapours after placing the mask back on after a break, replace the filters immediately. Sometimes, charcoal filters last less than 4 hours. Store the respirator in a sealed bag when not in use. If working with toxic materials for an extended period of time, a supplied air mask and hood are recommended.

Avoid skin contact with the fibres and other particles by wearing long pants and long sleeves along with gloves or barrier creams. The eyes must be protected using leak-proof goggles (no vent holes) when working with resins or solvents because chemical damage to the eyes is usually irreversible.

### **1.2.3 Fibre Reinforced Materials**

The purpose of reinforcement in reinforced plastics is to provide most of the strength. The three main forms of fibre reinforcements are particles, whiskers, and fibres.

A particle is a square piece of material. Glass bubbles (Q-cell) are hollow glass spheres, and since their dimensions are equal on all axes, they are called a particle.

A whisker is a piece of material that is longer than it is wide. Whiskers are usually single crystals. They are very strong and used to reinforce ceramics and metals.

Fibres are single filaments that are much longer than they are wide. Fibres can be made of almost any material, and are not crystalline like whiskers. Fibres are the bases for most composites. Fibres are smaller than the finest human hair and are normally woven into cloth-like materials. The most used fibres in aeronautic are the carbon ones, the glass ones, the aramidic ones. For each of them, different types of fibres are commercially available having different properties and characteristics.

### **1.2.4 Laminated Structures**

Composites can be made with or without an inner core of material. Laminated structure with an inner core is called a sandwich structure. Laminate construction is strong and stiff, but heavy. The sandwich laminate is equal in strength, and its weight is much less; weight saving is mandatory for aerospace products.

The core of a laminate can be made from nearly anything. The decision is normally based on use, strength, and fabricating methods to be used.

Various types of cores for laminated structures include rigid foam, wood, metal, or the aerospace preference of honeycomb made from paper, Nomex, carbon, fiberglass or metal. Fig. 1.3 shows a typical sandwich structure.

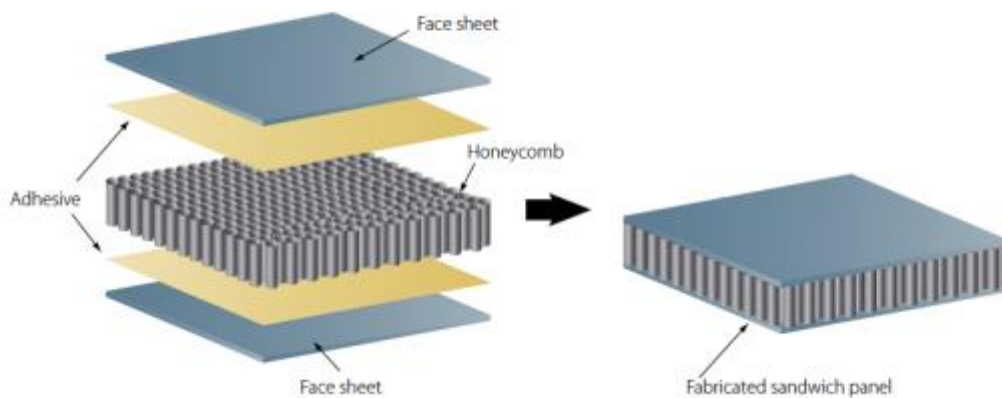


*Fig. 1.3 – Sandwich structure.*

It is very important to follow proper techniques to construct or repair laminated structures to ensure the strength is not compromised. Taking a high-density laminate or solid face and backplate and sandwiching a core in the middle make a sandwich assembly. The design engineer, depending on the intended application of the part, decides the selection of materials for the face and backplate. It is important to follow manufacturer' maintenance manual specific instructions regarding testing and repair procedures as they apply to a particular aircraft.

The reasons of the use of CFRP can be easily understood looking at the following picture, reporting, as a function of the material density, the Young's modulus, for several families of materials.

CFRP are ideally located above the diagonal of the diagram area, being characterize by a modulus similar to that of stainless steel, but saving a density absolutely lower.

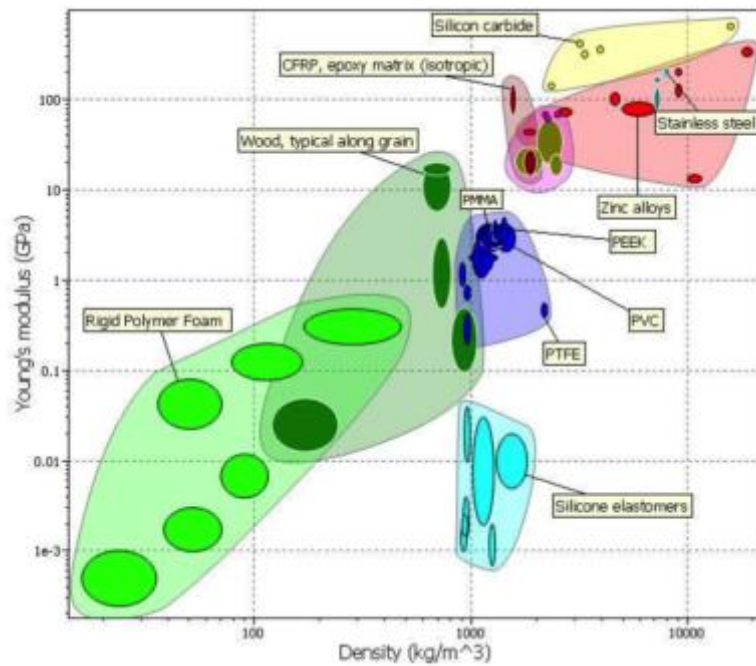


Fig. 1.4 – Young's modulus vs. density for main materials.

In the figure 1.5 a diagram similar to the previous one is proposed. In this case, the Young's modulus of material is reported vs. the tensile strength to density ratio.

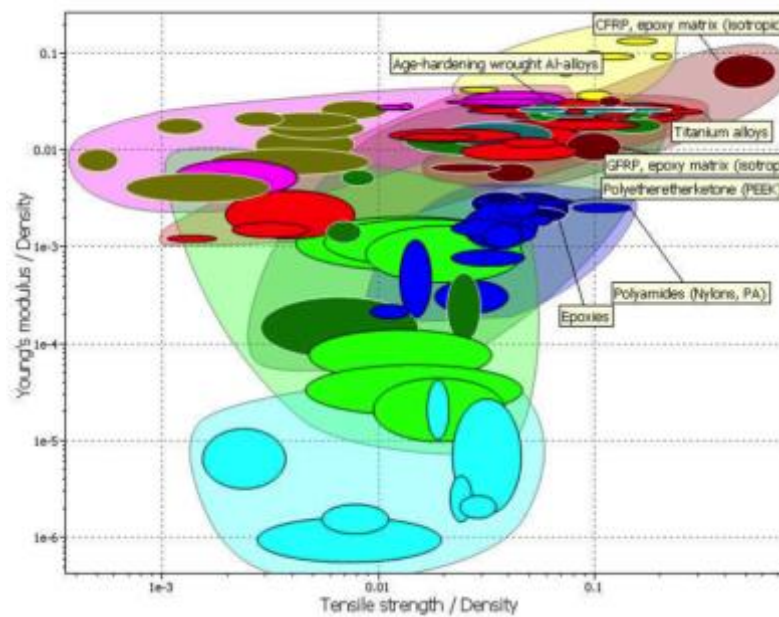


Fig. 1.5 - Young's modulus vs. the tensile strength to density ratio.

Also in this case, the CFRP are located at the very top of the diagram area. For their intrinsic characteristics, as a consequence, the CFRP represent the most promising material for the present and the future of aeronautic industry.

### 1.3 Aluminium alloys

Even if the aluminium alloys are not the materials under investigation in the present work, they have represented, without any doubt, the most important family of materials in aeronautic in the last decades. Almost every aircraft flying now are still made mainly with these alloys, so a brief description, even in terms of a comparison with CFRP and titanium alloys can be absolutely useful.

Looking at the figure 1.6, in fact, one can easily understand the importance of this material in aeronautic.

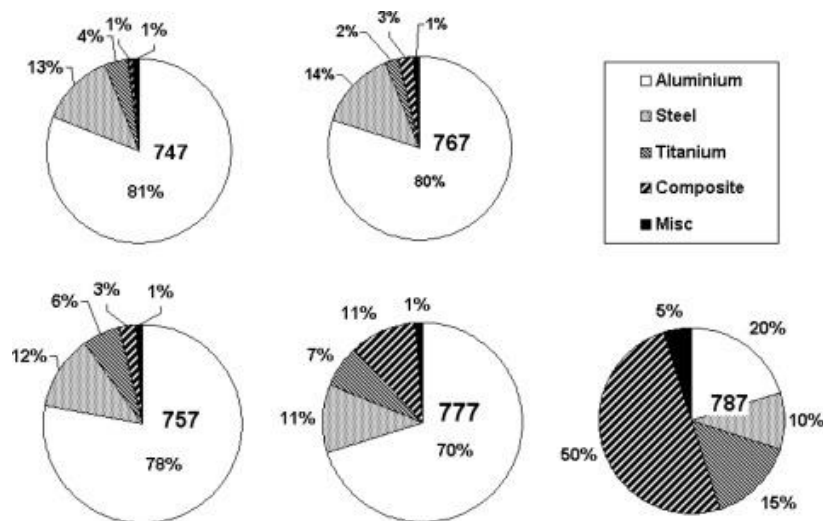


*Fig. 1.6 – Percentages of materials used in the most common Boeing commercial aircrafts.*

Even in the case of 787, the amount of aluminium alloy used is impressive: about 20 tons of aluminium alloys are used for each single aircraft.

Looking at the value of the global aeronautic market, the gross demand of aluminium alloys is approximately one half of the whole demand of raw materials:



Fig. 1.7 – Raw materials global demand for aeronautic in 2014.

As it can be easily understood, one of the most important issues remain the high value of the buy-to-fly ratio, which means that meanly, only one sixth of the acquired materials will participate to the aircraft, the largest part resulting in scraps.

Commercially pure aluminium is a white lustrous metal that stands second in the scale of malleability, sixth in ductility, and ranks high in its resistance to corrosion. Aluminium combined with various percentages of other metals forms alloys that are used in aircraft construction.

Aluminium alloys in which the principal alloying ingredients are manganese, chromium, or magnesium and silicon show little attack in corrosive environments. Alloys in which substantial percentages of copper are used are more susceptible to corrosive action. The total percentage of alloying elements is seldom more than 9% or 10% in the wrought alloys.

Aluminium is one of the most widely used metals in modern aircraft construction. It is vital to the aviation industry because of its high strength to weight ratio and its comparative ease of fabrication. The outstanding characteristic of aluminium is its lightweight. Aluminium melts at the comparatively low temperature of 660°C. It is nonmagnetic and is an excellent conductor.

Commercially pure aluminium has a tensile strength of about 90 MPa, but rolling or other cold working processes may noticeably increase its strength. By alloying with other metals, or by using heat-treating processes, the tensile strength may be raised to as high as 550 MPa or to within the strength range of structural steel.

Aluminium alloys, although strong, are easily worked because they are malleable and ductile. They may be rolled into sheets as thin as 40 microns or drawn into wire 0,1 mm in diameter. Most aluminium alloy sheet stock used in aircraft construction range from 0.4 mm to 2,5 mm in thickness; however, some of the larger aircraft use sheet stock that may be as thick as 9,0 mm.

The various types of aluminium may be divided into two general classes: (1) casting alloys (those suitable for casting in sand, permanent mould, or die castings) and (2) wrought alloys (those which may be shaped by rolling, drawing, or forging). Of these two, the wrought alloys are the most widely used in aircraft construction, being used for stringers, bulkheads, skin, rivets, and extruded sections.

### **1.3.1 Cast alloys**

Aluminium casting alloys are divided into two basic groups. In one, the physical properties of the alloys are determined by the alloying elements and cannot be changed after the metal is cast. In the other, the alloying elements make it possible to heat treat the casting to produce the desired physical properties.

A letter preceding the alloy number identifies the casting alloys. When a letter precedes a number, it indicates a slight variation in the composition of the

original alloy. This variation in composition is simply to impart some desirable quality. In casting alloy 214, for example, the addition of zinc to improve its pouring qualities is indicated by the letter A in front of the number, thus creating the designation A214.

When castings have been heat treated, the heat treatment and the composition of the casting is indicated by the letter T, followed by an alloying number. An example of this is the sand casting alloy 355, which has several different compositions and tempers and is designated by 355-T6, 355-T51, or C355-T51.

Aluminium alloy castings are produced by one of three basic methods: (1) sand mould, (2) permanent mould, or (3) die cast. In casting aluminium, it must be remembered that in most cases different types of alloys must be used for different types of castings. Sand castings and die-castings require different types of alloys than those used in permanent moulds.

Sand and permanent mould castings are parts produced by pouring molten metal into a previously prepared mould, allowing the metal to solidify or freeze, and then removing the part. If the mould is made of sand, the part is a sand casting; if it is a metallic mould (usually cast iron) the part is a permanent mould casting. Sand and permanent castings are produced by pouring liquid metal into the mould, the metal owing under the force of gravity alone.

The two principal types of sand casting alloys are 112 and 212. Little difference exists between the two metals from a mechanical properties standpoint, since both are adaptable to a wide range of products.

The permanent mould process is a later development of the sand casting process, the major difference being in the material from which the moulds are made. The advantage of this process is that there is less porosity than in sand castings. The sand and the binder, which is mixed with the sand to hold it together, give off a certain amount of gas that causes porosity in a sand casting.

Permanent mould castings are used to obtain higher mechanical properties, better surfaces, or more accurate dimensions. There are two specific types of permanent mould castings: (1) permanent metal mould with metal cores, and (2)

semi-permanent types containing sand cores. Because finer grain structure is produced in alloys subjected to the rapid cooling of metal moulds, they are far superior to the sand type castings. Alloys 122, A132, and 142 are commonly used in permanent mould castings, the principal uses of which are in internal combustion engines.

Die-castings used in aircraft are usually aluminium or magnesium alloy. If weight is of primary importance, magnesium alloy is used because it is lighter than aluminium alloy. However, aluminium alloy is frequently used because it is stronger than most magnesium alloys.

Forcing molten metal under pressure into a metallic die produces a die-casting and allowing it to solidify; then the die is opened and the part removed. The basic difference between permanent mould casting and die-casting is that in the permanent mould process the metal flows into the die under gravity. In the die casting operation, the metal is forced under great pressure.

Die-castings are used where relatively large production of a given part is involved. Any shape that can be forged can be cast.

### **1.3.2 Wrought aluminium alloys**

Wrought aluminium and wrought aluminium alloys are divided into two general classes: non-heat-treatable alloys and heat-treatable alloys.

Non-heat-treatable alloys are those in which the mechanical properties are determined by the amount of cold work introduced after the final annealing operation. The mechanical properties obtained by cold working are destroyed by any subsequent heating and cannot be restored except by additional cold working, which is not always possible. The “full hard” temper is produced by the maximum amount of cold work that is commercially practicable. Metal in the “as fabricated” condition is produced from the ingot without any subsequent controlled amount of cold working or thermal treatment. There is, consequently, a variable amount of strain hardening, depending upon the thickness of the section.

For heat-treatable aluminium alloys, the mechanical properties are obtained by heat treating to a suitable temperature, holding at that temperature long enough to allow the alloying constituent to enter into solid solution, and then quenching to hold the constituent in solution. The metal is left in a supersaturated, unstable state and is then age hardened either by natural aging at room temperature or by artificial aging at some elevated temperature.

Wrought aluminium and wrought aluminium alloys are designated by a four-digit index system. The system is broken into three distinct groups: 1xxx group, 2xxx through 8xxx group, and 9xxx group (which is currently unused).

The first digit of a designation identifies the alloy type, and it refers to the main alloying element. The second digit indicates specific alloy modifications. Should the second number be zero, it would indicate no special control over individual impurities. Digits 1 through 9, however, when assigned consecutively as needed for the second number in this group, indicate the number of controls over individual impurities in the metal.

The last two digits of the 1xxx group are used to indicate the hundredths of 1% above the original 99% designated by the first digit. Thus, if the last two digits were 30, the alloy would contain 99% plus 0.30% of pure aluminium, or a total of 99.30% pure aluminium. Examples of alloys in this group are:

- 1100 — 99.00% pure aluminium with one control over individual impurities.
- 1130—99.30% pure aluminium with one control over individual impurities.
- 1275—99.75% pure aluminium with two controls over individual impurities.

As mentioned previously, in the 2xxx through 8xxx groups, the first digit indicates the major alloying element used in the alloy as follows:

2xxx—copper

3xxx — manganese

4xxx—silicon

5xxx—magnesium

6xxx — magnesium and silicon

7xxx — zinc

8xxx — other elements

In the 2xxx through 8xxx alloy groups, the second digit in the alloy designation indicates alloy modifications. If the second digit is zero, it indicates the original alloy, while digits 1 through 9 indicate alloy modifications.

The last two of the four digits in the designation identify the different alloys in the group.

Alloy	Percentage of alloying elements (aluminum and normal impurities constitute remainder)								
	Copper	Silicon	Manganese	Magnesium	Zinc	Nickel	Chromium	Lead	Bismuth
1100	—	—	—	—	—	—	—	—	—
3003	—	—	1.2	—	—	—	—	—	—
2011	5.5	—	—	—	—	—	—	0.5	0.5
2014	4.4	0.8	0.8	0.4	—	—	—	—	—
2017	4.0	—	0.5	0.5	—	—	—	—	—
2117	2.5	—	—	0.3	—	—	—	—	—
2018	4.0	—	—	0.5	—	2.0	—	—	—
2024	4.5	—	0.6	1.5	—	—	—	—	—
2025	4.5	0.8	0.8	—	—	—	—	—	—
4032	0.9	12.5	—	1.0	—	0.9	—	—	—
6151	—	1.0	—	0.6	—	—	0.25	—	—
5052	—	—	—	2.5	—	—	0.25	—	—
6053	—	0.7	—	1.3	—	—	0.25	—	—
6061	0.25	0.6	—	1.0	—	—	0.25	—	—
7075	1.6	—	—	2.5	5.6	—	0.3	—	—

Tab. 1.1 – Nominal composition of main wrought alloys used in aeronautic.

### 1.3.2.1 Effect of Alloying Element

#### 1000 series

99% aluminium or higher, excellent corrosion resistance, high thermal and electrical conductivity, low mechanical properties, excellent workability. Iron and silicon are major impurities.

#### 2000 series

Copper is the principal alloying element. Solution heat treatment, optimum properties equal to mild steel, poor corrosion resistance unclad. It is usually clad with 6000 or high purity alloy. Its best-known alloy is 2024.

### *3000 series*

Manganese is the principal alloying element of this group that is generally non-heat treatable. The percentage of manganese, which will be alloy effective, is 1.5%. The most popular is 3003, which is of moderate strength and has good working characteristics.

### *4000 series*

Silicon is the principal alloying element of this group, and lowers melting temperature. Its primary use is in welding and brazing. When used in welding heat-treatable alloys, this group will respond to a limited amount of heat treatment.

### *5000 series*

Magnesium is the principal alloying element. It has good welding and corrosion resistant characteristics. Moderate high temperatures (over 70°C) or excessive cold working will increase susceptibility to corrosion.

### *6000 series*

Silicon and magnesium form magnesium silicide, which makes alloys heat treatable. It is of medium strength, good forming qualities, and has corrosion resistant characteristics. The most popular alloy of the series is 6061.

### *7000 series*

Zinc is the principal alloying element. When coupled with magnesium, it results in heat-treatable alloys of very high strength. It usually has copper and chromium added. The principal alloy of this group is 7075.

### *Hardness Identification*

Where used, the temper designation follows the alloy designation and is separated from it by a dash: i.e., 7075-T6, 2024-T4, and so forth. The temper designation consists of a letter indicating the basic temper that may be more

specifically defined by the addition of one or more digits. These designations are as follows:

F	as fabricated
O	annealed, recrystallized (wrought products only)
H	strain hardened
H1	(plus one or more digits) strain hardened only
H2	(plus one or more digits) strain hardened and partially annealed
H3	(plus one or more digits) strain hardened and stabilized

The digit following the designations H1, H2, and H3 indicates the degree of strain hardening, number 8 representing the ultimate tensile strength equal to that achieved by a cold reduction of approximately 75% following a full anneal, 0 representing the annealed state.

### **Introduction**

The drilling is one of the oldest and well known machining process, as a consequence an enormous number of books and papers have been written on it during the last decades.

Nevertheless, speaking about the drilling of advanced materials in some specific applications, such as aeronautic, the issues arising due to the peculiarities of the materials themselves and, above all, the high standards required, result in the opportunity to carefully define the drilling process in every aspect.

In aeronautic, in fact, the drilling is the fundamental and starting machining operation to realize the assembly. The effectiveness of an assembly made by mean of fasteners is strictly related to the quality of the holes: their accuracy and, if the case, their defects dramatically govern the strength and the efficiency of the assembled structure.

For these reasons, it is mandatory to understand deeply all the concerns in the drilling of a stack of very dissimilar materials, such as CFRP and titanium alloys, in order to drill the parts to be assembled with the highest accuracy.

In this chapter, all the aspects involved in the drilling will be treated with the aim to emphasize the various concerns arising in the drilling of stacks of advanced materials.

### **2.1 The tools**

The tool represents the first and the most important element to take into account.

Several different kinds of tools have been proposed in last year, characterized by different shape and materials, and every time a new tool has been designed and realized with the aim to provide enhanced performances.

In particular, the tools have been proposed to minimize the occurrence of defects in the parts to be assembled.

Looking at CFRP, for instance, the delamination has always represented the most important issue. In order to prevent or minimize this defect, the tools have been designed with specific features, and they look very different from the conventional and well known classical twist tool drill.

In the drilling of metals, on the contrary, other defects can occur, such as the burr. The burr in the drilling of titanium alloys is even more easy to occur due to the specific properties of these materials, first of all the very low value of the coefficient of thermal conductivity, as it will be better explained in the following paragraphs. To this aim, dedicated tools with specific features and, above all, specific materials have been proposed in the recent years.

As a consequence, it is easy to understand how, in the drilling of a stack of these materials, the tool has to have a geometry representing the best possible compromise, having at the same time the task to perform at the best and minimize the defects occurrence in each single material of the stack.

In the next sections of this paragraph, all the aspects of a tool will be discussed, with a special eye on their impact on the quality of the drilling of a stack.

### **2.1.1 Geometry**

The drilling tools are rotary cutting tools, their conventional geometry, reported in the figure 2.1 (a), is made of two main parts: *shank* and *body* sometimes divided by the *neck*, a section of smaller diameter than the shank and body.

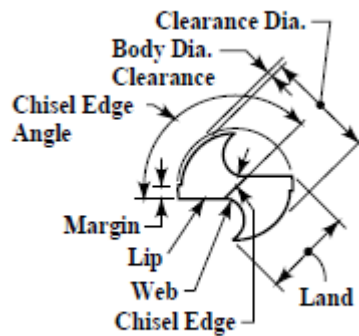
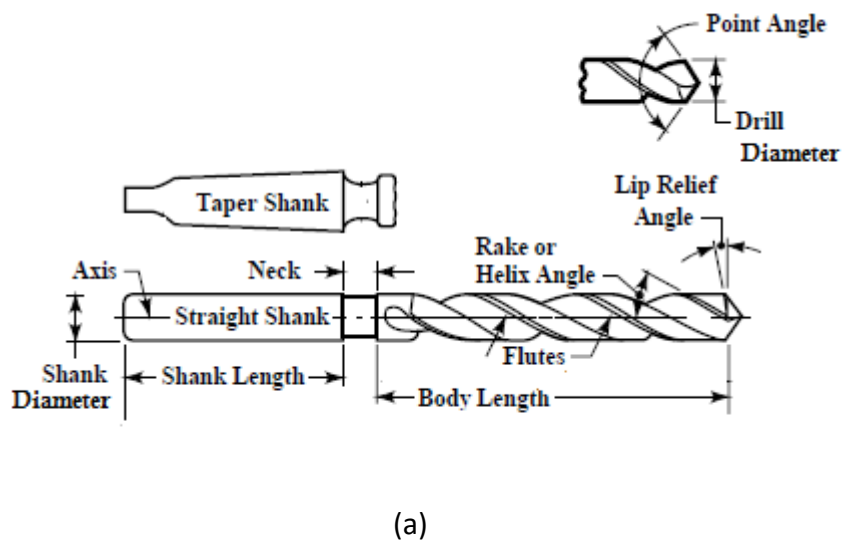


Fig. 2.1 – The geometry of conventional drilling tool (a) side view and (b) frontal view

The *shank* is the part of the drill by which it is held in the spindle. It may be straight or tapered: most have a straight shank. All but the smaller sizes are ground with “back taper,” reducing the diameter from the point toward the shank, to prevent binding in the hole when the drill is worn.

The cylindrical straight shank may be characterized by a same or of a different diameter than the body diameter of the drill and may be made with or without driving flats, tang, or grooves.

The taper shank is preferable to the straight shank for drilling medium and large size holes. The drills having conical shanks are suitable for direct fitting into

tapered holes in machine spindles, driving sleeves, or sockets. Tapered shanks generally have a driving tang, two opposite parallel driving flats on the end of a straight shank, which is the flattened end of a taper shank, intended to fit into a driving slot in the socket.

The *body* is the portion of the drill extending from the shank or neck to the outer corners of the cutting lips or edges. In the following list the nomenclature and the definitions of the main features of drilling tool are reported, shown in the figure 2.1 (a) and (b) (longitudinal and frontal view, respectively) like defined by the American National Standard.

- *Axis* is the imaginary straight line that forms the longitudinal centre of the drill.
- One or more *flutes* are the straight or helical grooves that allow removal of chips and the cutting fluids to reach the cutting edges.
- *Helix Angle* is made by the leading edge of the land with a plane containing the axis of the drill.
- *Lip Relief*, the axial relief on the drill point.
- *Lip Relief Angle* is the axial relief angle at the outer corner of the lip. It is measured by projection into a plane tangent to the periphery at the outer corner of the lip.
- *Point* is the cutting end of a drill made up of the ends of the *lands*, the *web*, and the *lips*. In form, it resembles a cone, but departs from a true cone to furnish clearance behind the cutting edges.
- *Point Angle* is the angle included between the lips projected upon a plane parallel to the drill axis and parallel to the cutting lips.
- *Body Diameter Clearance* is that portion of the land that has been cut away so it will not rub against the wall of the hole.
- *Chisel Edge* is the edge at the ends of the web that connects the cutting lips.
- *Chisel Edge Angle* is the angle included between the chisel edge and the cutting lip as viewed from the end of the drill.

- *Clearance Diameter* is the diameter over the cutaway portion of the drill lands.
- *Land* is the peripheral portion of the drill body between adjacent flutes.
- *Margin* is the cylindrical portion of the land which is not cut away to provide clearance.
- *Web* is the central portion of the body that joins the end of the lands. The end of the web forms the chisel edge on a two-flute drill. In some cases, when web thinning is realized, it is an operation of reducing the web thickness at the point to reduce drilling thrust.
- *Lips—Two Flute Drill* are the cutting edges extending from the chisel edge to the periphery; the drilling tools may be characterized by the presence of the *Lips—Three or Four Flute Drill*, in this case they are the cutting edges extending from the bottom of the chamfer to the periphery.

The drilling tools are classified into three groups, T, M and D, as reported in the figure 2.2 [1] according to the values of helix and point angles. The values of those features depend on the material to work: T group is characterized by the values larger than M and D groups because T group tools are appropriate to drill soft materials like aluminium alloys or copper; M and D group tools are suitable to drill harder material like HSS and titanium alloys.

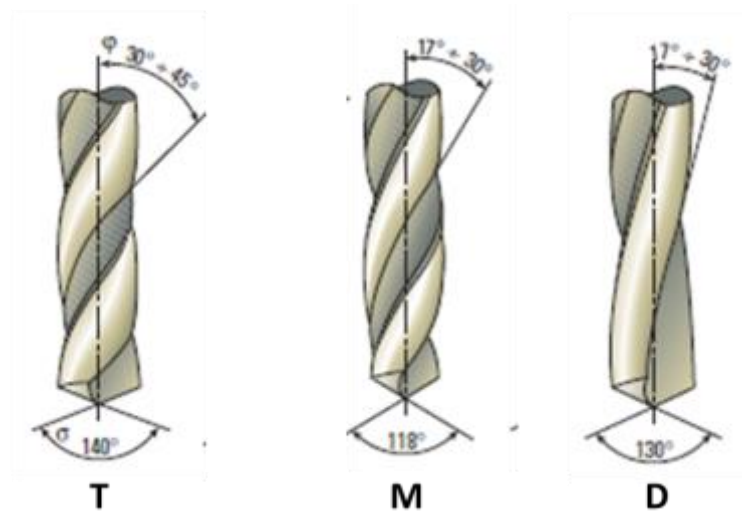


Fig. 2.2 – The classification of drilling tools based on the angle size.

### 2.1.2 Materials

The materials used to realize the drilling tool are mainly steel, High Speed Steel (HSS), sintered metal carbide, covered metal carbide, poly crystalline diamond, cubic boron nitride [2]. Among the sintered metal carbide, the tungsten carbide (WC) in Cobalt (Co) binder is mostly used to machine the titanium and its alloys.

This material, known as hard material, is made by the sintering of grains of Tungsten Carbide in a Co binder; the figure 2.3 shows the  $\alpha$  allotropic form of WC.

The use of this material is due its physical and mechanical proprieties as:

- High compressive strength
- Good abrasion resistance
- High elastic modulus
- Good impact resistance
- High corrosion resistance
- Toughness
- High temperature resistance

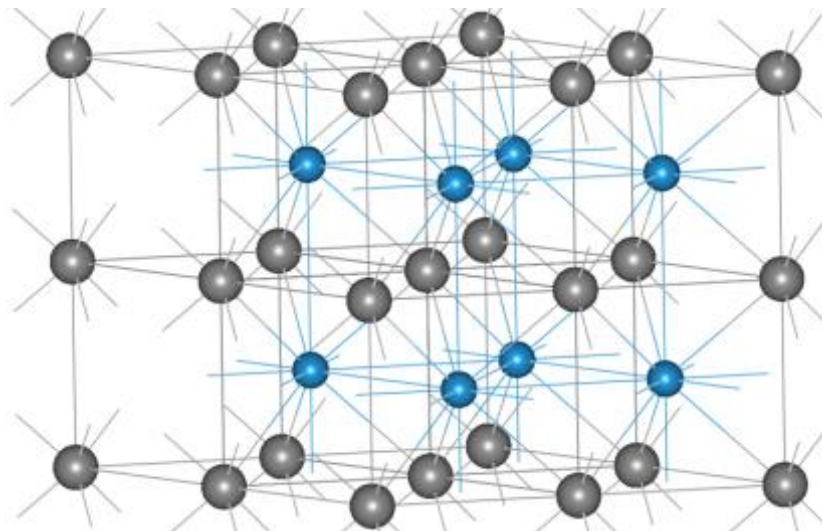


*Fig. 2.3 –  $\alpha$ -WC structure, carbon atoms are grey.*

According to the standard ISO, this material is classified into three main groups, K, M and P, identified with different colors: red, yellow and blue. They differ about the percentages WC and Co, as reported in the table 2.1.

ISO	Chemical composition			Mecanichal property		
	WC [%]	TiC+TaC (NbC) [%]	Co [%]	HRA	Elastic Modulus [GPa]	Color code
<b>K01</b>	97	-	3	93	665	<b>Red</b>
<b>K10</b>	95.5	0.5	4	92.5	630	
<b>K30</b>	92	2	6	91.5	630	
<b>K40</b>	93	-	7	90.5	600	
<b>K50</b>	86.5	0.5	13	89	530	
<b>M10</b>	72	23	5	92.5	-	<b>Yellow</b>
<b>M20</b>	80	12	8	91.5	580	
<b>M30</b>	83	8	9	90.5	-	
<b>M40</b>	75	14	11	90	560	
<b>P01</b>	50	38	12	91.5	-	<b>Blue</b>
<b>P10</b>	50	40	10	91.5	530	
<b>P20</b>	71	20	9	91.5	-	
<b>P30</b>	83	7	10	90.5	560	
<b>P40</b>	77	10	13	90	560	
<b>P50</b>	65	15	20	88	500	

*Tab. 2.1 – Chemical composition and mechanical property of WC-Co.*

Each material is used to realize different drilling tool based on the kind of drill material. The K group is suitable to realize the tools to machine materials that produce short chips as, for example, cast iron or aluminum. The M group is

suitable to machine HSS. Finally, the P group is correct to drill material as stainless steel because produce fluent chips.

The WC is divided into 7 groups based on the dimension of grains:

- Nano  $<0.2 \mu\text{m}$
- Ultra-fine  $0.2 \div \mu\text{m}$
- Submicron  $0.5 \div 0.9 \mu\text{m}$
- Fine  $1.0 \div 1.3 \mu\text{m}$
- Medium  $1.4 \div 2.0 \mu\text{m}$
- Medium Coarse  $2.1 \div 3.4 \mu\text{m}$
- Coarse  $3.5 \div 5.0 \mu\text{m}$
- Extra Coarse  $>5.0 \mu\text{m}$

The figure 2.4 reports the grain observed at the microscope.

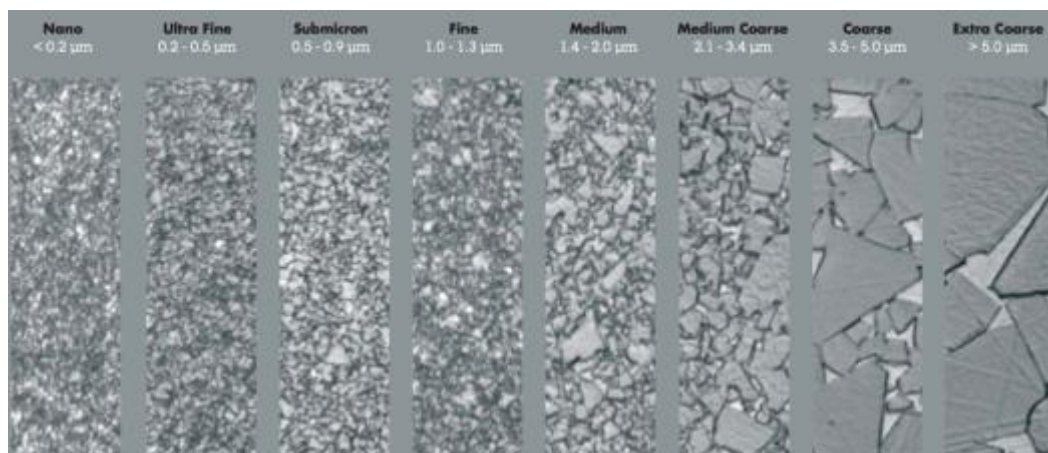


*Fig. 2.4 – Grain size of WC.*

### **2.1.3 Coatings**

There is more and more the need to enhance the manufacturing performance as to improve the mechanical strength and wear resistance. To this aim, the use of the coating is increasingly widespread.

The main materials used as coating are Titanium nitride (TiN), Titanium carbide (TiC), Aluminium oxide (Al<sub>2</sub>O<sub>3</sub>), Titanium carbon nitride (TiCN), Diamond Like Carbon (DLC). They enhance the toughness at high temperature, improve chemical stability with the workpiece, reduce the thermal conductivity, increase the adhesion with the substrate and lower the friction coefficient with the chip.

The thickness of the coating layer has to be very thin: it ranges from 5 to 10 µm to prevent the possibility to detachment of the coating. In some cases, to further enhance the performances of the coating, it is preferable to apply a double or triple layer. Some noticeable examples are:

- Substrate + (TiC) + (TiN)
- Substrate + (TiC) + (Al<sub>2</sub>O<sub>3</sub>)
- Substrate + (TiC) + (Al<sub>2</sub>O<sub>3</sub>) + (TiN)

In the last years, the use of multi layers coating is developing, each single layer having a thickness ranging usually from 2 µm to 10 µm. This allows to increase the hardness: the lower the grain size the higher the hardness of the layer.

Two deposition methods are used to produce thin films and coatings: the Chemical Vapour Deposition (CVD) and the Physical Vapour Deposition (PVD).

CVD is a thermo-chemical treatment and it is based on the chemical reaction among different gases at temperatures higher than 1000°C. This technique is suitable to coat substrates in sintered metal carbide and it allows forming of a homogenous and uniform coating.

PVD is a process in which the material goes from a condensed phase to a vapour one and then back to a thin film condensed phase. It occurs at low temperatures, about 500°C and it is suitable to coat tool in HSS, and with a very sharp shape (like twist drilling tool and milling tool) since it allows minimizing the distortion of the tool during the cooling phase.

## 2.2 Issues in drilling of materials

Different issues occur in drilling of the different materials since they depend on the nature of the material. For this reason, it is appropriate to define the issues in drilling of each material as reported in the following paragraphs.

### 2.2.1 Issues in drilling of CFRP

As mentioned in the previous chapter, the CFRP is a multi-phase material characterized by a given number of layers but, above all, it is an anisotropic material. The figure 2.5 shows the main features of a plate of CFRP: it is made by stack of several plies with fibres disposed with different angles; each layer has an average thickness of 0.25 mm and each fiber has a diameter of  $5 \div 10 \mu\text{m}$ .

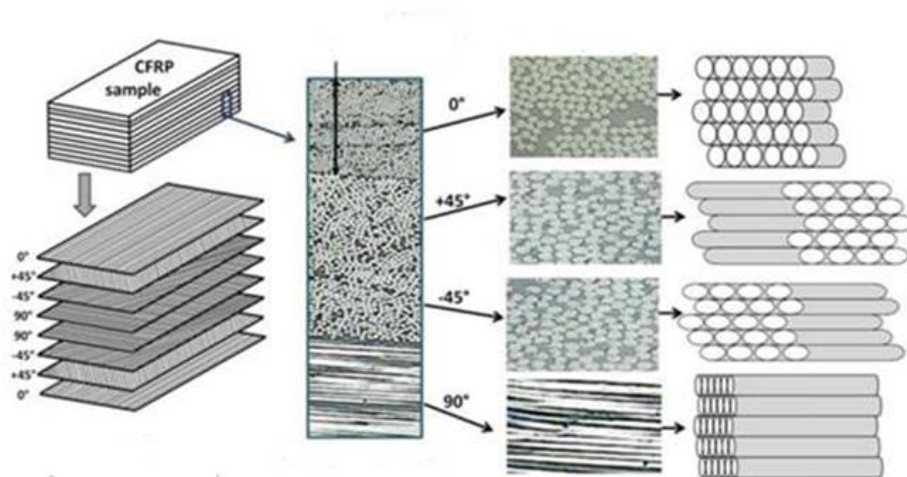
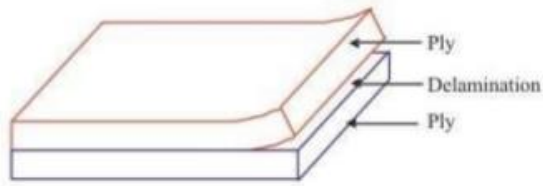


Fig. 2.5 – The main features of CFRP.

For its nature, some defects can occur during drilling of CFRP as the *delamination* and *pull-out*.

The delamination (figure 2.6) is the separation of the adjacent plies due to the failure of their interface. Its extension is measured as the difference between the maximum diameter of the damage zone ( $d_{\text{max}}$ ) and hole nominal diameter ( $d_{\text{nom}}$ ).



*Fig.2.6 – The sketch of the delamination.*

A skilled operator can easily detect the delamination and its entity via visual inspection (looking only at the external surfaces) or with an ultrasonic control. The figure 2.7 reports an image CFRP hole in which the defect of delamination is appreciable and quantifiable.

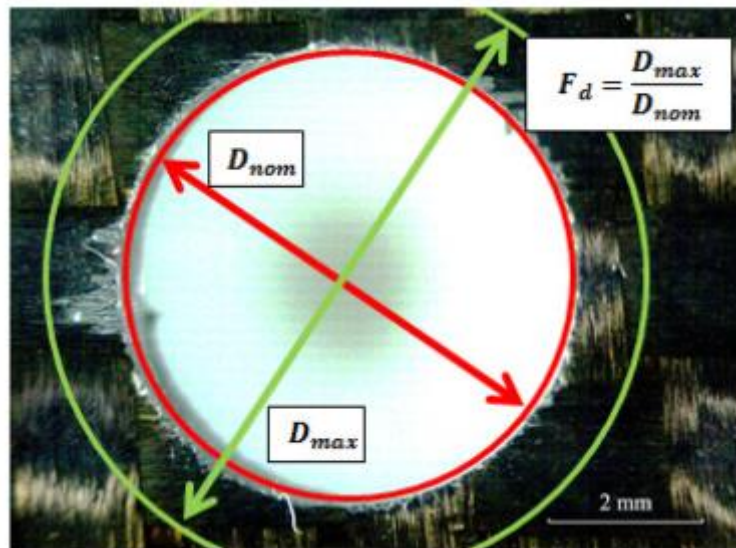


*Fig. 2.7 – Extension of the delamination of the CFRP hole.*

This defect preferentially occurs in external layers, both at the entry side of the tool and at the exit one, as shown in the figure 2.8. in the former case, it is named peel-out, in the latter is named push down.

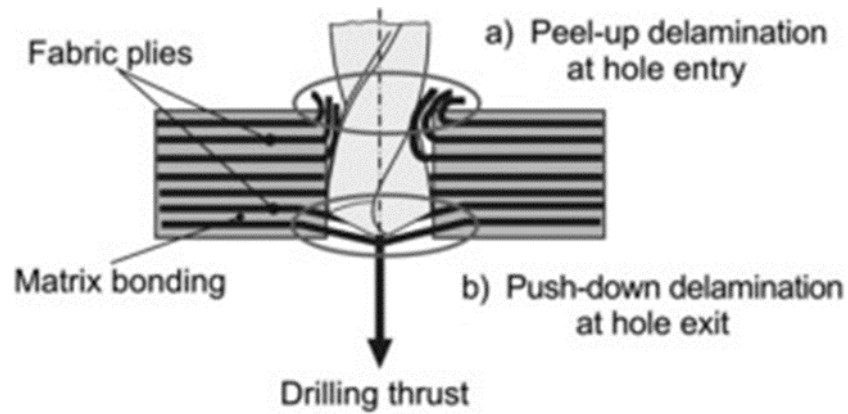


Fig. 2.8 – Delamination in entry and exit hole.

The pull-out (figure 2.9) is a defect that occurs in the borehole; it consists in uncut fibres that come out from the matrix.

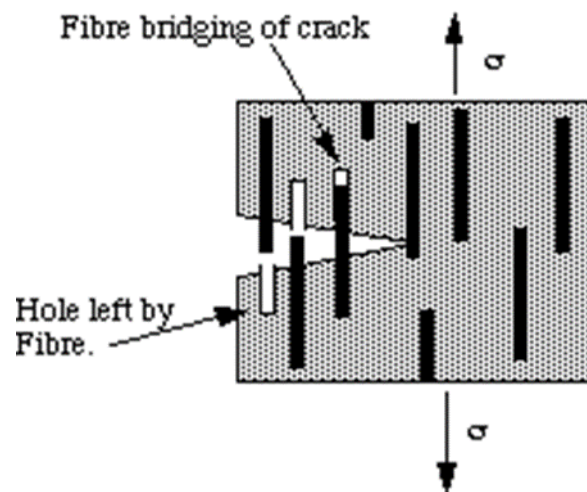
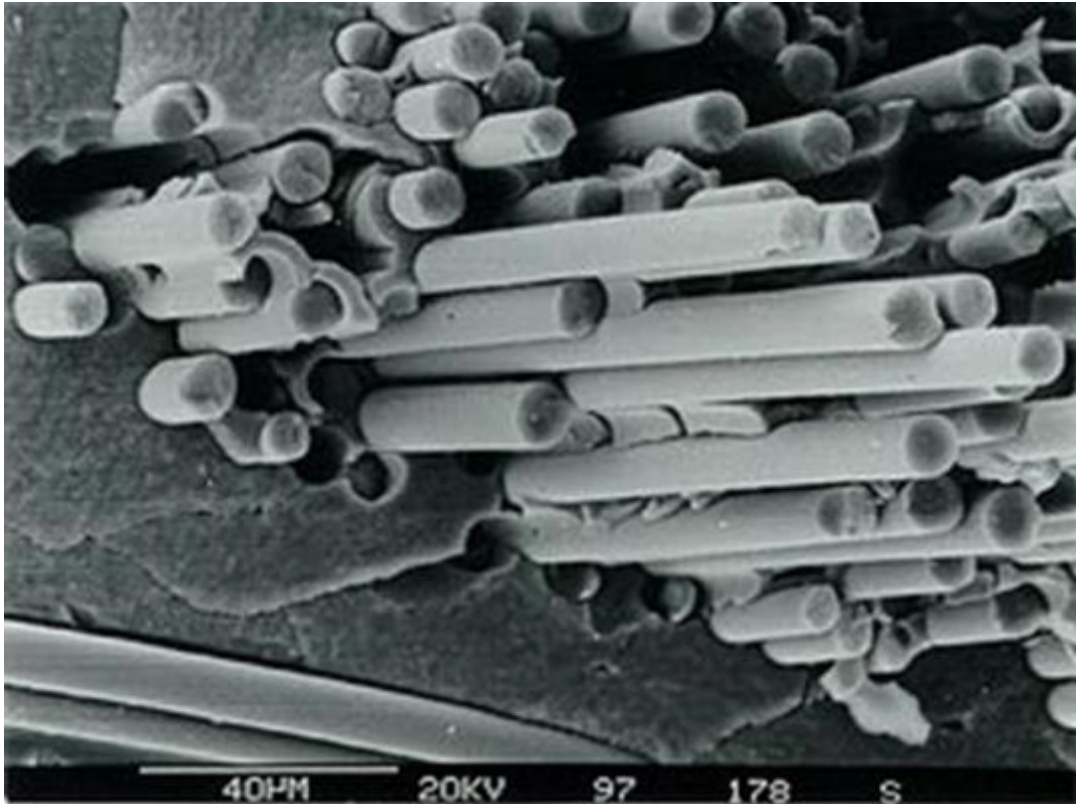


Fig.2.9 – Defect of CFRP borehole: Pull – out.

This defect can be observed only through an accurate inspection of the borehole with a microscope. The figure 2.10 shows an image of CFRP borehole acquired at SEM microscope.



*Fig. 2.10 – SEM image of pull-out in CFRP borehole.*

### **2.2.2 Issues in drilling of titanium alloys**

As described in the previous chapter the titanium is a metal characterized by low values of elastic modulus and coefficient thermal conductivity if compared to the steel.

Due to the low value of elastic modulus, in machining and especially in drilling, part of the thrust forces put to work the titanium sheet are spent to deform the workpiece. This results into a change of the angle between the cutting edge and the surface of the material; this leads to an increase of friction and, as consequence, in an increased amount of heat in the cutting zone. Due to the low value of the coefficient of thermal conductivity, this amount of heat remains confined in the cutting zone. The effect is hence a rise of the cutting temperature. The most of the heat goes away with the chip.

The hot chip can either attach to the tip of the tool (resulting in the so called built up edge) and damage the borehole during its evacuation, mainly on the CFRP borehole, since the matrix is noticeable softer than the chip itself.

Furthermore, the built-up edge, changing the shape of the cutting edge, results in a worsening of the chipping mechanism and the hole quality decay more and more.

Finally, the low value of the coefficient thermal conductivity involves also the defect of burr, a plastic deformation of the material that occurs at tool exit side. The figure 2.11 illustrates the stages of the formation of the burr: when the drilling tool approaches the bottom of the material (Initiation), the friction development and the heat generation result in a cutting temperature rise because the material become thinner and thinner (Development). Consequently, the material softens and, instead of being cut, deforms plastically until to the fracture (Initial fracture).

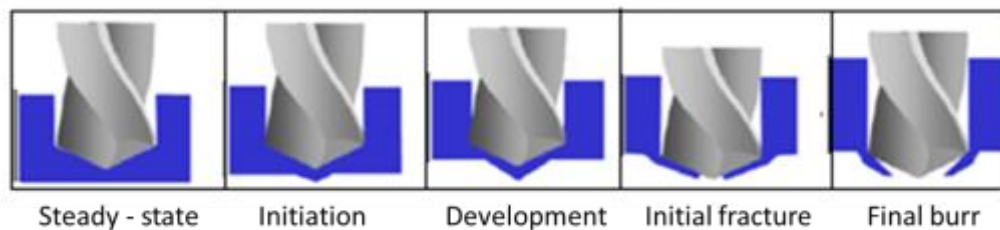


*Fig. 2.11 – The stages of burr formation.*

The entity of the burr is defined as the height of the maximum peak of the burr itself along the hole circumference at the exit side of the tool.

It is an important output and a threshold value is defined as acceptance limit. In fact, if the burr height overcomes this value, part of the tightening torque imposed on the fasteners is spent to deform the burr. For this reason, a given acceptable value of the maximum burr height has to be defined: above this value, the clamping pressure loses effectiveness.

### 2.2.3 Issues in drilling of CFRP-Ti stacks

The issues in the drilling of a stack of dissimilar materials are not simply the sum but a kind of combination of the issues concerning the drilling of the single material. They don't depend only on the materials but also on the stacking sequence.

In the case under investigation in the present research, i.e. on a stack of CFRP and Ti6Al4V, there are only two possible stacking sequences: CFRP in top and Ti6Al4V in bottom in figure 2.12 (a) and vice versa in figure 2.12 (b).

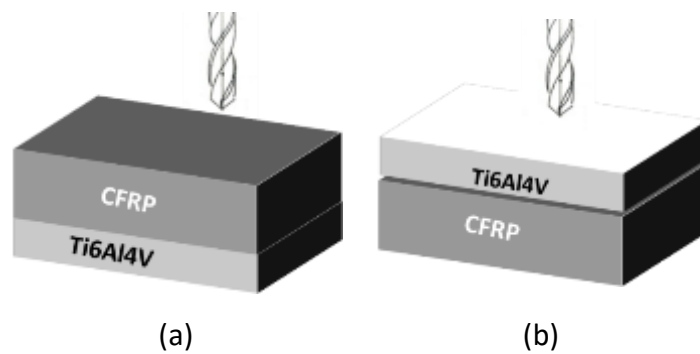


*Fig. 2.12 – Stacking sequence (a) top CFRP and bottom Ti6Al4V or (b) top Ti6Al4V and bottom CFRP.*

The presence of the CFRP on the top of the stacking sequence (fig. 2.12 (a)) is preferable for two main reasons. The former since the push-down, i.e. the delamination in exit hole of CFRP, is reduced due to the titanium in bottom that acts as a support. The latter because the BUE (see previous paragraph) is reduced since the formation of the BUE at the drilling of the previous hole is smoothed by the uncut abrasive carbon fibres during the drilling of the successive hole. The drawbacks are the damages that can occur in the CFRP borehole due to the evacuation of the sharp and hot chips of titanium.

Vice versa the presence of the titanium at the bottom involves a better borehole quality of CFRP due to the fact that the titanium chip does not go through the CFRP borehole but, at the same time, the burr formation of exit hole of titanium causes the change of the shape of CFRP top.

### **2.3 Strategies and cutting fluids**

The difficulty to break and remove the chip, the generation of the excessive heat and the related rise of the temperatures, are the most important factors affecting the efficiency and the productivity of the drilling.

Different methods, i.e. hot machining, high-pressure coolant application, application of minimum quantity lubrication (MQL) have been tried by researchers to enhance machining performance. Among these methods, the use of the peck drilling strategy and the application of the cutting fluids are included. A peck drilling strategy, i.e. a stepwise strategy, can be adopted to both facilitate the chip break and removal and to reduce the cutting temperatures.

In each single step, the tool plunges in the workpiece up to a given depth and then it is retracted by the workpiece. This action is repeated step by step, the tool goes deeper and deeper, until the hole is finished.

There are two kind of peck strategies: the fixed position pecking and the adaptive pecking. The former involves the repeating of the pecking movements to a specified and fixed step set up by the computer numerical control (CNC) machine; the application of the latter method involves the switching of the tool to Z-axis extraction when the difference between the cutting torque at the hole entrance and the actual cutting torque exceeds a given and predetermined allowable difference. This second method can be used only if drilling torque and forces are monitored during the process. In this case, the adaptive system executes pecking only when chips over-accumulate during cutting, thus reducing the number of pecks in order to reduce power consumption.

The application of the cutting fluids plays a very important role in machining operations, particularly in cutting of the metal. It can increase the tool life and dimensional accuracy, decrease cutting temperatures, improve surface roughness and finally reduce power consumption.

Their purposes are mainly two: the cooling, since they reduce the cutting temperature, and the lubrication, since they decrease the friction between the tool, the chip and workpiece.

Yildiz and Nalbant's studies [3] concerned the cutting fluids carrying out an in-deep study about cryogenic coolant and their application. Based on their studies conventional cutting fluids are classified into two groups, as reported in figure 2.13. Water-soluble fluids are preferable for operations where cutting speeds are very high and pressures on the tool are relatively low. Neat cutting oils are straight mineral oils, or mineral oils with additives. They are preferred when cutting pressures in the interface chip and tool are very high and where the primary consideration is lubrication. Some researches proved that cutting fluids cannot penetrate the chip–tool interface at high-cutting speeds.

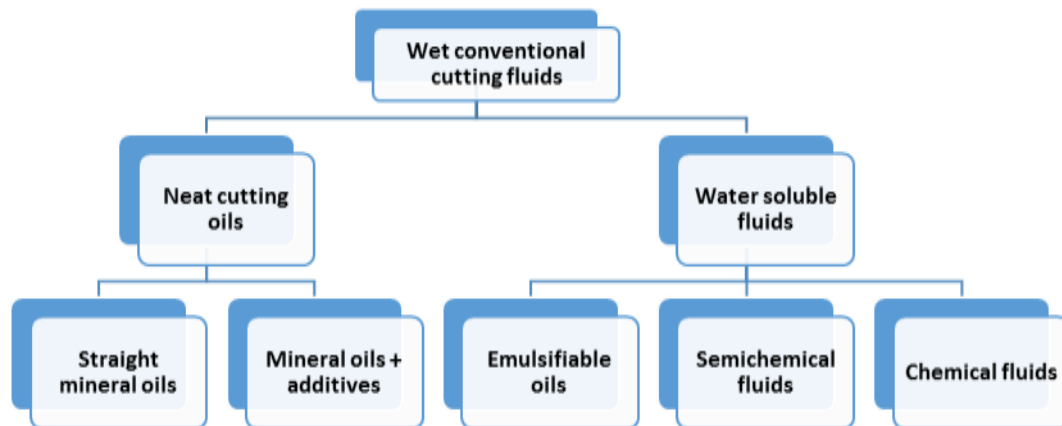


*Figure 2.13 – Conventional cutting fluids.*

On the other hand, the application of conventional cutting fluids in industry involves several health and environmental problems. Environmental pollution due to chemical degradation of the cutting fluid at high temperature; water pollution and soil contamination during their ultimate disposal; biological (dermatological) ailments to operator's health coming in fumes, smoke, physical contact, bacteria and odours with cutting fluid; requirement of extra floor space and additional systems for pumping, storage, filtration, recycling, chilling, etc. For example, according the statistical data of 2002 [4], total environmental expenditure of Turkey was \$402,947,766. There were 272,482 firms in

manufacturing industry in the same year. If each of these firms had one machine (lathe or mill) and if each of these machines held 100 L of cutting fluid, tons of waste cutting fluid must have released to environment.

It is mandatory to use an environmentally acceptable coolant in manufacturing industry. For this purpose, liquid nitrogen as a cryogenic coolant has been explored since the 1950s in metal cutting industry. The cryogenic cooling consists in the application of gases during the machining at very low temperature, below boiling point.

Uehara and Kumagai's studies [5,6] have pioneered to today's cryo-machining works. Their experimental findings were considerable in terms of machining performance. The subject has been further studied in different views and gaining interest due to its remarkable success on machinability. From the machining tests and cost analysis in a study, the following advantages of cryogenic cooling over conventional emulsion cooling were determined such as longer tool life, better chip breaking and chip handling, higher productivity, lower productivity cost, better work surface finish, environmentally safer, healthier for the worker.

The main gases used are helium, hydrogen, neon, nitrogen, oxygen, normal air at cryogenic temperature. Liquid nitrogen is the most commonly fluid used in cryogenics. It is produced industrially by fractional distillation of liquid air and is often referred to by the abbreviation LN<sub>2</sub>. Nitrogen melts at 210.01 °C and boils at 198.79 °C; it is the most abundant gas, it is a colourless, odourless, tasteless and non-toxic gas. These characteristics of liquid nitrogen have made it as a preferred coolant.

The methods to supply the cutting fluids in general could be classified into four groups (fig. 2.14):

1. *pre-cooling*;
2. *treatment*;
3. *indirect cooling*;
4. *spray or jet cooling*.

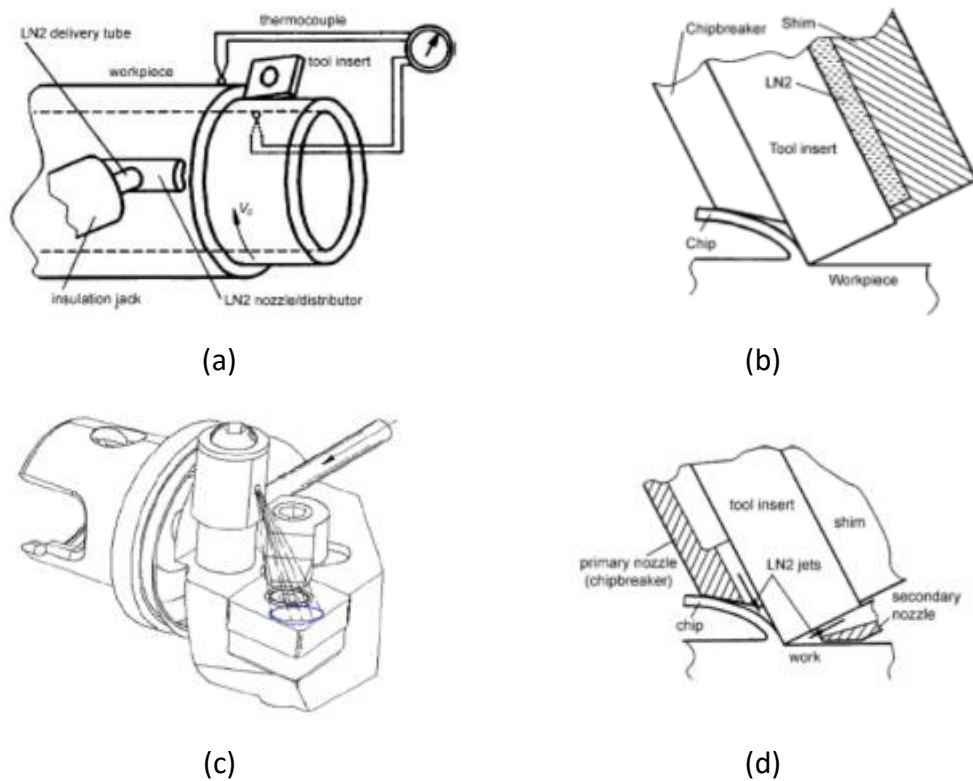


Fig. 2.14 – Supply method of the cutting fluids (a) Pre-cooling, (c) Indirect cooling, (c) Spray cooling, (d) Jet cooling.

The first and the second are suitable mainly to cryogenic cooling; indirect cooling and jet cooling for application of both kinds of cutting fluids.

In the *cryogenic pre-cooling* the workpiece is cryogenically cooled with an enclosed bath or general flooding. The aim is to cool workpiece in order to change from ductile to brittle the mechanical behaviour of the material. This method supports the break of the chip but may be impractical in the production line and negatively increase the cutting force and the abrasion; in addition, they can cause dimensional change of the workpiece and huge liquid nitrogen consumption.

The *cryogenic treatment* is a process similar to heat treatment. In this method, the parts are cooled down to cryogenic temperature and maintained at this temperature for a long time and then heated back to room temperature to improve their wear resistance and dimensional stability. However, the effectiveness of the cryogenic treatment can vary according to the different

machining processes and cutting conditions. To author's knowledge, however, scientific literature suffers the lack of a comparison between this cooling technique and the others.

The *indirect cooling*, also called cryogenic back cooling or conductive remote cooling. Looking at the couple tool-workpiece, the aim is to cool the fixed one through heat removal, via conduction, from a cutting fluid chamber located on it. In other words, the cutting fluid is not supplied to the contact area between the tool and the workpiece, it doesn't cause significant change in properties of the workpiece, furthermore the cooling effect is stable. However, the effect of this approach is highly dependent on thermal conductivity of the cooled material, its thickness and the distance from the cutting fluids source to the highest temperature point at the cutting edge. To author's knowledge, however, relevant scientific results have been proposed only in the case of turning by Evans et al. [7,8].

The objective of the spraying and jet cooling is to cool directly the cutting zone, particularly the tool-chip interface. In the former method, the tool-chip interface is cooled spraying the fluids on the cutting zone; in the latter method, the cooling of the tool-workpiece interface is provided by the coolant flooding, supplying it through one or more external nozzles, or injecting cutting fluids in the coolant channels of the tool.

In the spraying and flooding coolants, the consumption of the cutting fluids could be high. This is even more true in the case of cryogenic coolant since the cryogenic gases, like LN<sub>2</sub> for instance, cannot be circulated inside the machine like the conventional cooling fluids. In this way, the cryogenic gases are released into normal atmospheric pressure, absorb heat during the cutting process and they quickly evaporate.

There are several advantages when the cutting fluids are supplied through the coolant channels. The cooling power is not wasted on any unnecessary area and thus workpiece will stay at constant temperature and will not be subjected to dimensional inaccuracy and geometrical distortion. This localised cryogenic

cooling reduces the tool face temperature, enhances its hardness, and so reduces its wear rate; this approach also embrittles the chip by cold temperature.

Furthermore, this approach eliminates the BUE problem on tools because the cold temperature reduces the possibility of chips welding to the tool and the high pressure of the cryogenic jet also helps to remove possible BUE formation, therefore it will produce better surface quality.

3. The drilling of stacks comparison between Wet and Cryogenic conditions
- 

### 3. Material & Methods

This chapter illustrates the first phase of the research activity of this thesis, which has been partially carried out in the TU Chemnitz laboratories under the supervision of Dr. Dix. The drilling tools used were provided by HTT srl, an Italian company that produces drilling tools for important company as Leonardo®. The main geometric characteristics of the tools and their materials will be shown in details. The workpieces were provided by Leonardo®, an Italian company that realizes parts of aircraft for other companies as The Boeing Company.

The first experimental campaign was carried out in order to establish the influence of the process condition as the working parameters and the influence of cutting fluids, i.e. conventional lubricant (in the following named “wet condition”) and cryogenic coolant (in the following named “cryogenic conditions”). The recorded outputs have been the thrust force and torque diagrams, the hole diameters and the burr height. The former to investigate the tool wear in indirect way and the latter in order to define the influence of the cutting conditions on the hole quality.

The tool wear was studied using an indirect method, as mentioned before, in according to the procedure proposed by Rawat and Attia [9]. They examined the wear mechanisms of WC tools during dry drilling of woven carbon fibre reinforced composites and found that both the thrust force and cutting force ( $F_c$ ) increase with the increase in flank wear and, as consequence, the hole quality gets worse. Thrust force was found to be higher than the cutting force in the primary and the secondary wear regions. However, in the tertiary wear region, the cutting force increases beyond the thrust force. This is likely due to the high temperature built up on the tool with continuous drilling at such high speeds [9]. The increase of cutting force implicates the increase of torque ( $M$ ) for the relationship  $M = F_c \cdot b$  where  $b$  depends on the diameter of the tool.

Fernandes and Cook [10] focused their studies on drilling of CFRP and CFRP stacks and found that thrust force and torque increase with increasing of feed, but correlated to drill tool, thickness of workpiece and tool wear, too.

The investigation reported by Sushinder et al. [11] on drilling of Ti6Al4V using WC tool at various cutting speed resulted in thrust force and torque higher at low cutting speed due to higher resistance to plastic deformation. A material with low thermal conductivity like titanium deforms easily at higher cutting speeds and thermal softening effects dominate.

### 3.1.1. The used tool

The cutting tool used in the first phase of this experimental analysis, named K1R, was made of sintered tungsten carbide (WC) in a cobalt (Co) binder and coated with Diamond-Like Carbon (DLC). The drill tool was made using WC particles of an average size of  $0.5\ \mu\text{m}$  (micro-grain according to the definition provided in the previous chapter) and a percentage of 5.0% of Co. K1R was a short drill tool characterized by a diameter of 7.94 mm and a body length of 34 mm with a point angle of  $150^\circ$ , it was made with the presence of a countersink angle of  $100^\circ$  as shown in figure 3.1. A drill is defined short when the length to diameter ratio is lower than 5.

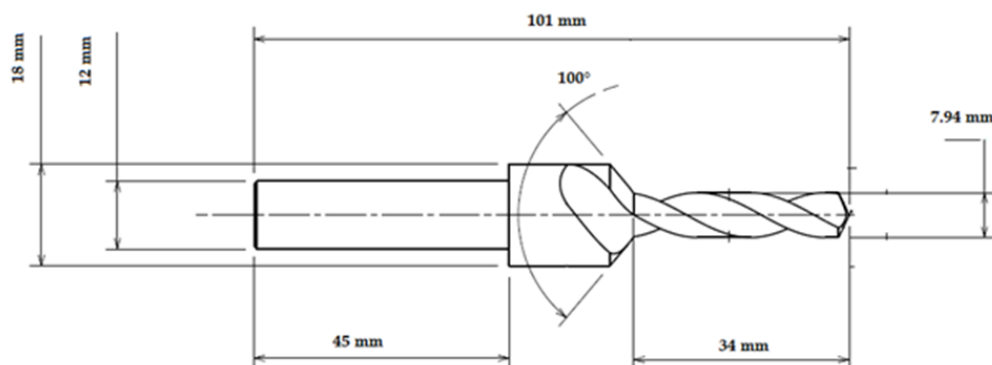


*Fig. 3.1 - Geometry of tool K1R.*

The tool has two coolant channels, so the cooling method used is the jet one, as described in the previous chapter.

### 3.1.2. The workpieces

The CFRP/Ti6Al4V stack used in the experiment was composed of CFRP laminate puts on Ti plate. The CFRP laminate was made of woven carbon fabric of 200 g/m<sup>2</sup> in an epoxy matrix with full thickness of 18 mm. The titanium plate used in the experiment was Ti6Al4V with thickness of 10 mm. Both materials were cut by means of an abrasive water jet. The workpieces were provided by Leonardo® and they are the materials used to realize the BOEING 787.

This stacking sequence, CFRP on top and Ti6Al4V on bottom, has been chosen since it represents the real case to face. As in fact, on the aircraft, the CFRP is the outside of the fuselage and titanium parts are inside and it is not possible to put the drilling machine inside the fuselage.

The samples used for the wet and cryogenic drilling were made by the same material and thickness but they differ in the shape. A square specimen of CFRP laminate laid on the top of the Ti6Al4V plate of the same size (300mm x 300mm) was drilled on wet condition. The figure 3.2 shows the workpiece fixed on the worktable of the drilling machine.

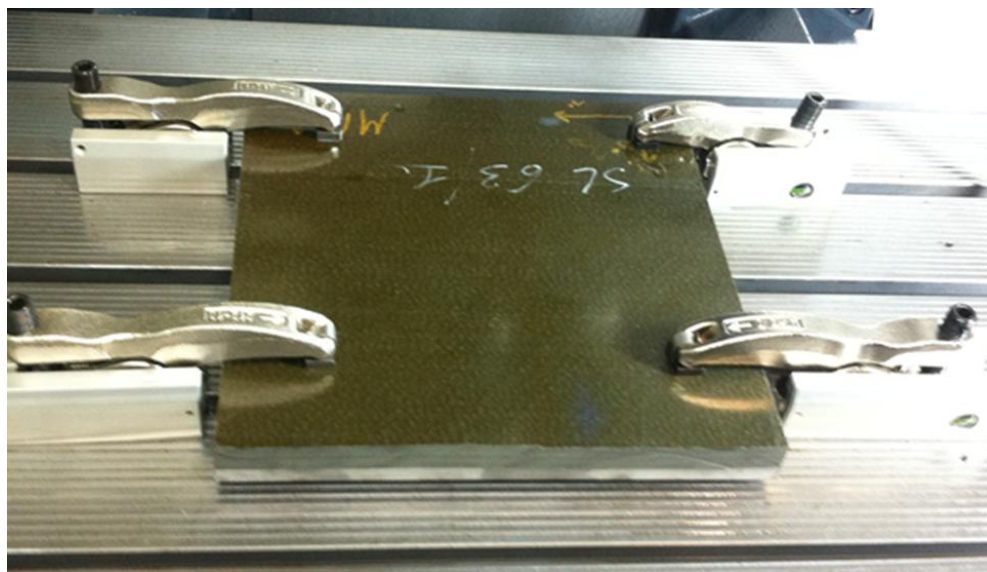


*Fig. 3.2 – Sample for wet drilling.*

The samples used for the cryogenic drilling were cylinders with 30 mm of diameter. The figure 3.3 shows the sample before (a) and after (b) the drilling. In this case, the two materials were joined mechanically using stainless steel bolts. The difference is due to the different ways used to perform the tests as it will be described in the following.

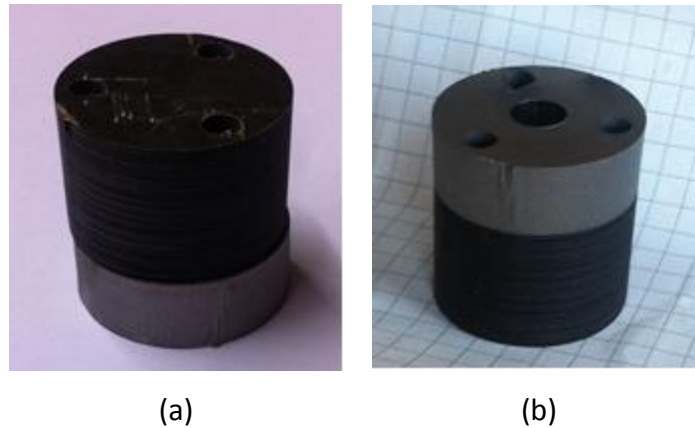


*Fig. 3.3 – Sample for cryogenic drilling (a) before and (b) after the drilling.*

### **3.1.3. Drilling machine**

The drilling tests were performed on a conventional Computer Numerical Control (CNC) machine DMC 850 V (figure 3.4), a 3-axis machine with a work volume of 850 mm X-axis, 520 mm Y-axis and 475 mm Z-axis.



*Fig. 3.4 – CNC machine DMC 850 V.*

It is not equipped to drill in cryogenic condition so it was adapted for the scope. As in fact, while in wet condition the workpiece was conventionally clamped on the worktable, in cryogenic drilling the tool was fixed on the worktable (fig.3.5) and the workpiece was clamped by drill chuck taking the necessary shape. In this way, the spindle speed and the feed were given to the sample. This has been forced by the need to supply liquid nitrogen through tool coolant channels: clamping the tool on the worktable, it is easy to supply the cutting fluid using a flexible pipe (see bottom side of fig. 3.5) attached to a LN<sub>2</sub> tank independent by the CNC machine.



*Fig. 3.5 – Set up cryogenic drilling.*

#### **3.1.4. Process conditions**

The CFRP laminate was always drilled using the same working parameters: 3560 RPM and feed rate of 630 mm/min, independently by the cooling conditions.

Conversely, four drilling conditions were used to work titanium for both cooling conditions, as reported in the following lists:

- 700 RPM and 30 mm/min
- 700 RPM and 70 mm/min
- 995 RPM and 30 mm/min
- 995 RPM and 70 mm/min

The lowest values were suggested by Leonardo® Company being the conventional parameters used in their process. The highest values were suggested by Dr. Dix of TU Chemnitz based on his experience.

A drilling strategy with fixed position pecking was used to drill the titanium in order to facilitate the chip removal and to reduce the cutting temperature. A peck value of 1.00 mm was chosen as suggested by Dr. Dix instead of 0.5 mm as proposed by Leonardo® Company. In this way, the number of pecks is reduced to drill the stack with a number of 10 pecks and a final peck of 3 mm to conclude. The drilling experiments consisted of 40 holes: 20 holes in wet conditions and 20 holes in cryogenic coolant, i.e. five replicates for each set of parameters.

### **3.1.5. Measuring instruments**

The experimental investigation was carried out through the study of the thrust force and torque acquired during drilling and the analysis of hole quality. This quality has been evaluated by burr height and hole diameter measurements. A Kistler® 9170A dynamometer was used to acquire the thrust force and torque, a diameter digital gauge to measure hole diameter and conventional digital gauge to measure the burr height, both made by Mitutoyo.

A rotating 4-component dynamometer Kistler® 9170A (fig. 3.6) was used to acquire the thrust force and torque during the drilling. Energy and measured values are transmitted on a non-contact basis. A data acquisition software was used to record the data. The complete measuring system comprises a rotor, stator, connecting cable and signal conditioner. The spindle type on the machine tool determines which rotor version is required. The piezoelectric 4-component sensor, four charge amplifiers and the digital transmission electronics are integrated into the rotor. It measures the radial forces  $F_x$  and  $F_y$ , the axial force  $F_z$  and the torque  $M_z$ .



*Fig. 3.6 – Dynamometer Kistler®.*

The hole diameters were measured with a Mitutoyo® Absolute digital shown in figure 3.7.

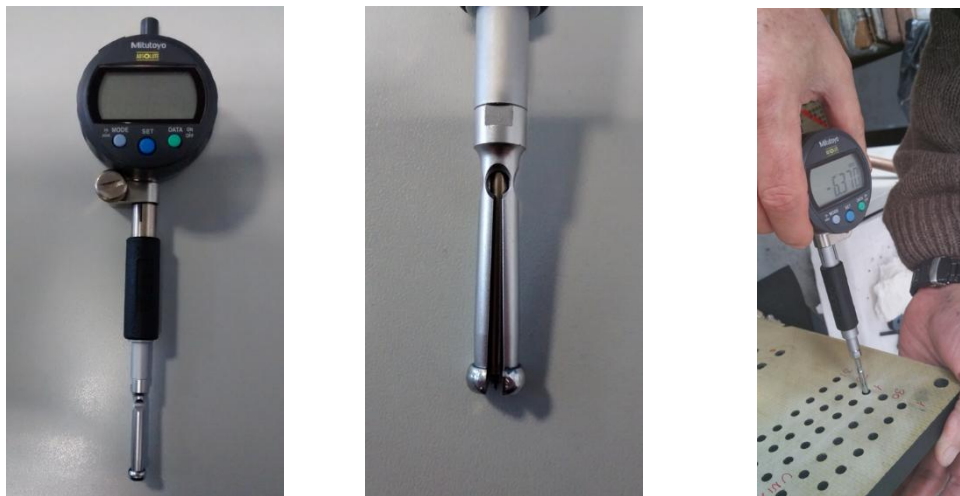


*Fig. 3.7 – Mitutoyo® Absolute digital*

The measure of the burr height was carried out with the instrument shown in the figure 3.8 Mitutoyo® Absolute. The three-points instrument is put on the specimen with the three points disposed around the hole to measure. A little disc belonging to the moveable part of the gauge (with a diameter slightly higher than the diameter of the hole to measure and laying on a plane parallel to the

three points plane), is put on the top of the burr to be measured: the measure consists of the distance between the three points plane and the plane of the disk. In this way, the burr height is defined as the height of the highest peak of the burr profile.

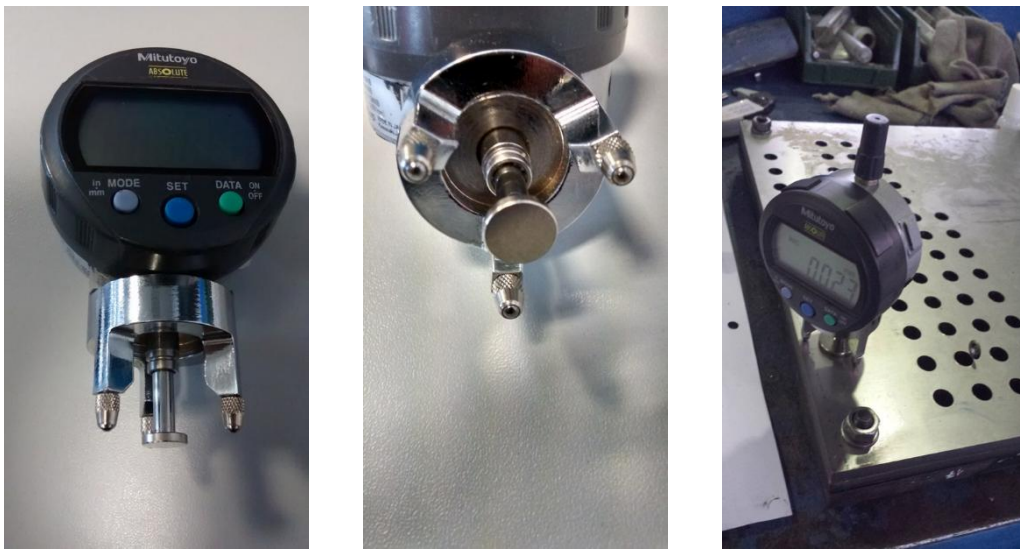


*Fig. 3.8 – Mitutoyo Absolute digital gauge.*

Finally, the tool wear has been considered too. Due to the well-known difficulties to carefully measure it, it has been decided to measure it indirectly, taking into account both thrust force and torque growth, according to the same procedure proposed by Rawat and Attia [9].

### **3.2. Results & discussions**

In the following sections the main results of this first experimental campaign will be given and deeply discussed.

As a result, we will be able to define the best procedure (i.e. the best cooling condition and the best set of process parameters) that can allow to make the hole with the best quality.

### 3.2.1. Thrust forces

The figure 3.9 shows the typical trend of the thrust force acting along the longitudinal axis Z acquired during the realization of one hole.

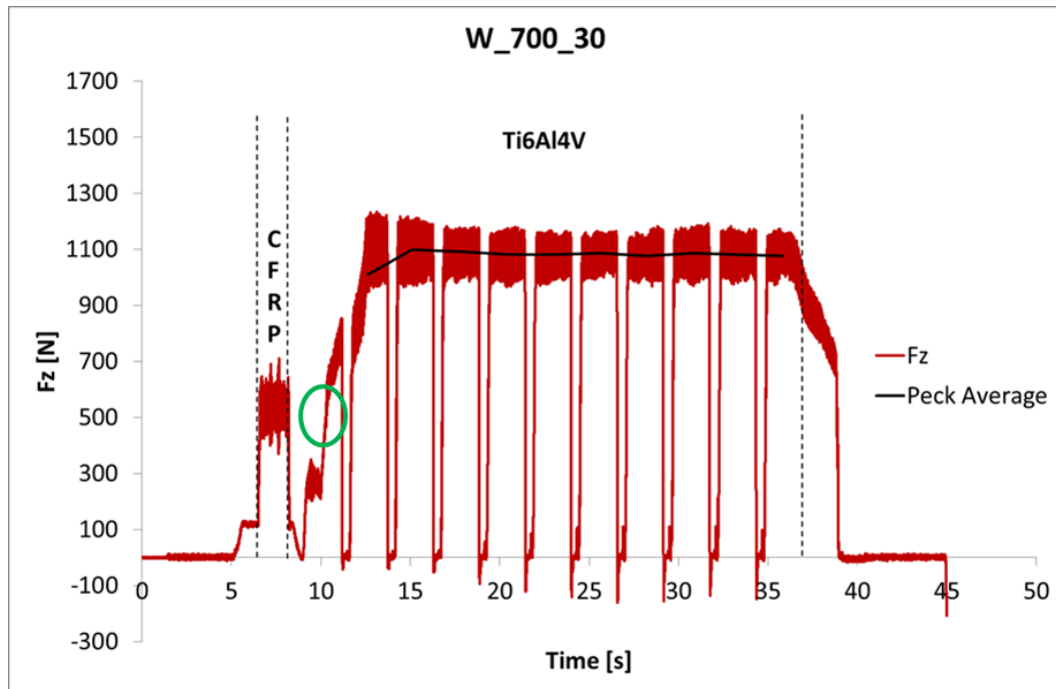


Fig. 3.9 – A typical trend of thrust force.

This graph shows two phases: the former regarding the drilling of CFRP and the latter the drilling of Ti6Al4V.

As reported in the previous paragraph, the CFRP drilling consists of a single step; the working parameters were the same in all diagrams and, as consequence, the values of the acquired forces are always the same.

Due to the peck strategy adopted in the drilling of Ti6Al4V, the force diagrams are characterized by 11 pecks. The black continuous line represents the medium force values calculated on each peck of force trend, respectively.

It may be noted that the first peck of Ti6Al4V drilling is lower than the following pecks; this difference is due to various causes:

- During the first peck in titanium sheet the tool is still partially working on CFRP since at the end of the first phase only the chisel edge arrived at the

bottom surface of the CFRP; as a consequence, during the first peck in Ti6Al4V the tool completes the drilling of CFRP, with the cutting parameters used for titanium, and begins to drill titanium.

- When the tool comes into contact with the titanium sheet a certain instability occurs causing the increase of tool vibrations [12]. This phenomenon implicates an abrupt discontinuity in both the recorded force and torque, as emphasized in green circles reported in fig. 3.9.
- The tool went through the clearance between the two materials for the not perfect coupling of the two plates.

The figures 3.10 and 3.11 show the thrust force trend acting along the longitudinal axis Z acquired during drilling of each single set of parameters under Wet and Cryogenic cooling conditions, respectively.

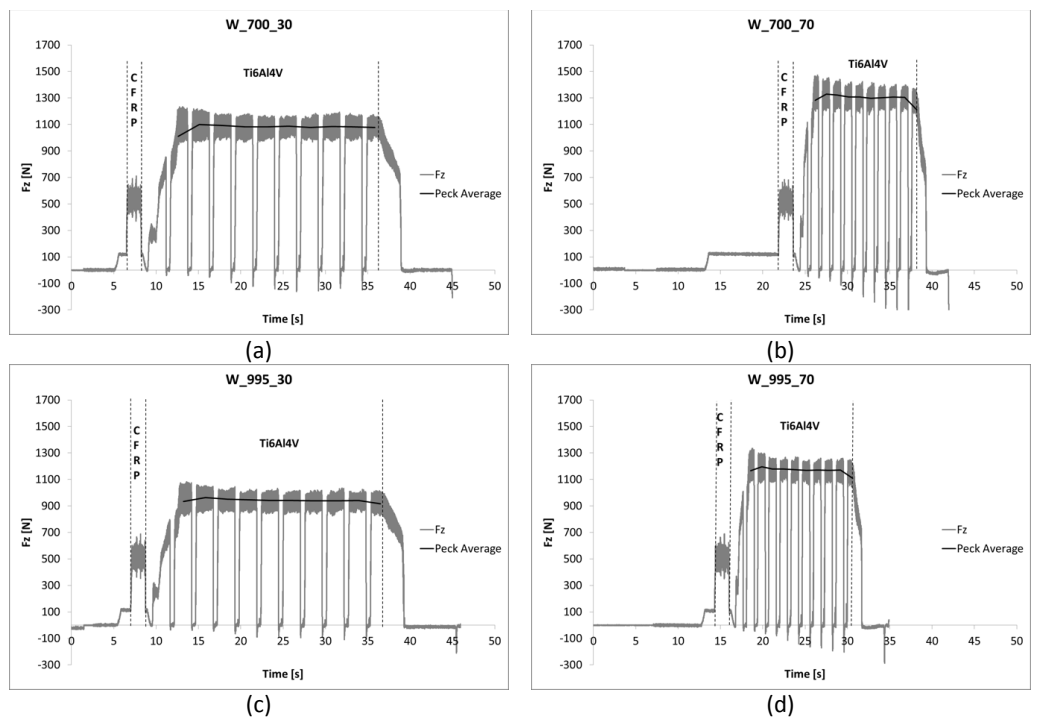


*Fig. 3.10 – The force acquired during wet drilling at different spindle speed and feed rate: (a) 700 RPM and 30 mm/min, (b) 700 RPM and 70 mm/min, (c) 995 RPM and 30 mm/min, (d) 995 RPM and 70 mm/min.*

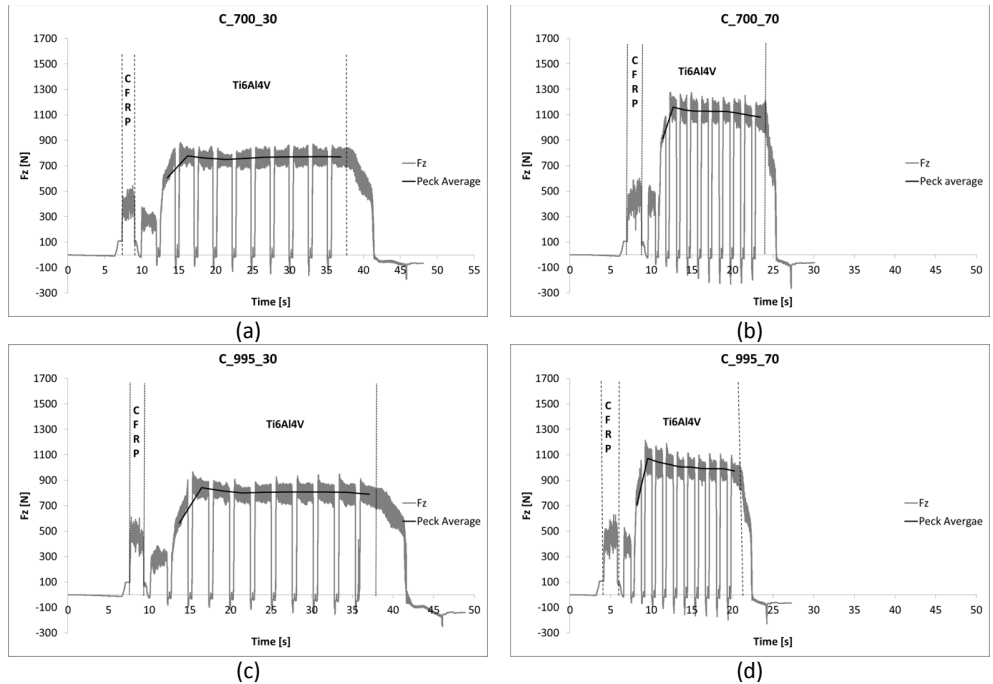


Fig. 3.11 – The force acquired during cryogenic drilling at different spindle speed and feed rate: (a) 700 RPM and 30 mm/min, (b) 700 RPM and 70 mm/min, (c) 995 RPM and 30 mm/min, (d) 995 RPM and 70 mm/min.

As concerning CFRP it is possible to observe in table 3.1 that the force in wet condition is higher than in cryogenic condition. The following table reports the mean  $F_z$  value related at the single peck for both cooling condition.

n [RPM]	$v_f$ [mm/min]	f [mm/rev]	Mean $F_z$ [N]	
			Wet	Cryo
3560	630	0.17	526	442

Tab.3.1 – Mean  $F_z$  values of CFRP drilling for both cooling condition.

As concerning Ti6Al4V force trend, it is possible to observe that the higher the feed rate the higher the measured forces, independently by spindle speed; this parameter seems to play a negligible role regarding the forces. The next table

reports the  $F_z$  mean values of Ti6Al4V drilling and the feed value corresponding at the set cutting parameters.

n [RPM]	$v_f$ [mm/min]	f [mm/rev]	Mean $F_z$ [N]	
			Wet	Cryo
700	30	0.043	1179	850
	70	0.100	1415	1227
995	30	0.030	1028	903
	70	0.070	1261	1130

Tab. 3.2 – The Mean  $F_z$  values of Ti6Al4V drilling for both cooling condition.

In order to enhance the readability of data reported in table 3.2, in figure 3.12 the same data are graphically reported in form of histograms as function of feed.

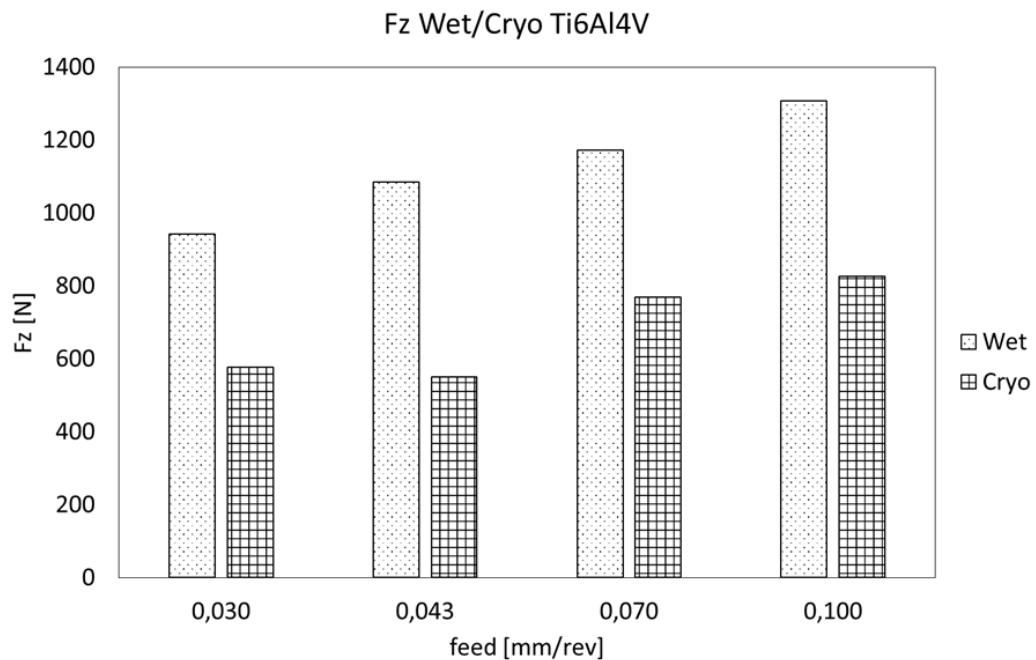


Fig.3.12 – The Thrust force during wet and cryogenic drilling as a function of feed.

It is appreciable, especially for the wet conditions, an increase of forces as the feed increases. The forces achieved the maximum value for 0.100 mm/rev feed corresponding the lower spindle speed (700 RPM) and the high feed rate (70

mm/min) while the minimum value was achieved by lower feed corresponding the higher spindle speed (995 RPM) and the lower feed rate (30 mm/min)

The forces acquired during wet drilling are considerably higher compared to those recorded in cryogenic conditions; in particular, the reduction in the force ranges from 10% in the case of feed set equal to 0.070 up to 28% in the case of feed set equal to 0.043.

### 3.2.2. Torque

The figure 3.13 shows a typical torque diagram acquired during drilling of the stack. As for the force, the torque curve is divided in two phases: the former regarding the drilling of CFRP and the latter the drilling of Ti6Al4V. It is appreciable an abrupt discontinuity in the first peck of titanium drilling also in the torque curve.

It is possible to observe how the torque increases as the depth increases in each single peck and, in wet condition, peck by peck up to achieve a steady condition.

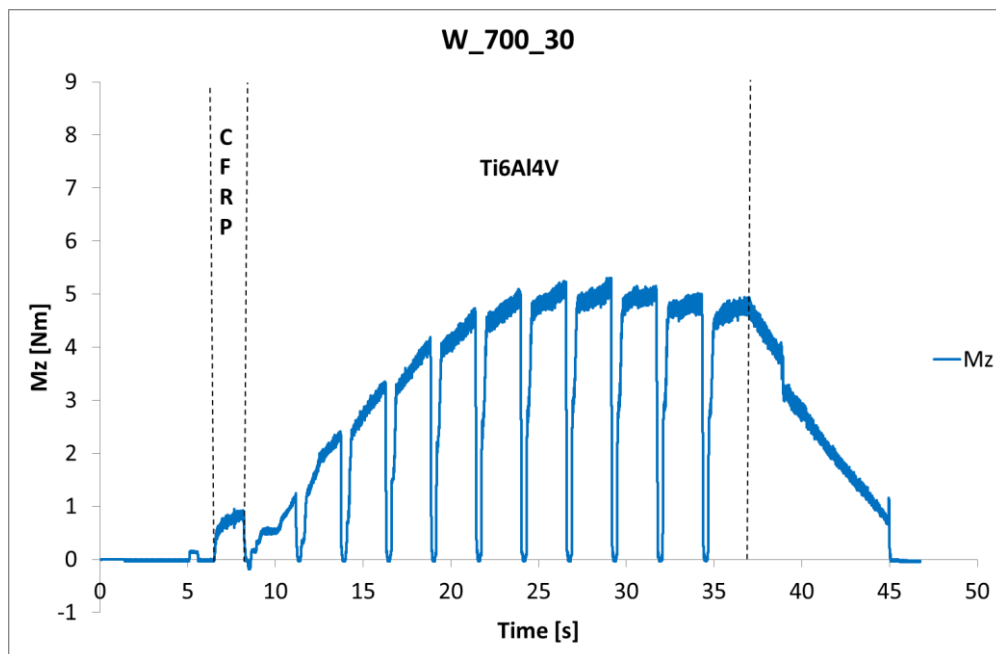
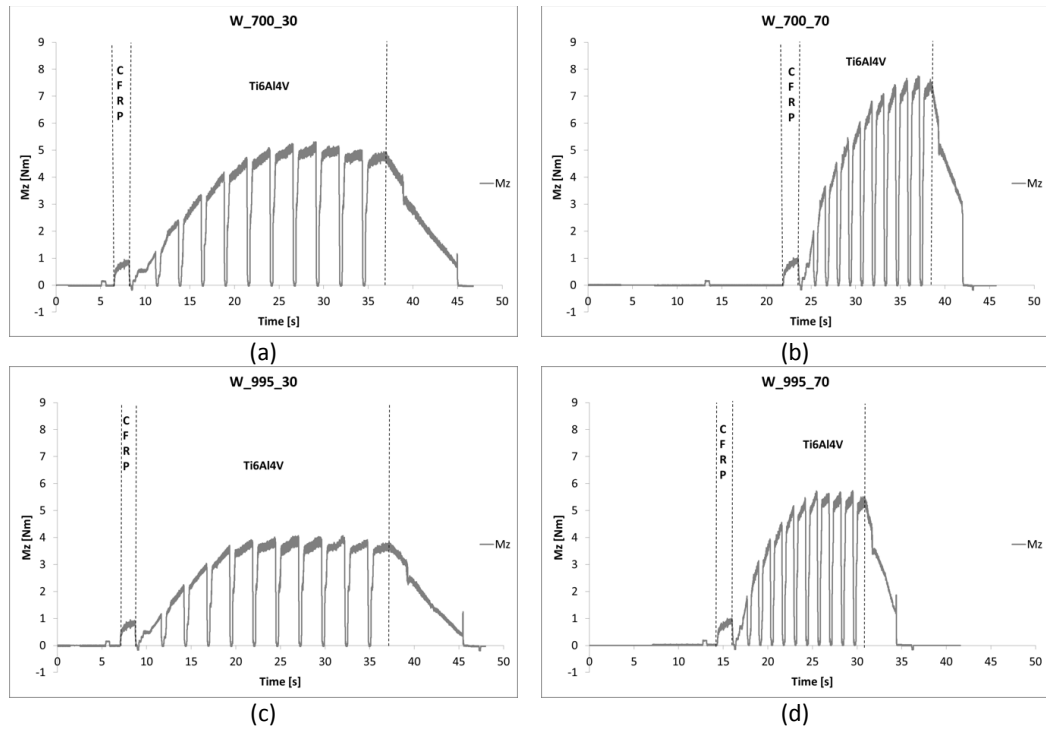


Fig. 3.13 – A typical trend of torque.

The figures 3.14 and 3.15 show the torque trend acquired during drilling of each single set of parameters under Wet and Cryogenic cooling conditions, respectively.



*Fig 3.14 - The torque acquired during wet drilling at different spindle speed and feed rate: (a) 700 RPM and 30 mm/min, (b) 700 RPM and 70 mm/min, (c) 995 RPM and 30 mm/min, (d) 995 RPM and 70 mm/min.*

With respect to the consideration drawn in describing the single diagram in fig. 3.13, looking at the fig. 3.14 it is possible to note that the higher the feed rate the higher the torque and the later the achieving of the steady conditions.

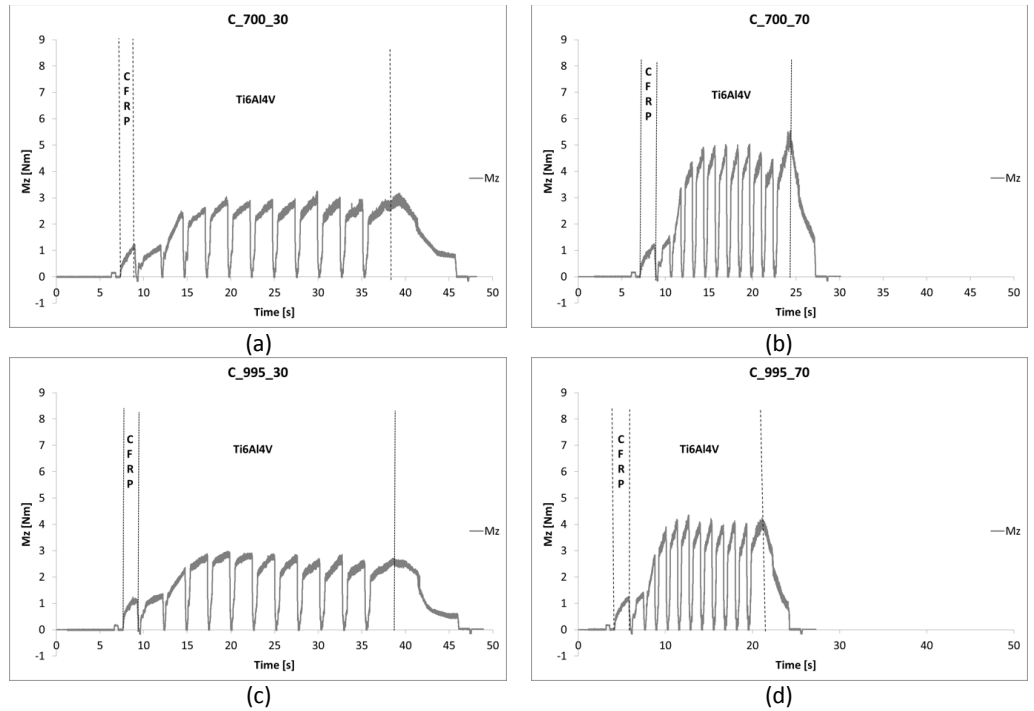


Fig. 3.15 - The torque acquired during cryogenic drilling at different spindle speed and feed rate: (a) 700 RPM and 30 mm/min, (b) 700 RPM and 70 mm/min, (c) 995 RPM and 30 mm/min, (d) 995 RPM and 70 mm/min.

In the first phase of the diagrams, limiting the attention on the drilling of CFRP, independently by coolant conditions, it is possible to observe how the torque increases as the depth increases. According to the literature [13], a growth is much more evident in cryogenic condition, as confirmed by the mean values reported in table 3.3.

n [RPM]	$v_f$ [mm/min]	f [mm/rev]	Mean Mz [Nm]	
			Wet	Cryo
3560	630	0.17	0.7	0.9

Tab. 3.3 - The mean value acquired during CFRP drilling for both cooling condition.

The lack of lubricant in cryogenic condition induces different mechanism in the interaction of the tool with respectively fibers and polymer matrix resulting in areas of uncut carbon fibers and consequent fiber pullout, encouraged also by matrix embrittlement. Those fibers protrude out into the borehole resulting in higher resistance to the rotation of the tool. Higher cutting forces are needed to drill the material and, as a consequence, higher torque is needed.

In the second phase of the diagram regarding the drilling of titanium alloy plate, independently from the cooling conditions and the process parameters, it is possible to note how, in each single peck, the torque increases, and the higher the feed rate the higher the quick of the torque increases. Such a phenomenon is due to both the increase of temperature generated by the friction between the tool and the borehole and to chip accumulation.

Focusing attention on figure 3.14, it can generally be assessed that the lower the feed the lower the torque. In case of the lowest feed, the torque shows a stable plateau value starting from the fifth peck (figure 3.14 (c)). As the feed increases, see figure 3.14 (a), the plateau value slightly increases and it is reached later, at the sixth peck. The plateau value is higher and it is reached even later in case of feed equal to 0,07, at the seventh peck (figure 3.14(d)). Finally, for the highest feed, no plateau value is reached, since the torque continuously increases peck by peck (figure 3.14 (b)). In all cases, the torque quickly decreases in the last and longest peck.

In cryogenic condition (see figure 3.15), the torque shows a behavior quite different and the acquired values in this case are slightly lower than in the previous one. First of all, the feed rate plays a significant role: the higher the feed rate the higher the recorded torque and this value is quite constant as rotational speed varies. In all cases the torque shows to reach a steady condition and such a condition is reached slightly later when the feed rate increases.

It was observed that the torque increases slightly during this stage reaching its peak value when the area of the tool in contact with the surface of the hole is maximum.

Differently from the wet condition, in this case the torque always shows to reach the highest value during the last peck. This is due to the fact that the last peck, as reported in the previous paragraph, has a longer stroke than the others, and equal to 3 mm.

Since the feed is the same, the time in which the tool remains in contact with the material in this last peck is longer. This leads to a temperature increase resulting in a partial loss of benefits of cryogenic temperatures. Furthermore, when the tip of the tool comes out from the bottom side of the plate, the liquid nitrogen sprayed from the coolant channels do not come in touch with the material and the above-mentioned loss in total.

The next table reports the maximum of the mean values of each single peck acquired for each set of drilling parameters. Those values corroborate the above drawn hypothesis.

n [RPM]	v <sub>f</sub> [mm/min]	f [mm/rev]	Max M <sub>z</sub> [Nm]	
			Wet	Cryo
700	30	0.043	5.0	2.7
	70	0.100	7.4	4.3
995	30	0.030	3.8	2.6
	70	0.070	5.4	3.5

*Tab.3.4 - The maximum of the medium value of each single peck for both cooling condition.*

In figure 3.16 the same data are graphically reported in form of histograms as function of feed: it is clearly shown the increase of torque as the feed increases, with higher values in wet condition. Similar results have been found by Fernandes and Cook in the drilling of CFRP [10].

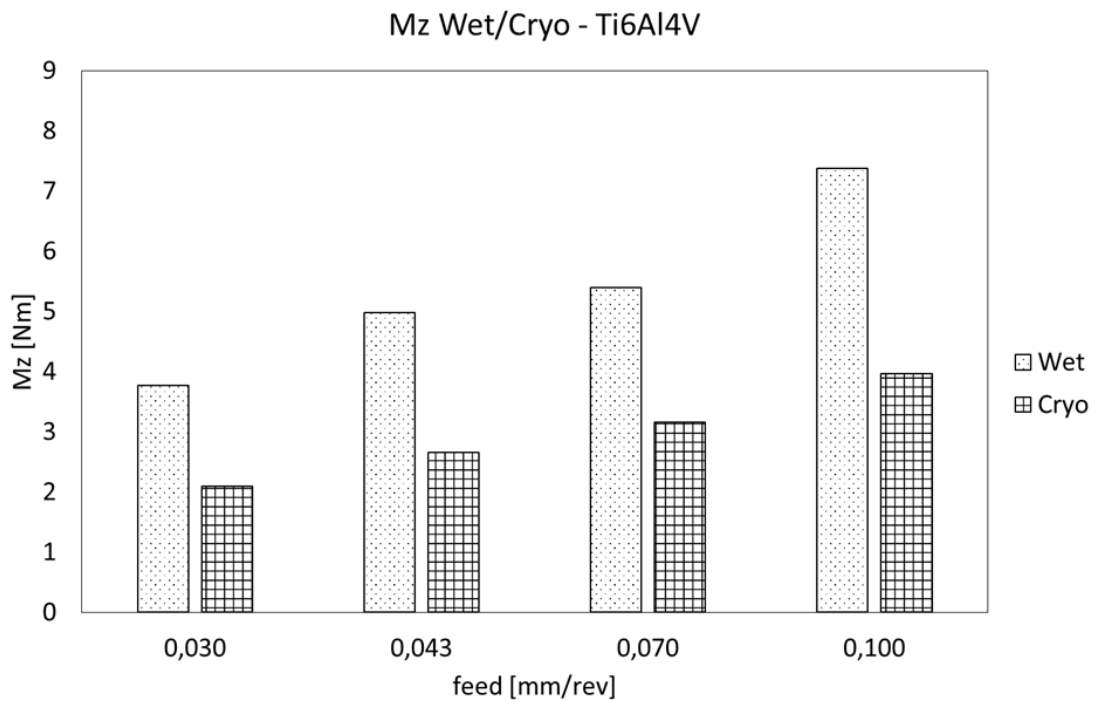


*Fig.3.16 – The torque during wet and cryogenic drilling as a function of feed.*

### 3.2.3. Hole diameters

The next figure shows the measurements of CFRP hole diameters as function of feed in wet (fig. 3.17) and cryogenic (fig. 3.18) conditions, both at the entrance and the exit of the drilled hole.

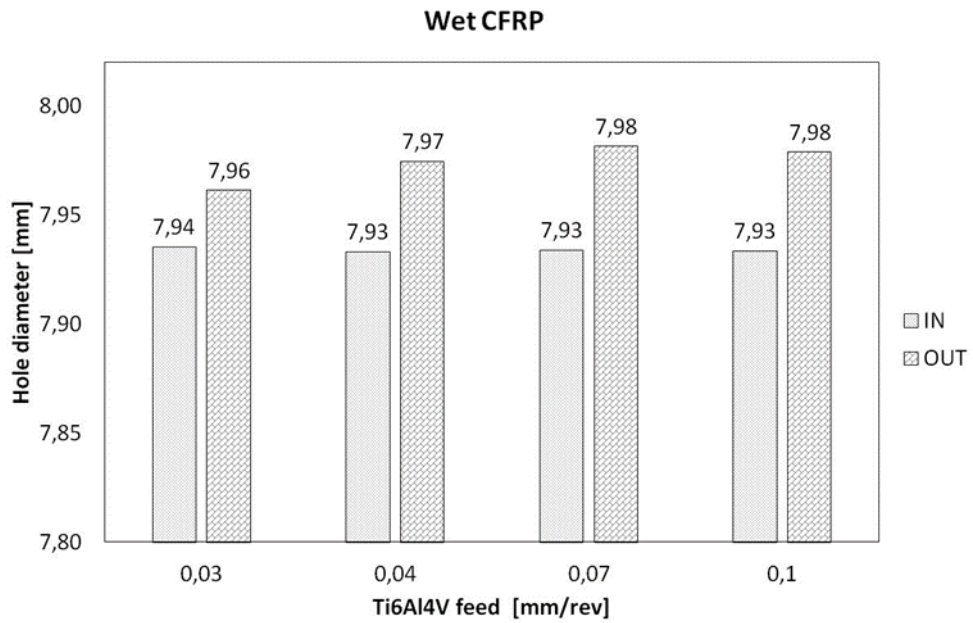


Fig. 3.17 – In and Out CFRP hole diameters as function of feed in wet conditions.

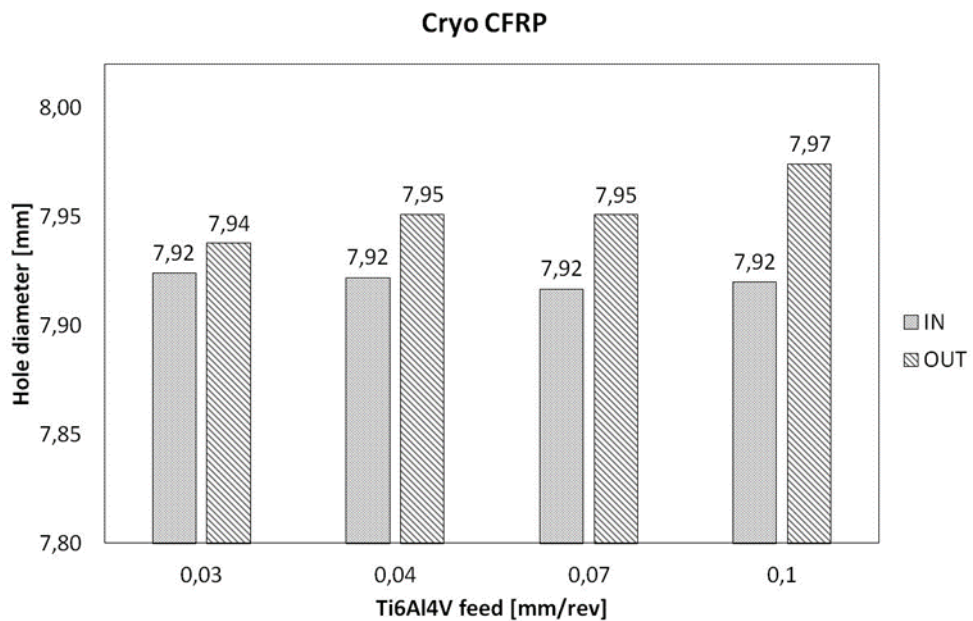


Fig. 3.18 – In and Out CFRP hole diameters as function of feed in cryogenic conditions.

The entry CFRP holes are often undersized, with respect to the tool nominal diameter, due to spring-back of both the matrix and the fibers [14].

It is appreciable, in each case, an increase of exit diameters with respect to the entry one; this is mainly due to what happens in the first drilling peck of titanium that is also the last step in CFRP drilling.

The instability phenomenon of the tool, mentioned in the previous section, occurs when it bursts through the bottom of CFRP and starts to penetrate the top of titanium plate. This phenomenon causes the tool vibrations leading to an enlargement of the circular motion of the drill and, as a consequence, resulting in the exit holes of CFRP with larger diameters. Furthermore, in this last phase, the tip of the tool works the CFRP with the cutting parameters used for titanium: the higher the feed the higher the vibrations and, finally, the larger the diameters, in both wet and cryogenic conditions.

Even if only slightly, the CFRP diameters of hole realized in cryogenic condition are smaller than those realized in wet condition with a difference ranging from 0.01 mm up to 0.03 mm (see fig. 3.19).

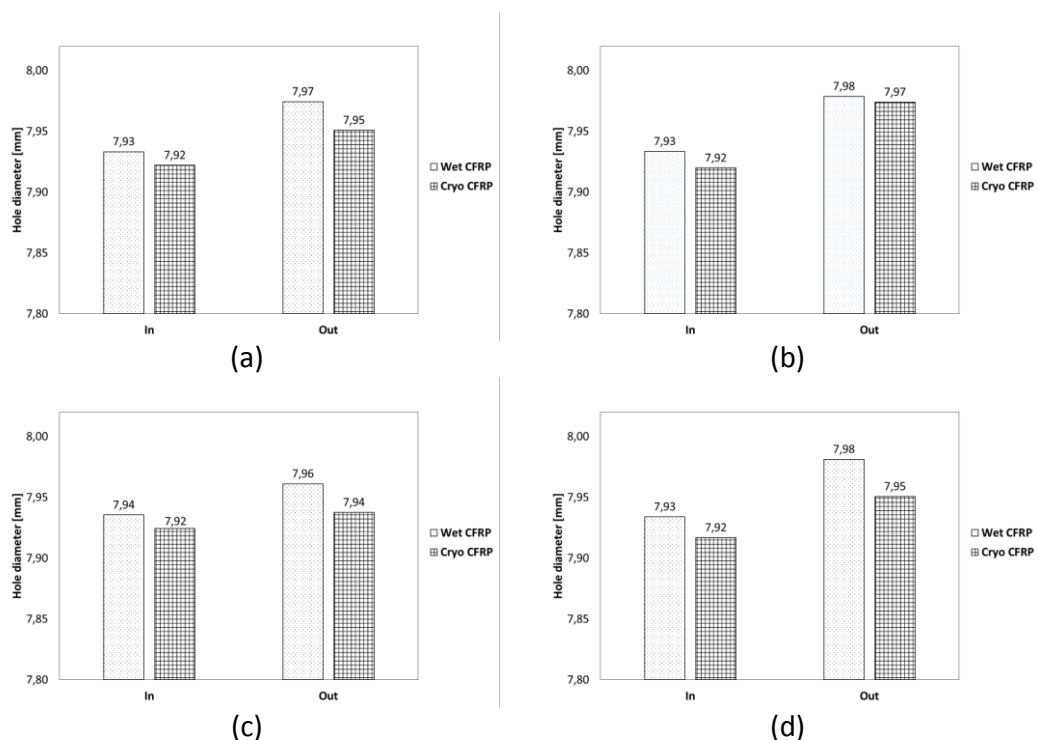
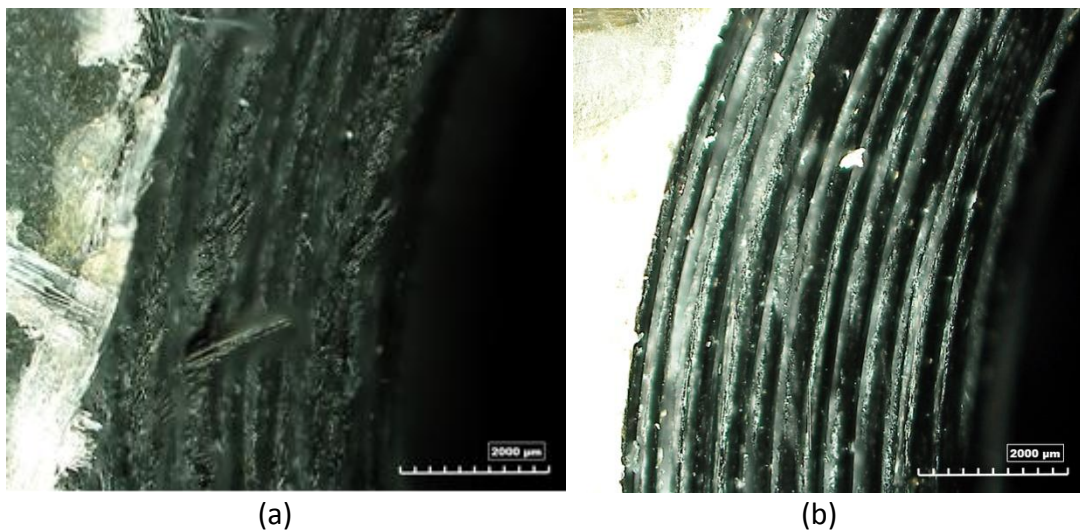


Fig. 3.19 – CFRP hole diameter in wet and cryogenic condition with different feed in Ti6Al4V (a) 0.04 mm/rev (b) 0.010 mm/rev (c) 0.03 mm/rev (d) 0.07 mm/rev.

The lower value of diameters of the holes made in cryogenic conditions is due to the occurrence of two different phenomena. The former regarding the operating temperature: the lower the temperature the lower the diameter of the tool. The latter regarding the lack of lubricant: this induces different mechanism in the interaction of the tool with respectively fibers and polymer matrix resulting in an evident fiber pull-out encouraged also by matrix embrittlement in cryogenic condition. This is evident in figure 3.20, where a comparison is proposed between the boreholes made respectively in cryogenic (a) and wet (b) conditions. The above described results are in good agreement with literature [12]: during cutting a large deflection of fibers occurs, the uncut carbon fibers protrude out into the drilled hole causing in deep fiber pull-outs affecting, in lowering, the measured diameters.



*Fig. 3.20 – A comparison of hole inner surface between cryogenic (a) and wet (b) conditions.*

Since measurements performed in CFRP holes result in hole diameter measurements that need a deeper understand, further, and more accurate measurements, have been performed using a CMM machine made by DEA, in order to try to describe with the highest accuracy the borehole.

To this aim, for each single hole made in the CFRP plate, limiting the attention and the measures to the holes made in cryogenic conditions, the whole borehole has been acquired with a scanning step in depth of 0.5 mm and 36-measurement positions equally distributed along each single circumference. As a consequence, since the measured thickness of the CFRP plate is a little higher than 18 mm, 38 different circumferences have been scanned.

In figure 3.21, as an example, a circumference scanned at a depth of 3.5 mm is reported in order to give evidence of the performed measurements.

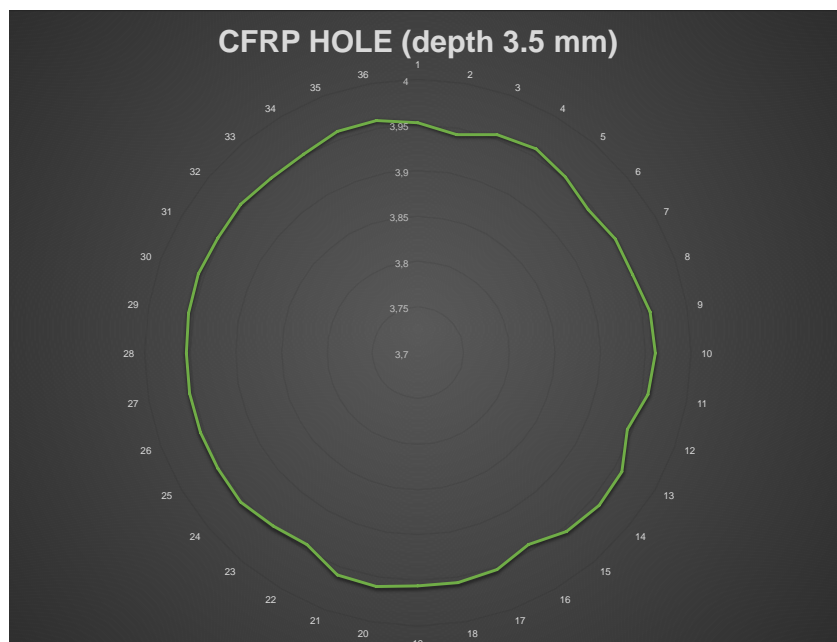
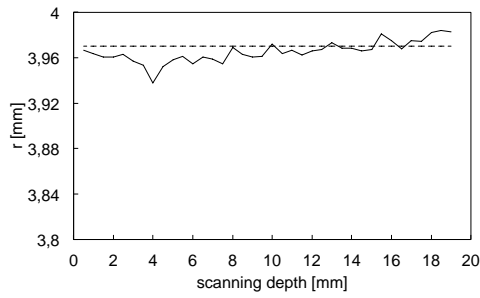


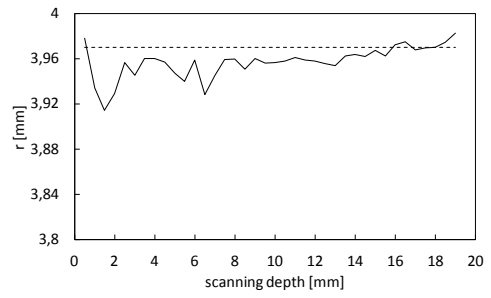
*Fig. 3.21 – Hole measurements performed via CMM machine on the CFRP hole made with 700 RPM and 30 mm/min in cryogenic conditions.*

For each single circumference, the center has been calculated with the mean square method. Finally, for each circumference, the radii calculated as the distance between the above described center and the four noticeable positions indicated respectively by 1, 9, 18 and 27 (according to the positions reported in figure 3.21) have been collected for each depth.

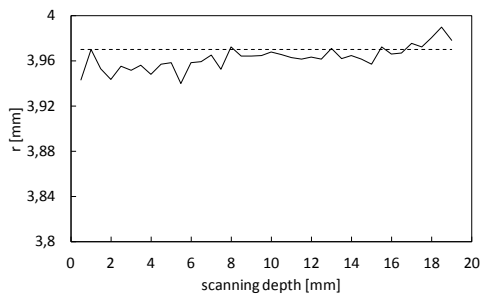
Figures from 3.22 to 3.25 report the trend of these radii as a function of the scanning depth. The dotted line reported in each graph represent the nominal radius value.



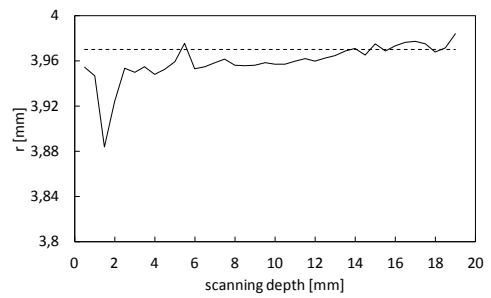
(a)



(b)

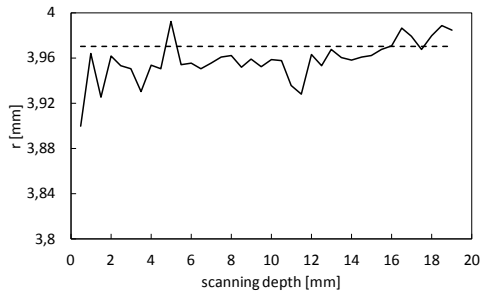


(c)

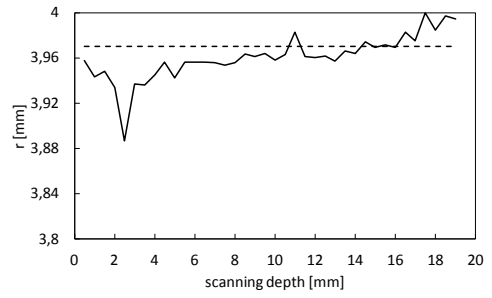


(d)

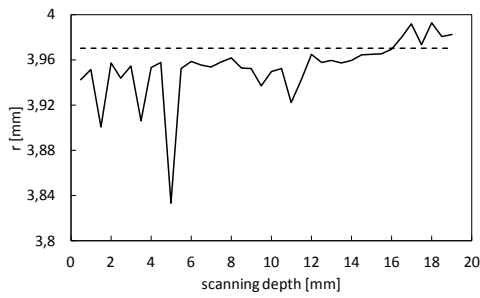
*Fig. 3.22 – Measured radii in CFRP borehole for hole made with 700 RPM and 30 mm/min in cryogenic conditions for 4 different positions equally distributed along the circumference.*



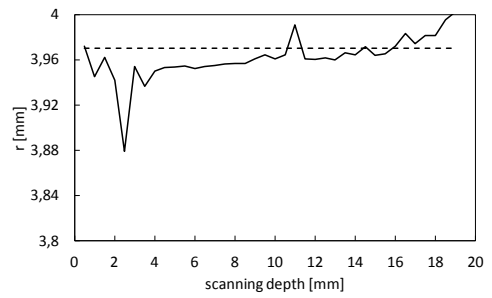
(a)



(b)

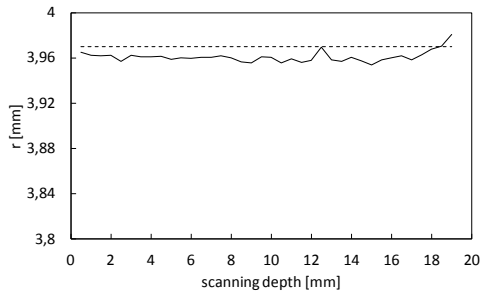


(c)

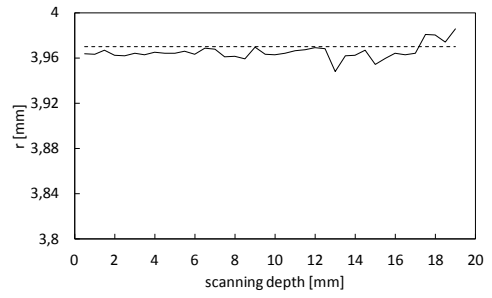


(d)

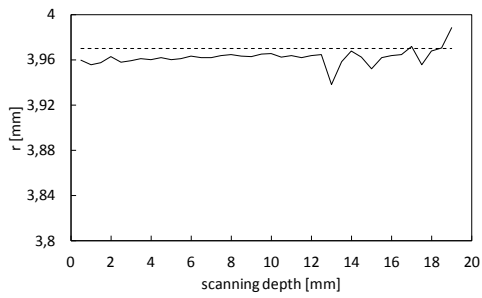
*Fig. 3.23 – Measured radii in CFRP borehole for hole made with 700 RPM and 70 mm/min in cryogenic conditions for 4 different positions equally distributed along the circumference.*



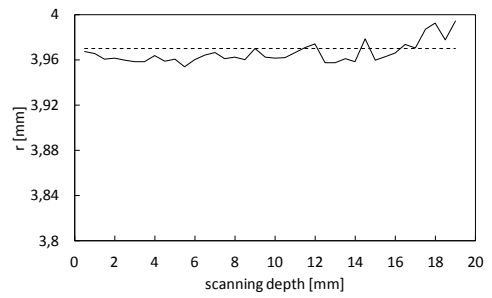
(a)



(b)



(c)



(d)

*Fig. 3.24 – Measured radii in CFRP borehole for hole made with 995 RPM and 30 mm/min in cryogenic conditions for 4 different positions equally distributed along the circumference.*

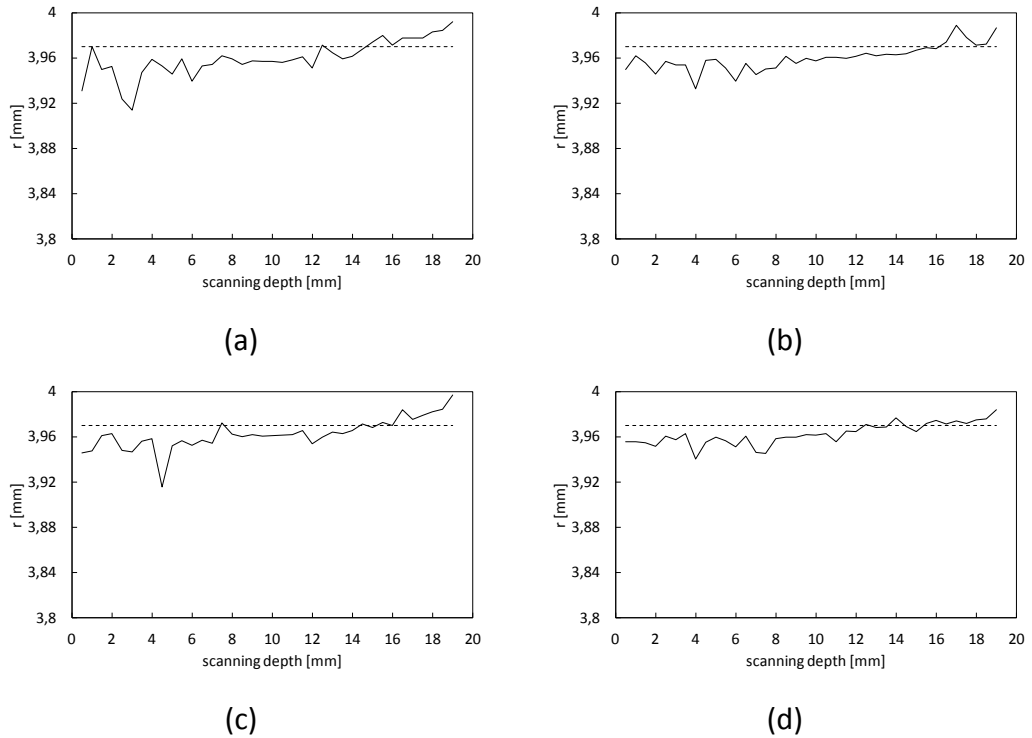


*Fig. 3.25 – Measured radii in CFRP borehole for hole made with 995 RPM and 70 mm/min in cryogenic conditions for 4 different positions equally distributed along the circumference.*

The data provided by the measurements made in this further campaign corroborate the data acquired with the Mitutoyo® Absolute digital shown in figure 3.7, since even in this case it is evident how the measured hole diameter in the entry side is lower than the nominal value, due to the material spring back that is emphasized in cryogenic conditions, and the hole diameter increases as the measuring depth increases, due to the tool instability occurring when the tool itself come in contact with the upper surface of the titanium sheet.

Finally, it is important to underline how, independently by the cooling conditions, the measured hole diameter on the entry side of CFRP plate is always lower than that on the exit side, ranging this difference from 0.02 mm, when the feed is equal to 0.03 mm/rev, up to 0.05 mm, when the feed is equal to 0.1 mm/rev.

In the histograms in the figures 3.26 and 3.27 one can observe that the effect of cutting parameters on Ti6Al4V diameters is negligible and the entry and exit

diameters are comparable recording a mean diameter in entry and in exit of 7.93 mm and 7.95 mm in wet and cryogenic conditions, respectively.

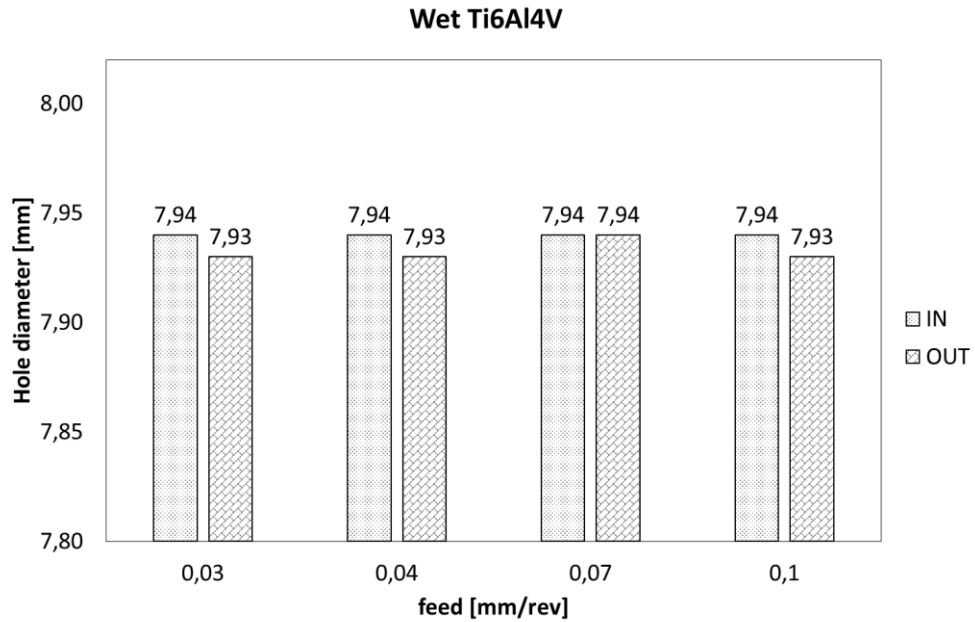


*Fig. 3.26 – In and Out Ti6Al4V hole diameters as function of working parameters in wet condition.*

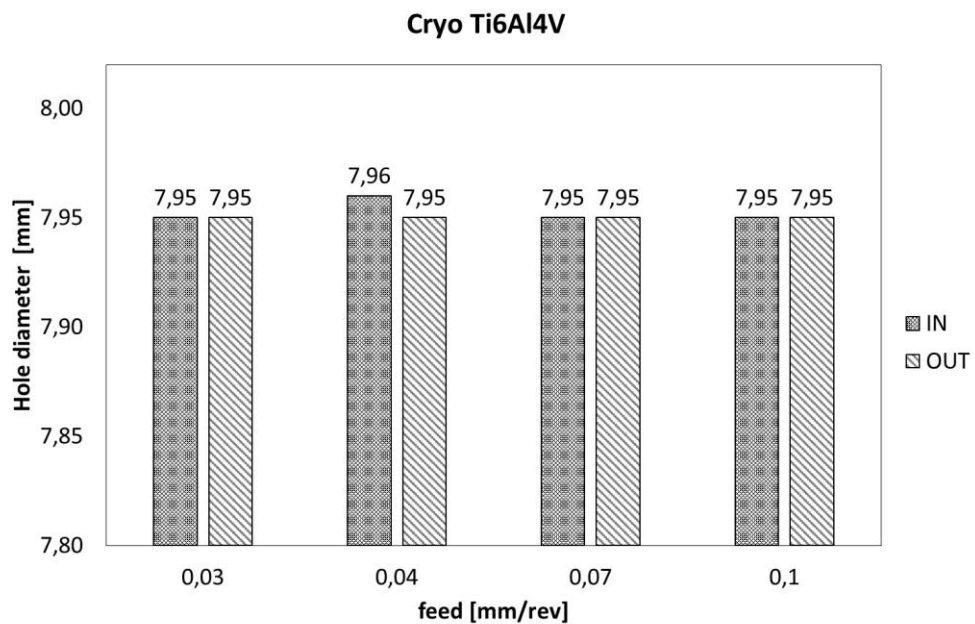


*Fig. 3.27 – In and Out Ti6Al4V hole diameters as function of working parameters in cryogenic condition.*

The figure 3.28 shows the comparison of the measured hole diameters in wet and cryogenic conditions.

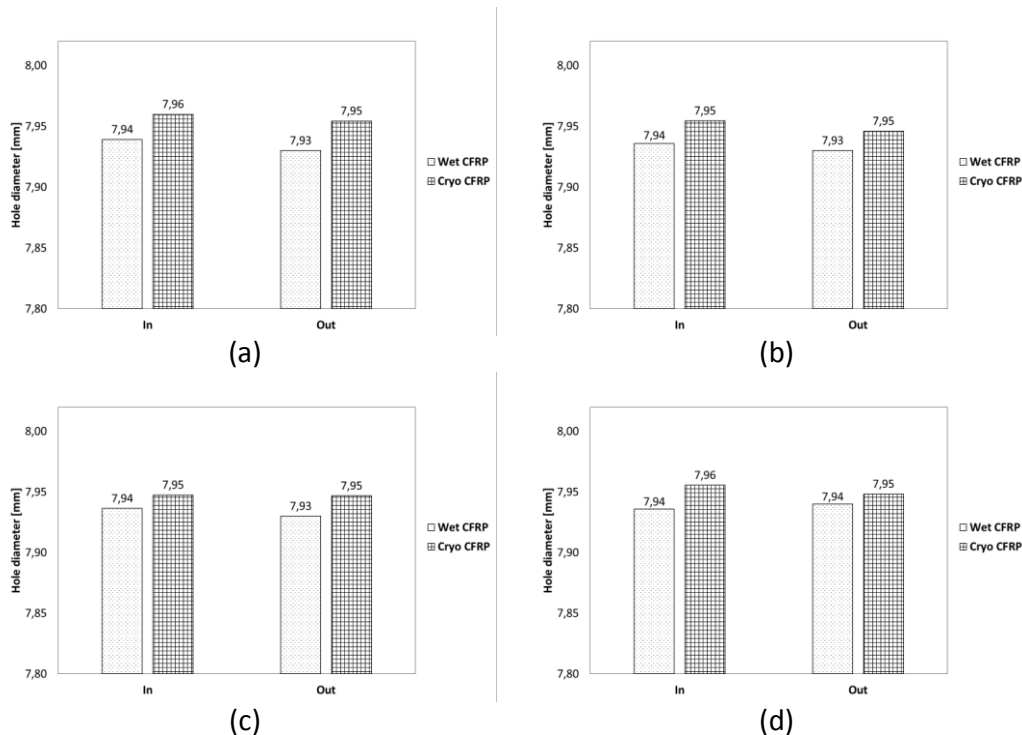
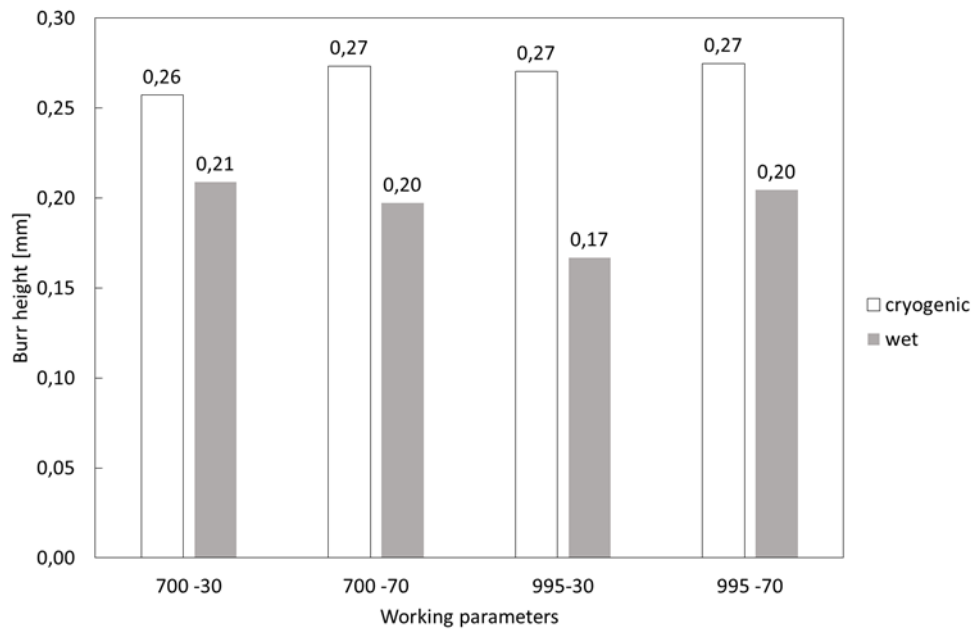


Fig. 3.28 – Ti6Al4V hole diameter in wet and cryogenic condition with (a) 0.04 mm/rev (b) 0.10 mm/rev (c) 0.03 mm/rev (d) 0.07 mm/rev.

The figure allows seeing how, in case titanium sheet drilling, the situation is completely changed: the diameter values are always higher in cryogenic than in wet conditions, independently by drilling parameters and measuring sides. This is due to the loss of benefits of cryogenic temperatures. After drilling 18 mm of CFRP, the friction generated during the process results in a temperature increase that vanishes the continuous addition of liquid nitrogen. To this aim, even the adopted peck strategy is unable to avoid the phenomenon.

### 3.2.4. Burr height

The figures 3.29 shows the burr height at the exit hole for Ti6Al4V in both wet and cryogenic conditions respectively.



*Fig. 3.29 – The burr height of wet and cryogenic holes as function of drilling parameters.*

The increasing of burr height in exit hole of titanium sheet is a function of heat generation. The low thermal conductivity of titanium generates heat which enables to extrude the soften titanium at the tool margin area. The cryogenic coolant should reduce the temperatures during drilling and, as a consequence, should reduce titanium plastic flow. It is then expected that burr height be lower than in case of wet drilling. In our case, on the contrary, burr height is higher. This is due to the fact that, as reported in the previous section regarding hole diameters measurements, during the drilling of 18 mm of CFRP plus 10 mm of titanium, the heat generated by friction increases the temperature more and more up to vanish completely the benefits of cryogenic coolant. Furthermore, when the tip of the tool comes out, the liquid nitrogen does not come into contact with titanium sheet [15] causing the complete loss of refrigerant and lubricant action.

### 3.3. Conclusions

On the basis of the above described activities one can conclude that the drilling of stack of different materials in cryogenic condition can provide some noticeable benefits (reduction of thrust forces and torque, reduced environmental impact, acceptable hole quality) but further developments need. Analyzing in details the various investigated aspects, the following partial conclusions can be drawn:

- Focusing attention on CFRP drilling, the first material encountered by the tool, and with respect to the recorded forces, it can be assessed that the use of cryogenic conditions reduces the thrust force.
- Looking at the titanium sheets, the lower the feed the lower the recorded thrust force in both coolant conditions. Also in this case, the thrust forces recorded in cryogenic conditions are always lower than in wet conditions for each set of process parameters. Furthermore, forces recorded in the first peck in titanium sheet allows to demonstrate the instability phenomena of to the tool coming in contact with titanium upper surface: this results in tool vibrations leading to enlargement of CFRP exit hole.
- In both coolant conditions, independently by process parameters, in each single peck the torque increases. This phenomenon is due to the increase of temperature generated by the friction between tool and inner surface of hole and to chip accumulation.
- As concerning CFRP drilling, differently by the thrust force, the mean value of the acquired torque in cryogenic is higher than in wet condition. The lack of lubricant in cryogenic condition induces areas of uncut carbon fibers and fiber pullout. The higher torque acquired means that higher cutting forces need to drill the material. The fiber pullouts protrude out into the drilled hole making more difficult the rotation of tool.
- Moving the attention on the Ti6Al4V sheet, the recorded torque values, in wet conditions, tend to a steady state condition. Such a state is reached later and later as the feed increases, and the plateau value achieved

grows as the feed increases. In cryogenic conditions, on the contrary, the steady conditions are suddenly achieved and the relative plateau value is lower than in wet conditions.

- Concerning the diameter measurements, the entry ones of CFRP holes are often undersized (w.r.t. tool nominal diameter) due to spring-back of both the matrix and fibers. Conversely the exit diameters are oversized because of the instability phenomenon experienced by the tool coming in contact with the upper surface of the titanium sheet during the first peck in titanium. This leads to tool vibrations resulting finally in hole enlargement at the exit side of CFRP plate. This phenomenon strictly depends on the adopted feed: it has been proven that the higher the feed the larger the exit diameter
- The CFRP diameters are always larger in wet than in cryogenic conditions, independently by drilling parameters and measuring sides. The situation is completely changed in case of titanium sheet drilling: this is due to the loss of benefits of cryogenic temperatures. In case of drilling of stack of different thick materials, the benefits expected by cryogenic conditions reduce more and more as drilling goes on up to vanish completely. The absence of lubricant becomes then the key point and even the adopted peck strategy is not capable to avoid the phenomenon.
- Finally, focusing attention on the titanium burr height, the holes in cryogenic conditions show values higher than in wet condition. This is due to the fact that, the heat generated by friction increases the temperature, vanishing completely the benefits expected by cryogenic conditions. Furthermore, when the tip of the tool comes out, the liquid nitrogen does not come into contact with titanium sheet causing the complete loss of refrigerant and lubricant action. An alternative to reduce this could consist in a different approach using directly a liquid nitrogen spray on the back surface of the titanium sheet. It has not been taken into account

in the present research due to the complexity of the system and the growth of the related costs.

#### **4.1. Materials & methods**

In this chapter, the procedures adopted and the main results of a long run campaign will be presented and discussed.

Long run campaign means that we have performed an experimental research in which we made 60 holes with each investigated tool, with the aim to verify the useful life of the tool itself. Four different tools have been used, having the same geometry, by differing in the WC grainsize, ultrafine and micrograin, and in the presence or absence of DLC coating.

Even in this case, as in the previous chapter, the main outputs have been the recorded thrust force and torque, the hole diameter and the burr height.

The aim was to find the best tool, in terms of base material and coating, with the further aim to perform a future tool regeneration in order to save the expensive tool material and total money.

In the following sections, the used tools, the workpiece and the process parameters will be presented in details.

##### **4.1.1. The used tools**

The cutting tools used in the second phase of this experimental analysis had the same geometry of the tools used in the first phase described in the previous chapter. Four different types of tools were used, all the tools were made of sintered tungsten carbide (WC) in a cobalt (Co) binder and they were named as reported in the following list (R means that the tool is coated):

- C8
- C8R
- K1
- K1R

The cutting tools C8 and C8R were characterized by the same dimension of the WC particles, that range from 0.2 to 0.5  $\mu\text{m}$  (ultrafine according to the definition

provided in the second chapter) and a percentage of 4.2% of Co. They differed for the coating: C8 was uncoated and C8R was DLC coated.

The cutting tools K1 and K1R were characterized by the same dimension of the WC particles of an average size of 0.5  $\mu\text{m}$  (micro-grain according to the definition provided in the second chapter) and a percentage of 5.0% of Co. They differed for the coating: K1 was uncoated and K1R was DLC coated.

#### **4.1.2. The workpieces**

The workpieces used for the second phase were made with the same materials and geometry of those used in the first phase in wet condition.

The CFRP/Ti6Al4V stack used in the experiment was composed of CFRP laminate puts on Ti plate. The CFRP laminate was made of woven carbon fabric of 200  $\text{g}/\text{m}^2$  in an epoxy matrix with full thickness of 18 mm. The titanium plate used in the experiment was Ti6Al4V with thickness of 10 mm. Both materials were cut by means of an abrasive water jet. The workpieces were provided by Leonardo® and they are the materials used to realize the BOEING 787.

This stacking sequence, CFRP on top and Ti6Al4V on bottom, has been chosen since it represents the real case to face. As in fact, on the aircraft, the CFRP is the outside of the fuselage and titanium parts are inside and it is not possible to put the drilling machine inside the fuselage.

#### **4.1.3. The drilling conditions and evaluated outputs**

the process parameters adopted in this phase are those selected in the previous experimental campaign. The CFRP laminate was always drilled using the same working parameters: 3560 RPM and feed rate of 630 mm/min as in the first phase. The working parameters used to drill the titanium sheet were those select in the previous phase, i.e. 995 RPM and 70 mm/min. In particular, the titanium was machined using the same drilling strategy used in the first phase: a strategy with fixed position pecking in order to facilitate the chip removal and to reduce the cutting temperature. A peck value of 1.00 mm was chosen, in this way, the

number of pecks for titanium drilling was been 10 pecks and a final peck of 3 mm to conclude.

The drilling experiments consisted of 240 total holes: 60 holes for each tool in wet condition.

## 4.2. Results & discussions

In the following sections the main results in terms of recorded thrust force and torque, hole diameter and burr height will be presented and discussed.

Since the long run campaign consisted of 60 holes for each tool, for brevity, the main results will be presented in terms of data regarding set of ten holes.

### 4.2.1. Thrust forces

In the figure 4.1 the thrust forces recorded in CFRP drilling in the long run campaign of K1 tool family are shown.

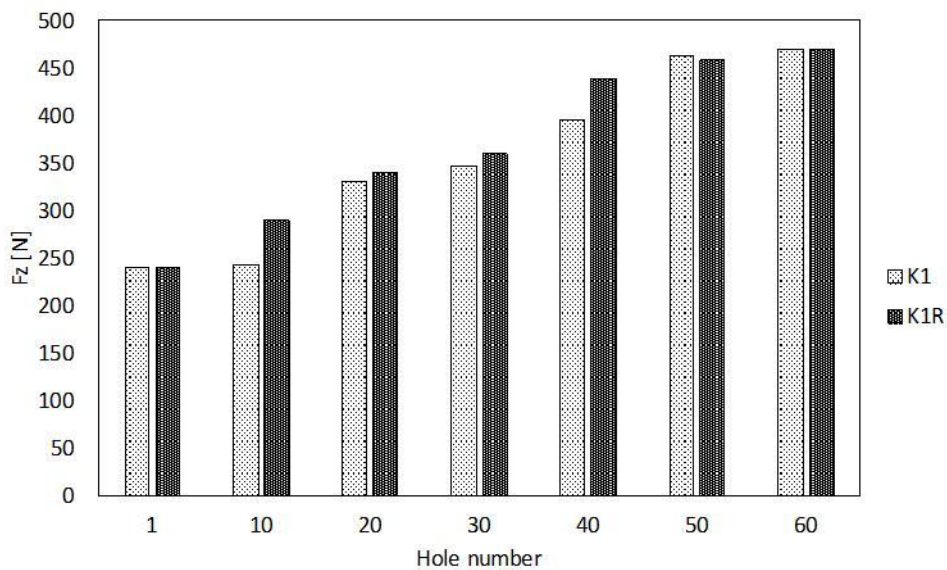


*Fig. 4.1 – Thrust force in CFRP: comparison K1 and K1R.*

It is evident how, the recorded thrust forces increase as the number of holes increase. By comparing the thrust force of the first hole with the same of the last hole, the force increases almost by the double. The performances shown by the

coated and uncoated tool seem to be slightly different along the campaign, but both in case of the first hole and in case of the last hole the recorded forces are almost the same.

In the figure 4.2 the thrust forces recorded in CFRP drilling in the long run campaign of C8 tool family are shown.

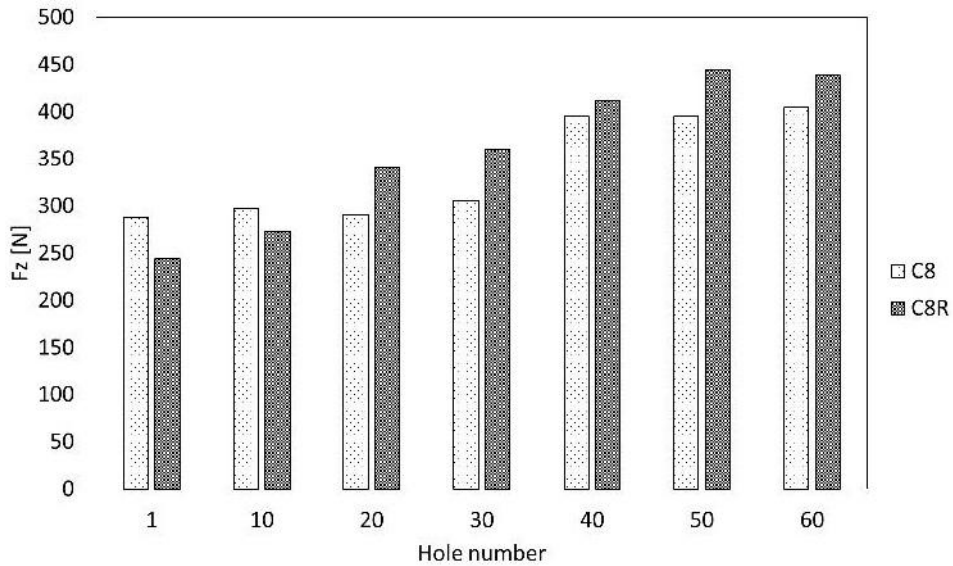


*Fig. 4.2 – Thrust force in CFRP: comparison C8 and C8R.*

Even if the forces increase as the number of holes increase, differently by the previous tool family, in the case of C8 tool family the recorded thrust forces increase slightly, since the differences between the first and the last hole are less evident. Furthermore, at the very beginning of the long run campaign, the coated tool seems to work better, but at the end the situation is changed. This means that at the beginning of the campaign, the coating seems to play an appreciable role, but, when the coating is worn, the performances abruptly drop down. Conversely, the performances shown by the uncoated tool seem to be more stable and, on the long distance, even better than those of the coated tool. In the figure 4.3 the thrust forces recorded in Ti drilling in the long run campaign of K1 tool family are shown.

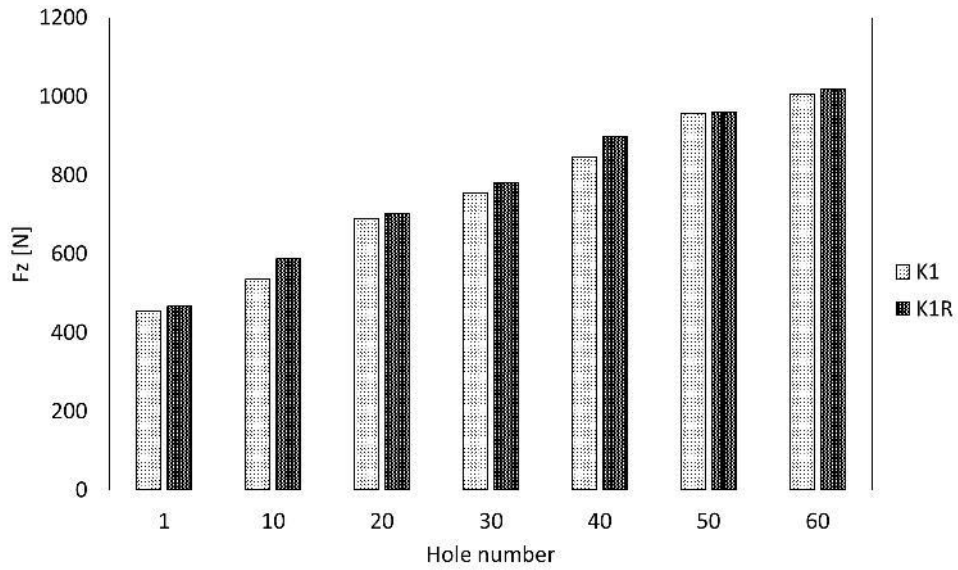


*Fig. 4.3 – Thrust force in Ti6Al4V: comparison K1 and K1R.*

In this case, the performances shown by both the coated and uncoated are very similar. In every case the performances decrease more and more, linearly, as the number of holes increase. As for the drilling of the CFRP, even in the case of Ti drilling, the forces recorded for the K1 family double moving from the first to the last hole.

In the figure 4.4, the thrust forces recorded in Ti drilling in the long run campaign of C8 tool family are shown.

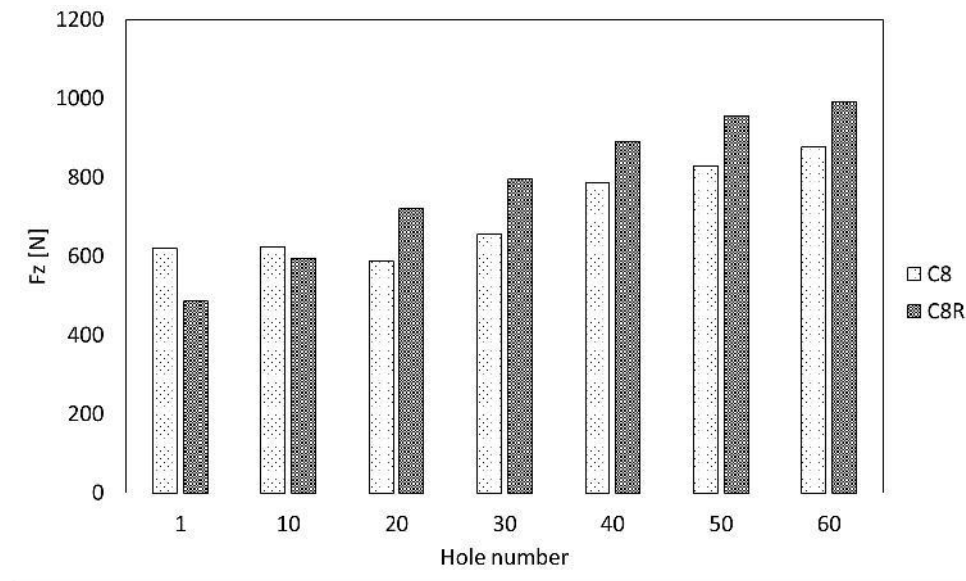


*Fig. 4.4 – Thrust force in Ti6Al4V: comparison C8 and C8R.*

In the case of drilling of Ti plate with the C8 family, considerations absolutely similar to those drawn for the drilling of CFRP with the same tool family can be made. In particular, at the very beginning of the long run campaign, the coated tool seems to work better, but at the end the situation changed. The coated tool seems to experience a greater wear than the uncoated one, so, at the end of the long run campaign, the latter shows better performances.

#### **4.2.2. Torque**

In the figure 4.5 the torque recorded in CFRP drilling in the long run campaign of K1 tool family is shown.

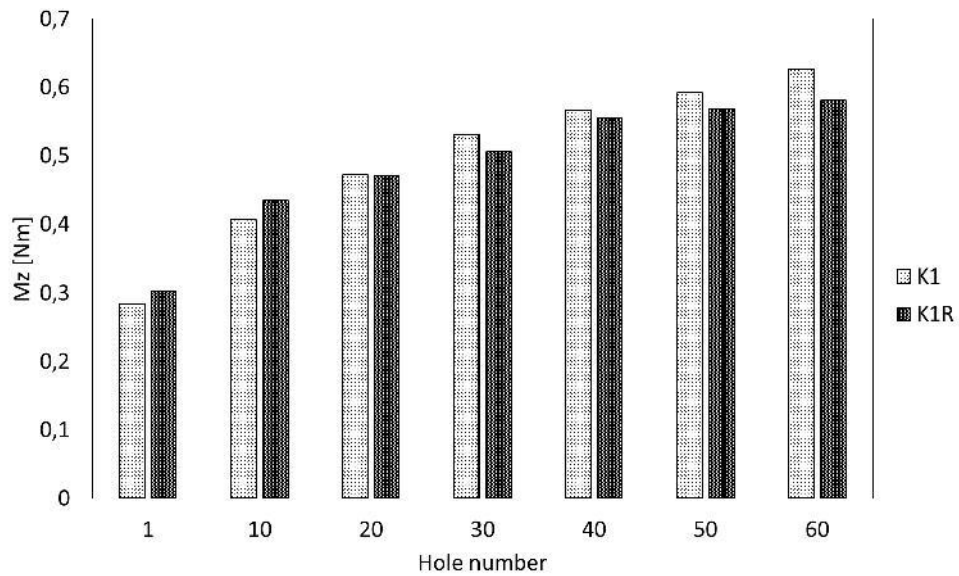


*Fig. 4.5 – Torque in CFRP: comparison K1 and K1R.*

It is evident how the recorded torque increases as the number of holes increases. By comparing the torque of the first hole with the same of the last hole, the torque increases almost by the double. The performances shown by the coated and uncoated tool seem to be slightly different along the campaign, since the torque recorded for the uncoated tool increases more than the torque of the coated one.

In the figure 4.6 the torque recorded in CFRP drilling in the long run campaign of C8 tool family is shown.

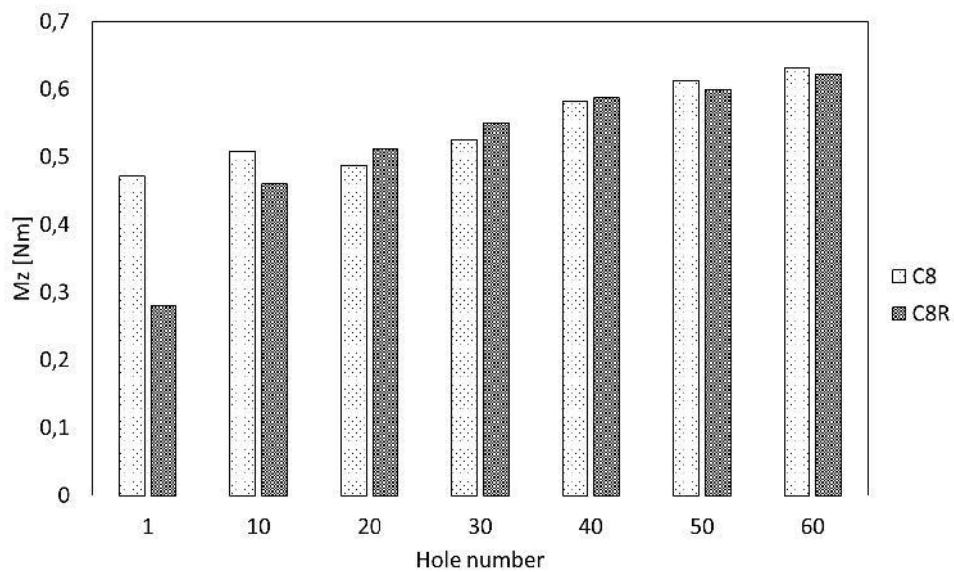


*Fig. 4.6 – Torque in CFRP: comparison C8 and C8R.*

As for the previous case, even in this one, the torque increases as the number of holes increases. At the beginning of the long run campaign the differences between the coated and uncoated tool are more evident but at the end they tend to even out. The value of the torque recorded in the first hole made with the uncoated tool is very high, probably something happens of strange and affects the measure. Anyway, the coated tool seems to work better recording a torque double moving from the first to the last hole.

In the figure 4.7 the torque recorded in Ti drilling in the long run campaign of K1 tool family is shown.

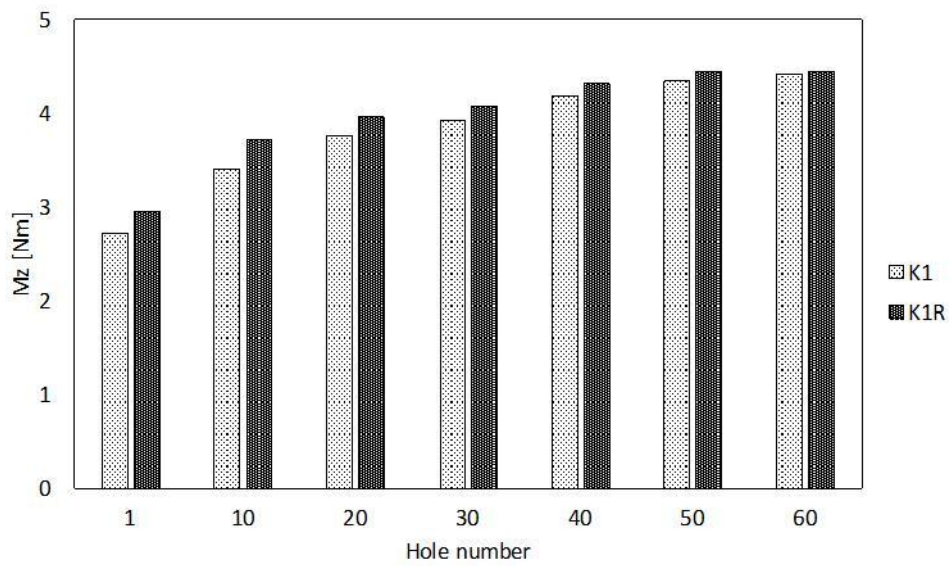


Fig. 4.7 – Torque in Ti6Al4V: comparison K1 and K1R.

In this case, the performances shown by both the coated and uncoated are very similar. Some differences are recorded at the beginning of the long run campaign but soon after they tend to even out. In every case the performances decrease more and more, linearly but slowly, as the number of holes increase.

In the figure 4.8 the torque recorded in Ti drilling in the long run campaign of C8 tool family is shown.

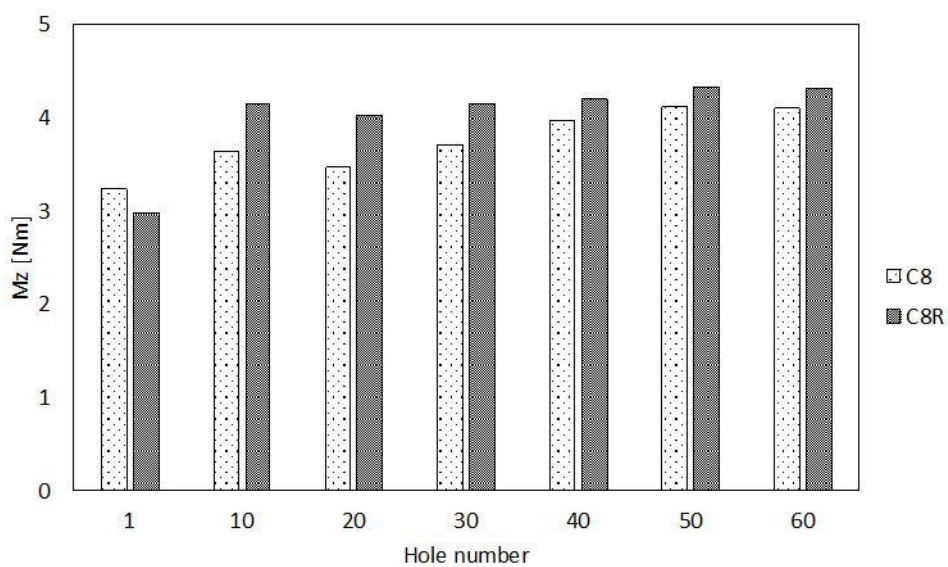


Fig. 4.8. – Torque in Ti6Al4V: comparison C8 and C8R.

In the case of drilling of Ti sheet with the C8 family, it is possible to note that the behavior of the torque is slightly different by the previous cases. The recorded torque in Ti drilling at the beginning of long run campaign do not respect a trend. Successively the coated and uncoated tools show a slightly different behavior. Looking at the outputs due to the uncoated tool, the recorded torque increase as the number of holes increase. This increase is less evident in coated tool characterized by a steady trend. The results in terms of recorded torque provided by the C8 tool family at the beginning of the long run campaign seem to be less linear than those provided by the other family of tool.

#### **4.2.3. Hole diameters**

Before to show and discuss the results of hole diameter, we define the “entry hole diameter” and the “exit hole diameter” respectively as the diameter of the hole measured in correspondence of the upper surface, e.g. the surface where the tool entered in the workpiece, and the diameter of the hole measured in correspondence of the lower surface, e.g. the surface of the workpiece where the tool comes out.

In the figure 4.9 the entry and exit hole diameters of the CFRP drilled with (a) K1, (b) K1R, (c) C8, (d) C8R, respectively.

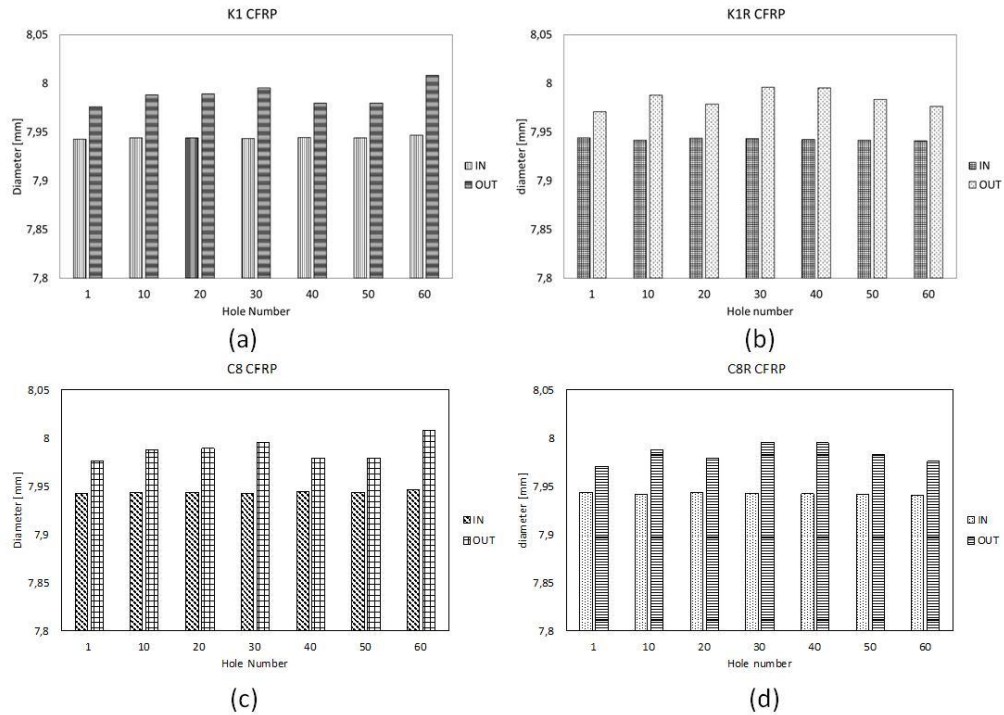
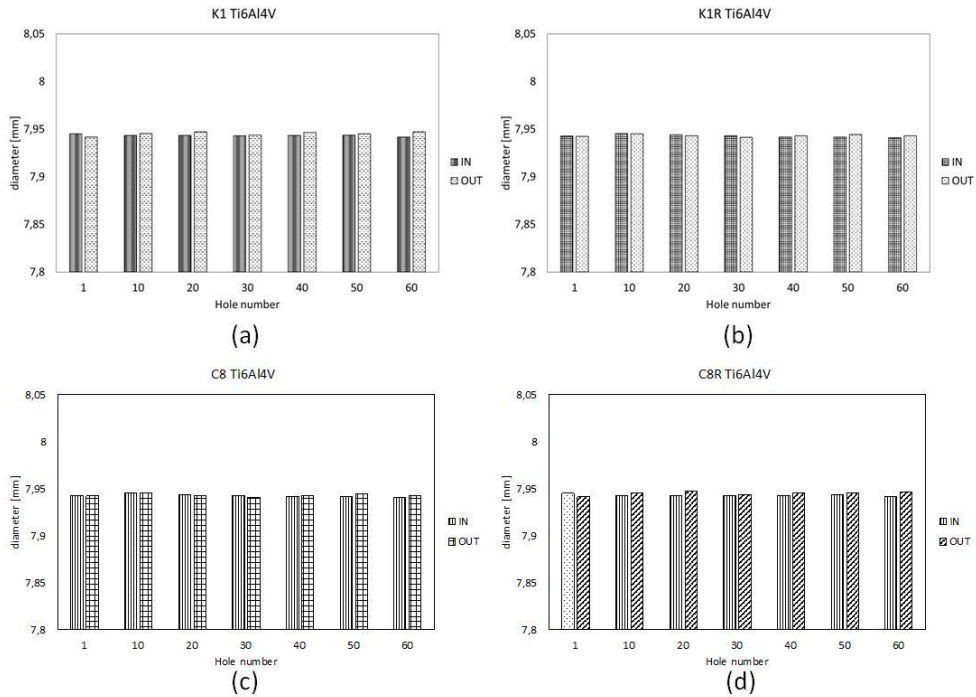


Fig. 4.9 - Entry and exit hole diameters of the CFRP: (a) K1(b) K1R, (c) C8, (d) C8R.

It is evident, for both the tool families, that the exit hole diameters are larger than the entry hole diameters. The CFRP entry diameters are often undersized due to spring-back of the matrix and fibers. The CFRP exit diameters are oversized for the presence of the Ti plate below. This is due to the instability of the tool coming in touch with the upper surface of the titanium plate that produces tool vibrations. When the tool starts to penetrate the top of the titanium, its circular motion enlarges resulting in the larger diameters.

Generally speaking, the measure of the entry side diameter seem to be absolutely stable, independently by the tool family, the presence of the coating and the number of holes. On the contrary, the measure of the exit side hole diameter seems to be unstable, even if the differences are negligible and no trends are evident. Finally, both the material grain size and the coating presence seem to play a very negligible role.

In the figure 4.10 the entry and exit hole diameters of the Ti6Al4V drilled with (a) K1, (b) K1R, (c) C8, (d) C8R, respectively.



*Fig. 4.10 - Entry and exit hole diameters of the Ti6Al4V: (a) K1(b) K1R, (c) C8, (d) C8R.*

Concerning titanium drilling there are no differences between the entry and exit hole diameters in every tool families, along the entire campaigns. The tool wear doesn't influence the diameter sizes, the trend is steady.

#### 4.2.4. Burr height

in this section, the burr height measurements will be presented and discussed. It is very important to remember that this is probably the most important output, as in fact, in the previous campaign, the process parameters and cooling conditions were selected according to it.

In the figure 4.11 the Ti6Al4V burr height of the exit holes drilled with K1 tool family is shown.

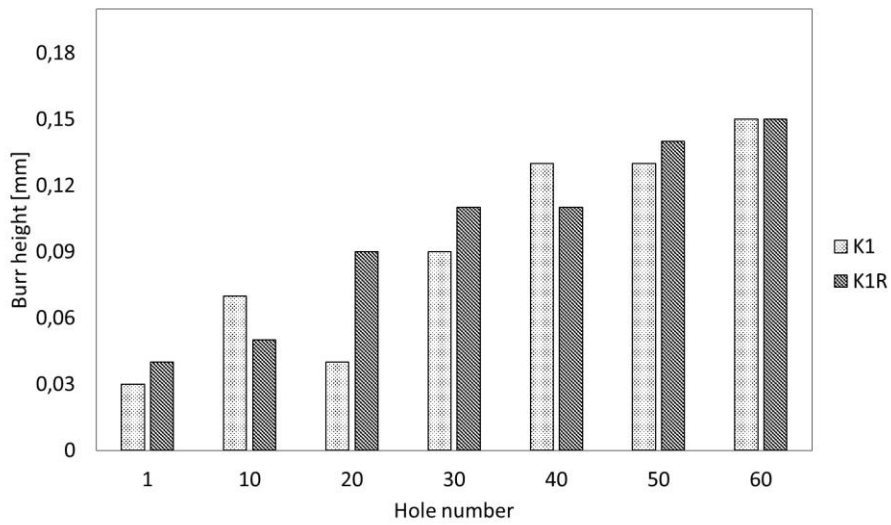


*Fig. 4.11 – The burr height due to the K1 tool family.*

The burr height increases as the number of holes increases. Since, in our research the burr height has been defined as the height of the highest peak of the burr itself along hole border, the measure itself is quite “unstable”, consequently it is not possible to justify any further trend.

In the figure 4.12 the Ti6Al4V burr height of the exit holes drilled with C8 tool family is shown.

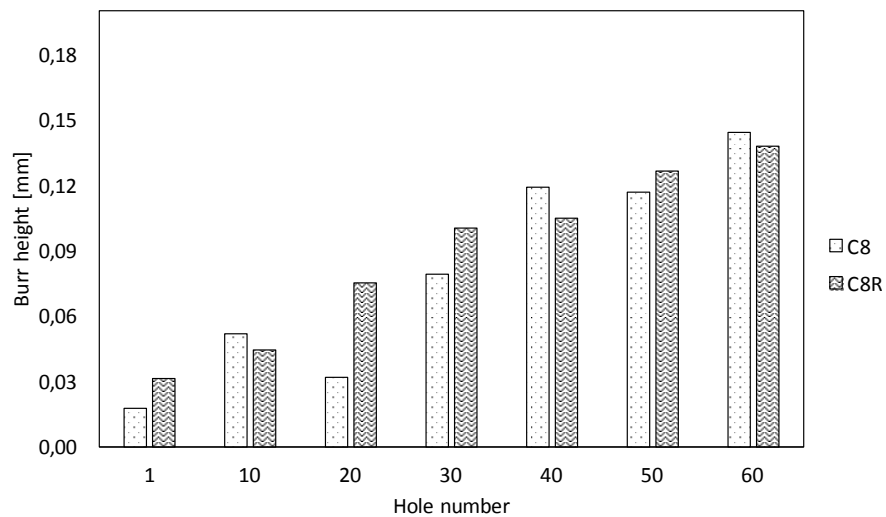


*Fig. 4.11 – The burr height due to the C8 tool family.*

In case of the burr height measurements of holes made with the tool of C8 family, it is possible to do considerations similar to those made for the other family. In this case, however, the values are lower.

#### **4.2.5. Tools visual inspection**

In the following, a series of pictures of both new and worn tools will be shown, with the aim to describe, by a qualitative point of view, the wear occurred in the different used tools. Since the C8 tool family showed better performances than the K1 family, and the performances of C8 and C8R tools are quite similar, but the former is cheaper than the latter, this phase of the research activity has been performed only on the C8 tool. Nevertheless, the results shown and the conclusions drawn are valid for both the tools of the family.

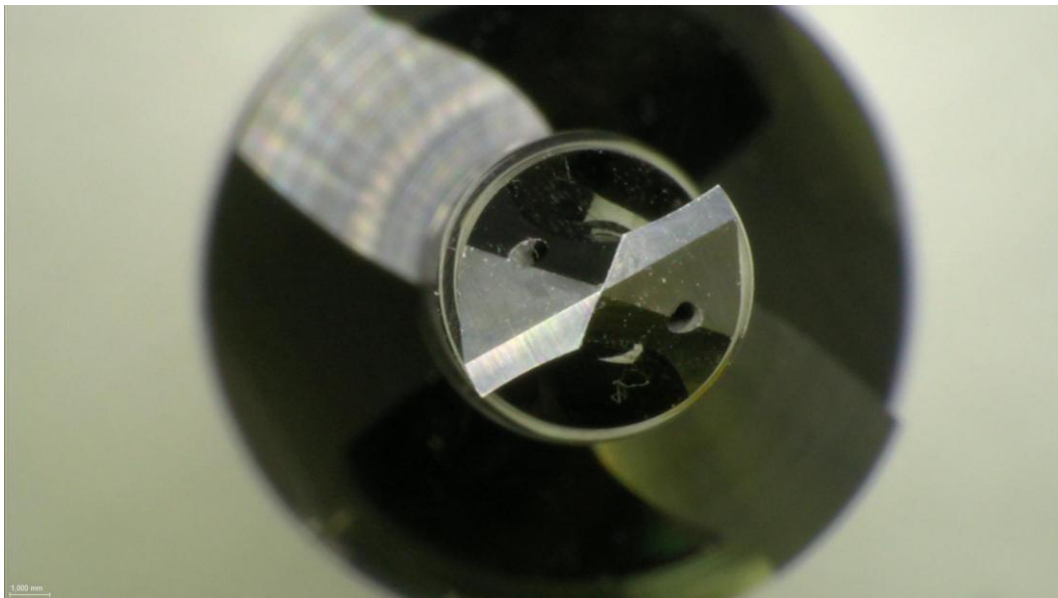


*Fig. 4.13 – frontal view of the new C8 tool.*

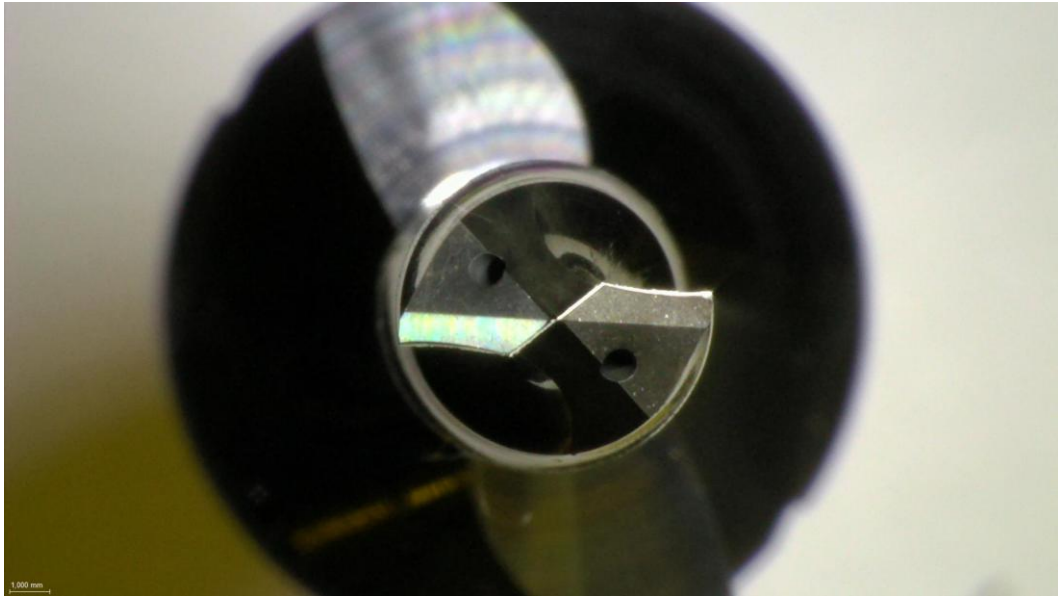


*Fig. 4.14 – frontal view of the worn C8 tool.*

By looking at the figures 4.13 and 4.14 it is possible to appreciate the flank wear (bright in the figure 4.14) as a comparison with the virgin flank in the figure 4.13. In more details, such a difference can be better appreciated looking at the figures 4.15 and 4.16.

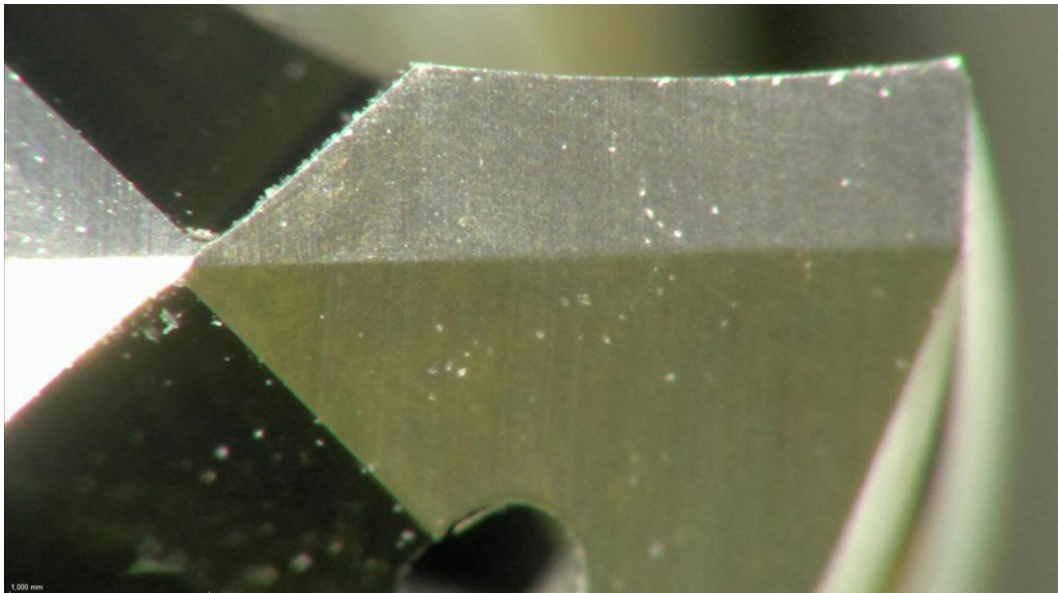


*Fig. 4.15 – frontal view of the new C8 tool: particular of the primary cutting edge.*

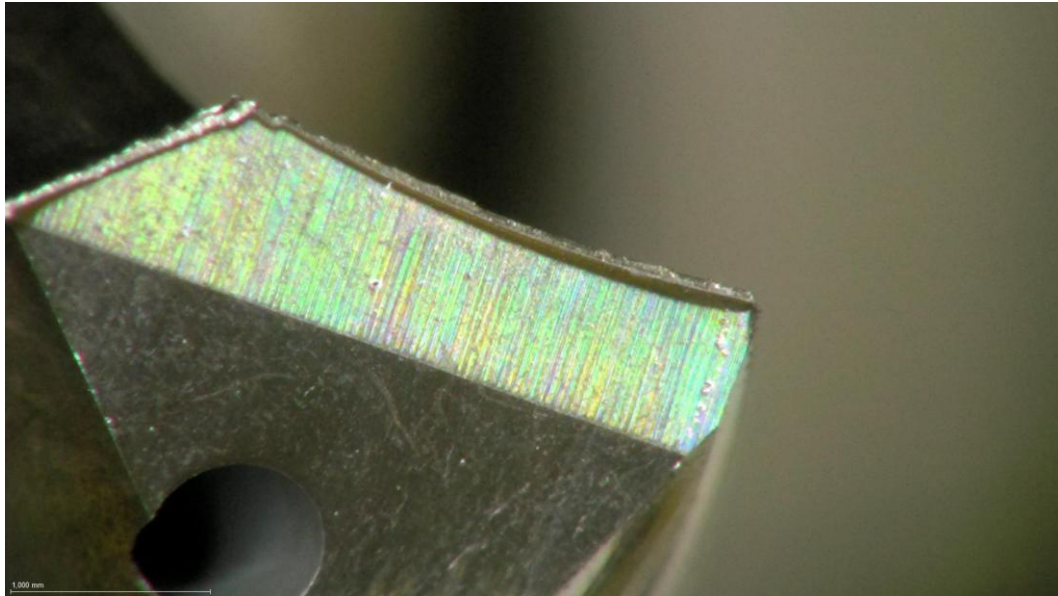


*Fig. 4.16 – frontal view of the worn C8 tool: particular of the primary cutting edge.*

As expected, the flank wear increases moving from the tool axis to tool outer side. The wear is quite stable along the whole flank. In figures 4.17 and 4.18, the rake face of both the virgin and worn tool are reported.

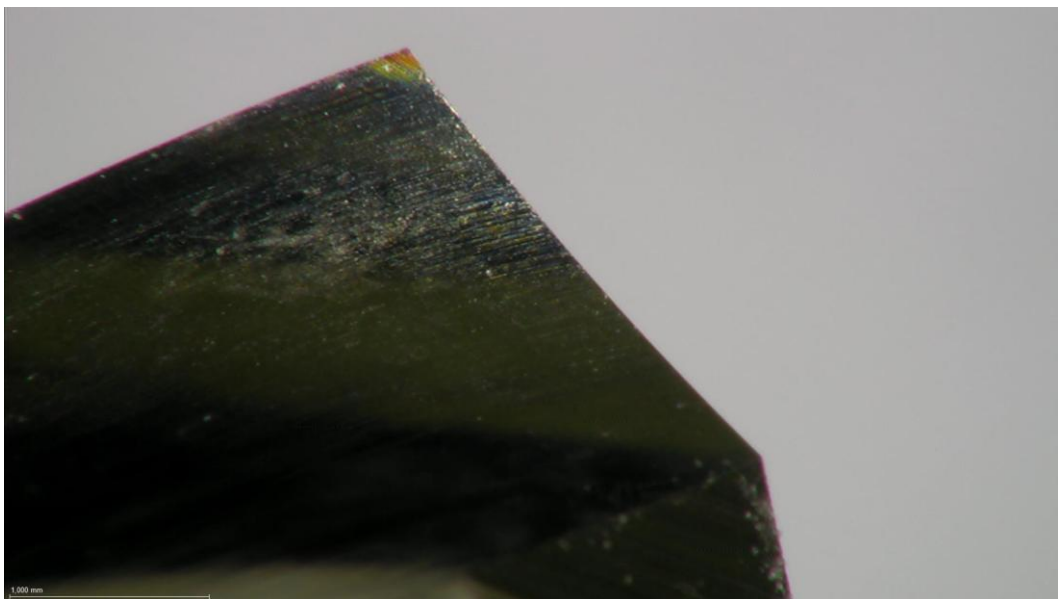


*Fig. 4.17 –Face of the new C8 tool.*

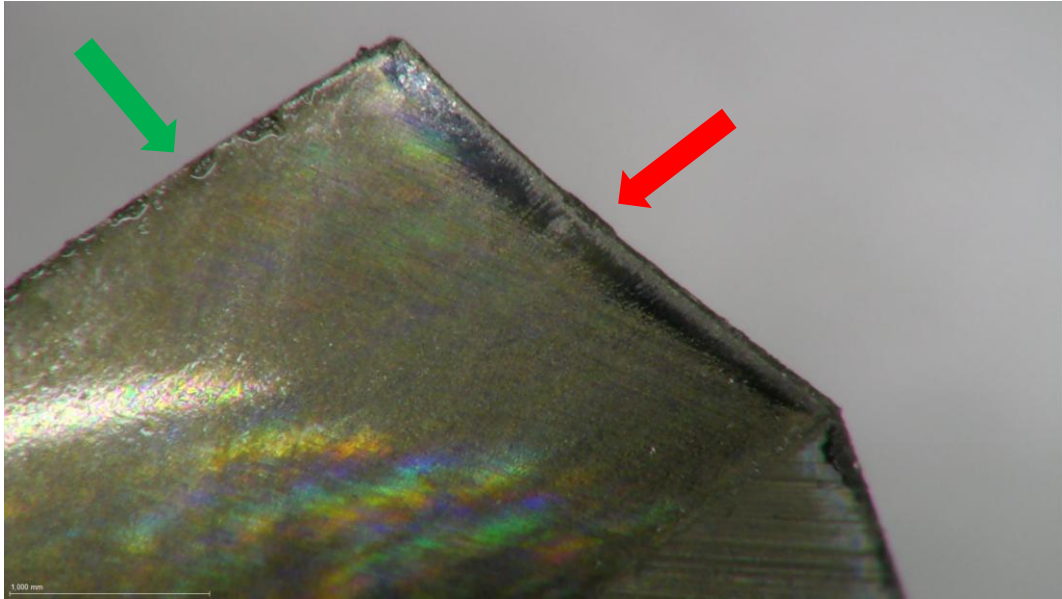


*Fig. 4.18 – Face of the worn C8 tool.*

By comparing them, it is possible to appreciate both the smooth and diffused wear of the face along the primary cutting edge (see red arrow in figure 4.18) and the interrupted and wear of the same face but along the secondary cutting edge (see green arrow in the same figure).

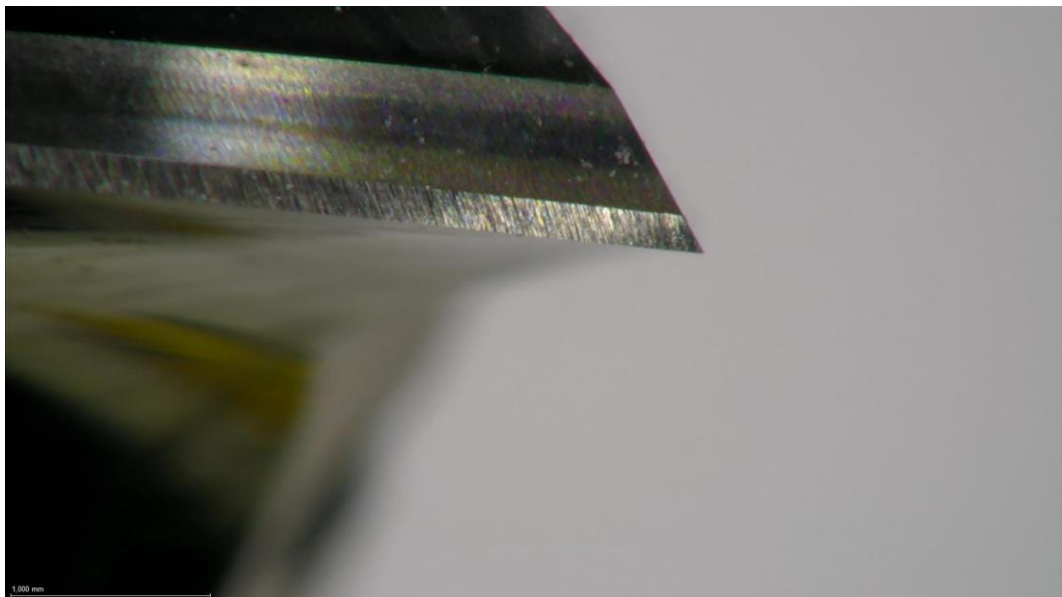


*Fig. 4.19 – Secondary cutting edge of the C8 new tool.*

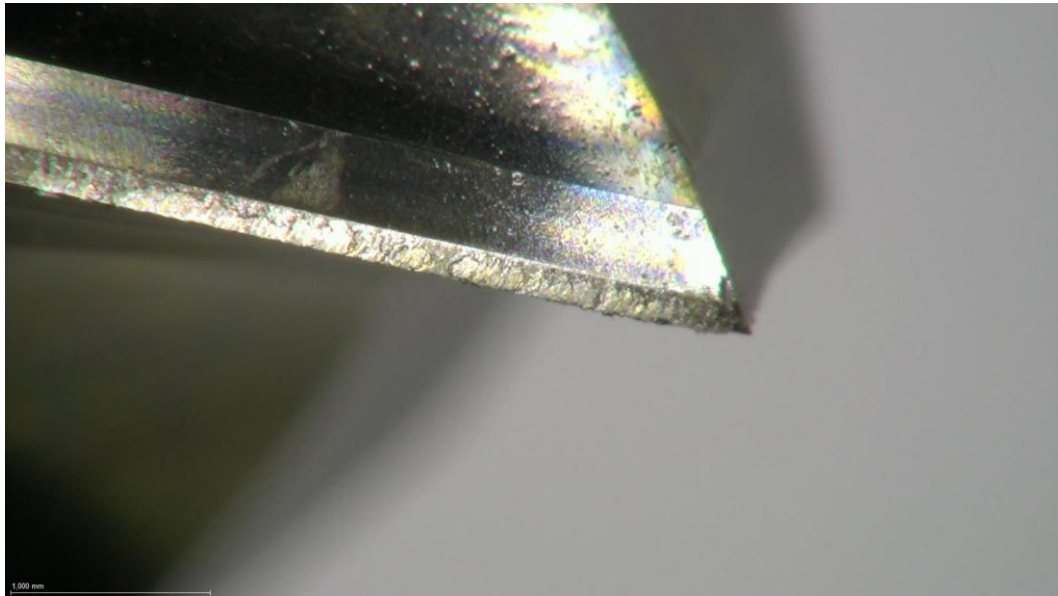


*Fig. 4.20 – Secondary cutting edge of the C8 worn tool.*

Finally, figures 4.19 and 4.20 show respectively the virgin and worn secondary cutting edge. It is possible to appreciate the abrasive wear occurred along the secondary cutting edge, and particularly in the corner (on the right in the figures).

### **4.3. Conclusions**

On the base of the results coming from the long run campaign, the following partial conclusions can be drawn.

Focusing attention on the recorded thrust force and torque:

- Independently from tool materials, the thrust force and the torque increase linearly for K1 tools and not for C8.
- In case of K1 tool family, the coating doesn't seem to be effective, since the recorded thrust force and torque are very similar for both the uncoated and coated tools.
- In the case of C8 tool family, the recorded thrust forces for the coated tool are higher than those recorded for the uncoated tool.

- On the long distance, i.e. after a large number of holes, the C8 tool leads to record the lowest forces.
- Looking at torque, the performances of all the tools on long run seem to be very similar.
- A partial contribution to the high values recorded for the coated tools, both in case of forces and torque, is not related to the wear but to the higher value of web thickness.

Focusing attention on the hole diameter measurements:

- In case of CFRP, the values measured for the diameters of the exit side are always appreciably larger than those of the entry side.
- This is due to the tool instability (resulting in tool vibrations) when the tool comes in touch with the upper side of titanium sheet.
- Anyway, according to acceptance threshold defined by Leonardo®, all the holes are in tolerance.
- All the tools show performances quite similar.
- Focusing attention on diameters of holes in titanium sheets, the tools are absolutely equivalent.
- In all cases, the influence of tool-life on hole diameter is negligible.

Finally, focusing attention on the burr height measurements:

- It is the measured output that is mostly influenced by tool life: in all cases, it quickly increases as the number of holes increases.
- On the long distances, due to the consumption of coating, the influence of the coating is negligible.
- The performances of C8 tool family seem to be better than those of K1 family.

## Conclusions

In this last chapter, I will provide the overall conclusions of the whole research activity carried out along my PhD course.

- Cryogenic condition seems to be very promising, since both the recorded thrust force and torque are always appreciably lower than in case of wet conditions. The major limit encountered, regarding the unacceptable value of the burr height, seems to be related to the very high value of the thickness of the entire stack.
- To this aim, in case like this, it could be more effective the use of a different cooling approach, based also on the direct cooling of the workpiece.
- Nevertheless, the advantages of cryogenic conditions are several, not only related to manufacturing aspects, but also to environmental ones, as described in the second chapter.
- Independently by the cooling conditions, in the holes made in the CFRP plate, the measured hole diameter on the entry side of the plate is always lower than that of the exit side, being the difference more and more evident as the feed rate increases. This is very probably due to the tool instability occurring when the tool comes in contact with the upper side of the titanium sheet. This phenomenon can be reduced by performing a prior hole with a lower diameter, even if in this case the manufacturing time increases dramatically.
- According to the thresholds imposed by the reference aeronautic sector (mainly the maximum acceptable burr height), at the end of the first experimental campaign, the wet condition has been preferred to the cryogenic one.
- Regarding the choice of process parameters and strategy, the highest values of both feed and spindle speed have been preferred, not only for

the reduced time consumption but also since they allow to record comparable values of force and torque. The same for the peck strategy: the highest value, reducing the number of pecks, reduce the manufacturing time and power consumption.

- According to the values chosen at the end of the first experimental campaign, the second one has been carried out in wet condition at the highest values of both feed and spindle speed with the highest peck.
- The partial conclusions have been provided at the end of the fourth chapter. Here I want to remark the effectiveness of the C8 tool, i.e. that characterized by the ultrafine grain structure, and the negligible role played by the coating on the long distance.
- Finally, the worn tool, described in details on each side face, allows to appreciate the kind of wear experienced by the tool (mainly abrasive) and its entity. This analysis allows to assess that, after a long run campaign of 60 holes, the wear of the tool is absolutely acceptable.
- As a consequence, as future developments, a tool regeneration can be performed with the aim to extend the tool life and save a huge amount of money.

## Bibliography

- [1] C. Amerio, R. De Ruvo, S. Simonetti, *Elementi di tecnologia*, SEI, 2011.
- [2] Serope Kalpakjian - Steven R. Schmid, *Tecnologia meccanica*, Pearson Educational Italia.
- [3] Yakup Yildiz, Muammer Nalbant, A review of cryogenic cooling in machining processes, *International Journal of Machine Tools & Manufacture*, 48 (2008), pp. 947–964.
- [4] <http://www.tuik.gov.tr/Start.do>
- [5] K. Uehara, S. Kumagai, Chip formation, surface roughness and cutting force in cryogenic machining, *Annals of CIRP*, 17 (1969), pp. 409–416.
- [6] K. Uehara, S. Kumagai, Characteristics of tool wear in cryogenic machining, *Annals of CIRP*, 18 (1970), pp. 273–277
- [7] C. Evans, Cryogenic diamond turning of stainless steel, *CIRP Annals*, 40 (1991), pp. 571–575
- [8] S.Y. Hong, Y. Ding, Cooling approaches and cutting temperatures in cryogenic machining of Ti–6Al–4V, *International Journal of Machine Tools and Manufacture*, 41 (2001), pp. 1417–1437.
- [9] Sanjay Rawat, Helmi Attia, Wear mechanisms and tool life management of WC–Co drills during dry high speed drilling of woven carbon fibre composites, *Wear*, 267 (2009), pp. 1022–1030
- [10] Marta Fernandes and Chris Cook, Drilling of carbon composites using one shot drill bit. Part I: Five stage representation of drilling and factors affecting maximum force and torque, *International Journal of Machine Tools & Manufacture*, 46 (2006), pp. 70-75.
- [11] Sushinder K, Shivaram PR, Nivedh Kannaa SB, Nisarg Gupta and Vijay Sekar KS, Investigation of Thrust forces, Torque and Chip microstructure during Drilling of Ti-6Al-4V Titanium alloy, *Applied Mechanics and Materials*, 787 (2015), pp. 431-436.

- [12] D. Kim, A. Beal, P. Kwon, Effect of tool wear on hole quality in drilling of carbon fiber reinforced plastic-titanium alloy stacks using tungsten carbide and polycrystalline diamond tools, *Journal of manufacturing science and engineering*, 138 (march 2016), pp. 031006-1-11
- [13] T. Xia<sup>1</sup> & Y. Kaynak<sup>2</sup> & C. Arvin<sup>1</sup> & I. S. Jawahir, Cryogenic cooling-induced process performance and surface integrity in drilling CFRP composite material, *International Journal of Advanced Manufacturing Technology*, 82 (2016), pp. 605-616.
- [14] Zitoune, Krihnaraj, Collombet, Studying of drilling composite material and aluminum stack *Composite Structures*, 92 (2010), pp. 1246 – 1255.
- [15] Xin Wang , Parick Y. Kwon, Caleb Sturtevant, Dave (Dae-Wook) Kim, Jeff Lantrip, Comparative tool wear study based on drilling experiments on CFRP/Ti stack and its individual layers, *Wear*, 317 (2014), pp. 265-276.